Subluminal and Superluminal Propagation of Electromagnetic Fields

A THESIS

submitted for the Award of Ph.D. degree of

Mohan Lal Sukhadia University

in the

Faculty of Science

BY

Tarak Nath Dey

Under the Supervision of

Prof. G.S. Agarwal

QUANTUM OPTICS & QUANTUM INFORMATION DIVISION
PHYSICAL RESEARCH LABORATORY, AHMEDABAD

MOHANLAL SUKHADIA UNIVERSITY, UDAIPUR

Year of submission: 2004

CERTIFICATE

This is to certify that the thesis entitled "Subluminal and Superluminal Propagation of Electromagnetic Fields" submitted for the award of the degree of Doctor of Philosophy of Mohanlal Sukhadia University in the faculty of Science is a record of bonafide investigations carried out by Shri. Tarak Nath Dey under my supervision and guidance.

This is an original piece of work on which no one has been awarded a degree in this University or in any other University.

The literary presentation of the thesis is satisfactory and it is in a form suitable for publication. The work presented in the thesis has been done after registration in this University.

Further, the candidate has put in attendance of more than 200 days in my institution as required under rule 7(b) and thus completed the residential requirement.

Prof. G.S. Agarwal
(SUPERVISOR)

In

memory of my father

. . . who has always been my source of inspiration

Contents

Acknowledgement

It gives me great pleasure to express my deepest sense of respect and sincere gratitude to Prof. G. S. Agarwal for his excellent guidance throughout the duration of this thesis work. His deep insight of getting to the heart of the problem and exceptional capacity to work, has been a source of inspiration for me. I have benefited immensely from the discussions with him and his critical evaluation for which I will always be obliged to him.

I am also grateful to Prof. V.B. Sheorey, Prof. S. Duttagupta, Prof J.H. Eberly, Dr. J. Banerji, Dr. Prasanta Panigrahi, Dr. R.P. Singh, Dr. K.P. Subramanian and Dr. Bimalendu Deb for their constant encouragement and suggestions during the Ph.D. work.

I would also like to thank Dr. Angom Dilip for useful discussions on parallelization in FORTRAN.

I thank all staff members of PRL for their kind cooperation at all stages; to name a few: Dholakiaji, Jigar, Purobi-di, Urmilaji, Nishthaji, Leelaji and Sudheenji.

I thank all my batch-mates Shubharangshu, Rajesh, Lokesh, Jayendra, Sanjoy, Sarika and Sudhesna for their encouragement and entertaining company during my Ph.D. period. I cherish the wonder moments shared with my friends, Alambhai, Subrata-da, Aninda-da, Dipu-da, Koushik-da Sunish, Pattu, Arun, Santosh, Neeraj, Manoj, Manish, Sanjeev, Harish, Vinay, Asoka, Pathak, Bhavesh, Charan, Rajneesh, Jayesh, Sanjoy, Yogesh, Dilip, Morthekai, Murali, Ravindra, P.K. Rajesh, Sudhree, Jaiswal, Utpal, Suranjana, Rudra, Subimal and Sumanta.

My heartfelt thank to Supriyo-da, Prakiti-di, Ashish-da, Sudipta-di, Soumen-da, Jhuma-di, Rajen-da, Jayshree-di, Sujoy, Sambita, Anirban, Prasanta and Malay who provided me constant inspiration during difficult period of my thesis.

It is a golden opportunity to me to express my sincere thanks towards the members of PRL football club.

Finally, I must remember the blessings of my family members which helped me to reach to this level. I am very much indebted to my parents for their endless sacrifice, love and affection.

Tarak Nath Dey

Abstract

The work in this thesis deals with the group velocity of electromagnetic fields in different atomic media. The main thrust of this work is that coherent control of group velocity is possible by manipulating the atomic coherence of the medium. In chapter 1, the basic theory of radiation-matter interaction is discussed. The theory of propagation equation is presented in Sec. 1.1. In Sec. 1.2 the derivation of interaction Hamiltonian is discussed. Sec. 1.3 and 1.4 present the manipulation of atomic coherence by applying an external coherent control field of suitable intensity. Sec. 1.5 presents the basic concept of group velocity and introduces the key theme of the thesis - manipulating atomic coherence to control the group velocity of light inside the medium. The coherent control of the group velocity produces subluminal propagation, storage and retrieval of light pulses as well as superluminal propagation are discussed in the following section. Many different applications of slow light, storage and retrieval of light and fast light are discussed.

In chapter 2, we study the propagation of a weak electromagnetic pulse through a Λ-system when the central frequency of the pulse is close to the atomic transition frequency. This weak pulse couples one arm of the Λ-system and a strong control field couples to the other arm. The lower metastable states of the atom are coupled by an additional field called lower level (LL) coupling field. An undistorted pulse propagation requires a stringent condition that the medium should be absorptionless when the pulse is near-resonance with atomic transition frequency. By properly selecting the parameters of control and LL coupling field intensity, we could achieve this condition and consequently distortionless pulse propagation. We show that the group velocity of the weak pulse can be controlled by suitably choosing the intensity of the control and LL coupling field. We also demonstrate

that such control can lead to a knob for changing the velocity of propagation of the pulse from subluminal to superluminal.

In chapter 3, we investigate the possibility of storage and retrieval of an intense probe pulse in a medium which can be modelled as a set of atoms with the relevant energy levels in Λ-configuration. We demonstrate that it is indeed possible to store and retrieve a probe pulse which is not necessarily weak. We find that the retrieved pulse remains a replica of the original pulse, although there is an overall broadening and loss of the intensity. The loss of intensity can be understood in terms of the dependence of medium absorption on the intensity of the probe. Our calculations include the dynamics of the control field, which becomes especially important as the intensity of the probe pulse increases. We use the theory of adiabatons [Grobe *et al.* Phys. Rev. Lett. **73**, 3183 (1994)] to understand our numerical results on the storage and retrieval of light pulses at moderate powers. We also demonstrate that a robust way of storage and retrieval of information on the weak modulating signal is possible by applying a suitable control pulse.

In chapter 4, we develop models for the propagation of intense pulses in solid state media which can have either saturated absorption or reverse absorption. We model subluminal propagation in ruby as a three level system and superluminal propagation in alexandrite as a four level system. The propagation dynamics is governed by the Maxwell's equations. We calculate the group velocity from the relative delay or advancement between the reference and output pulse. We present results well beyond the traditional pump-probe approach and explain the experiments of Bigelow *et al.*[Phys. Rev. Lett. **90**, 113903 (2003); Science **301**, 200 (2003).] on solid state materials. We also notice that the input pulse becomes distorted due to the intensity dependent nonlinearity of the medium.

In chapter 5, propagation of light pulses through a Doppler-broadened atomic medium is analyzed. It is shown that how Lamb dip and saturated absorption can be used to produce slow light with group indices of the order of 10^3 in a Doppler-broadened medium which otherwise exhibits very flat dispersion. We include all coherence effects in our numerical calculations.

In chapter 6, a new way to freeze light pulse inside a Doppler-broadened atomic medium through electromagnetically induced transparency is examined. It is shown that the application of an additional control field connecting the two lower level metastable states in the Λ-system can change the group velocity of the pulse inside the medium from negative to a

positive value. This change helps in stopping light provided the probe field as well as the suitable detuning of control field satisfies the two-photon resonance condition.

CHAPTER 1

Introduction

The meaning of group velocity in the context of light pulse propagation through resonant optical media has been puzzling the physicists for some time. Lord Rayleigh was the first to comment that the pulse travels in a medium with a group velocity rather than the phase velocity [1]. Later on, Sommerfeld and Brillouin developed a complete theory of the pulse propagation through a medium whose dielectric response was described by the Lorentz model [2]. They showed that anomalous dispersion always occurs in the region of absorption and leads to group velocity much larger than c, the speed of light in vacuum. They also pointed out that signal velocity is always less than c even in the case of anomalous dispersion, where the group velocity exceeds c. Manipulation of group velocity of the light pulse is possible by changing the dispersive property of the medium. The dispersive property can be dramatically modified by employing laser fields to drive the optical medium. The required dispersion and absorption can be obtained by the application of coherent control fields of suitable intensity. The precise control over the optical properties of the medium such as dispersion, absorption, and refractive index, gives rise to fascinating phenomena like coherent population trapping (CPT), electromagnetically induced transparency (EIT), lasing without inversion (LWI), ultraslow light and fast light. The recent demonstration on storage and retrieval of light in resonant media has tremendous technological implications. The ability to slow down the propagation velocity of light and to coherently stop and store it, holds the key to the ultimate control of light. This will have revolutionary impact in the area of optical communications and quantum information processing. It should be borne

in mind that the key feature underlying all these recent developments is *atomic coherence*. This thesis describe how atomic coherence can be manipulated using appropriate coherent control fields which will modify the propagation velocity of light through the medium.

1.1 Basic Propagation Equation

Light is an electromagnetic wave (em) consisting of oscillating electric and magnetic field vectors. The propagation of light (em) through an optical medium is governed by four fundamental Maxwell's equations, which in Gaussian units can be written as,

$$\vec{\nabla} \cdot \vec{D} = 4\pi\varrho, \qquad \text{(Gauss's Law)} \tag{1.1a}$$

$$\vec{\nabla} \cdot \vec{B} = 0, \tag{1.1b}$$

$$\vec{\nabla} \times \vec{E} = -\frac{1}{c}\frac{\partial \vec{B}}{\partial t}, \qquad \text{(Faraday's Law)} \tag{1.1c}$$

$$\vec{\nabla} \times \vec{H} = \frac{4\pi}{c}\vec{J} + \frac{1}{c}\frac{\partial \vec{D}}{\partial t}, \quad \text{(Ampere's Law)}. \tag{1.1d}$$

Here $\vec{E}$, $\vec{H}$ are the time-averaged values of the basic electric, magnetic field vectors at some space-time point $(\vec{r}, t)$, rather than the instantaneous values and c is the velocity of light in free space [3]. The electric displacement $\vec{D}$ and the magnetic induction $\vec{B}$ have "additive relations", coming from the interaction of matter and field,

$$\vec{D} = \vec{E} + 4\pi\vec{\mathcal{P}}, \tag{1.2a}$$

$$\vec{B} = \vec{H} + 4\pi\vec{\mathcal{M}}. \tag{1.2b}$$

Here $\vec{\mathcal{P}}$ and $\vec{\mathcal{M}}$ are the *electric* and *magnetic polarizations* respectively. In Eq. (1.2a) the contribution from the multipole moments (such as electric quadrapole moments) has been neglected, since at optical frequency the electric dipole moment is the most dominant quantity. In free space, both $\vec{\mathcal{P}}$ and $\vec{\mathcal{M}}$ vanish, hence, these quantities represent the influence of matter on the field. In this thesis, the system under consideration is *non magnetic* ($\vec{\mathcal{M}} = 0$), and *non conducting* ($\vec{J} = 0$), together with no free charge ($\varrho = 0$). Applying the curl operator in Eq. (1.1c), taking appropriate time derivatives and using the constitutive relation for $\vec{B}$, we obtain

$$\vec{\nabla} \times \vec{\nabla} \times \vec{E} + \frac{1}{c^2}\frac{\partial^2}{\partial t^2}(\vec{E} + 4\pi\vec{\mathcal{P}}) = 0. \tag{1.3}$$

Since $\vec{D} = \vec{E} + 4\pi\vec{P}$, for a charge free isotropic medium, $\vec{\nabla} \cdot \vec{D} = 0$, and thus $\vec{\nabla} \cdot \vec{E} = 0$. Therefore, the simplified wave equation can be written as

$$\vec{\nabla}^2\vec{E} - \frac{1}{c^2}\frac{\partial^2\vec{E}}{\partial t^2} = \frac{4\pi}{c^2}\frac{\partial^2\vec{\mathcal{P}}}{\partial t^2}. \tag{1.4}$$

This equation has the form of an inhomogeneous wave equation. The source term which appears on the right-hand side of this equation represents the nonlinear response of the medium. In the absence of the source term, the above Eq.(1.4) reduces to

$$\vec{\nabla}^2\vec{E} - \frac{1}{c^2}\frac{\partial^2\vec{E}}{\partial t^2} = 0. \tag{1.5}$$

In the optical wavelength limit, the variations of the field along the transverse directions is small. Therefore the general solution of this equation can be written in the form,

$$\vec{E} = \vec{E}_1(z - ct) + \vec{E}_2(z + ct), \tag{1.6}$$

where $\vec{E}_1$ and $\vec{E}_2$ are arbitrary functions. We see that the argument of $\vec{E}_1$ is unchanged when (z, t) is replaced by $(z + ct, t + \tau)$, where τ is an arbitrary parameter. Hence $\vec{E}_1(\vec{E}_2)$ represents a field which is propagating with velocity c in the positive (negative) z-direction.

Now in the presence of a polarized medium, the Maxwell's wave equation becomes nonlinear. In practice, it is very difficult to get the exact solution of nonlinear wave equation. But these equations can be solved analytically with few specialized approximations and, numerically, in the general case. For example, consider a linearly-polarized plane wave propagating in the z-direction, its electric field can be described by

$$\vec{E}(z,t) = \hat{e}\mathcal{E}_0(z,t)e^{-i(\omega t - kz)} + \text{c.}c. \tag{1.7}$$

where $\hat{e}$ is the direction of polarization, ω is the central angular frequency of the field, and the wave number, $k = \omega/c$. The complex conjugate (c.c.) term has been added to the electric field expression to make it real. The induced polarization of the medium can be written as

$$\vec{\mathcal{P}}(z,t) = \hat{e}\mathcal{P}_0(z,t)e^{-i(\omega t - kz)} + c.c. \tag{1.8}$$

We know that the bound state electron in an atomic medium experiences stronger electrostatic field due to the interaction with the nucleus as compared to the external field created

by an applied laser. Hence, we study the interaction of atom with the applied field perturbatively. The induced polarization can be expanded in a Taylor series, in powers of the applied electric field $\vec{E}$:

$$\mathcal{P}_\alpha(z,t) \equiv \mathcal{P}_\alpha|_{E=0} + \sum_\beta \left(\frac{\partial \mathcal{P}_\alpha}{\partial E_\beta}\right)\Big|_{E=0} E_\beta + \frac{1}{2!}\sum_{\beta,\gamma}\left(\frac{\partial^2 \mathcal{P}_\alpha}{\partial E_\beta \partial E_\gamma}\right)\Big|_{E=0} E_\beta E_\gamma + \cdots . \quad (1.9)$$

The first term in Eq. (1.9) corresponds to the permanent polarization of the system. This type of polarization is not present in our system. The second term represents the induced linear polarization. The term in the first bracket along with the summation in the second term of Eq. (1.9) can be regarded as the linear susceptibility of the medium. The higher order susceptibility term can be obtained by the subsequent terms in Eq. (1.9); these become important when the applied field is not weak, otherwise one can retain up to the first order. Therefore, the polarization $\mathcal{P}_\alpha$ is usually a complicated nonlinear function of $\vec{E}$. In the linear case, however, $\mathcal{P}_\alpha$ takes a simple linearized form

$$\mathcal{P}_\alpha(z,t) = \sum_\beta \int_{-\infty}^{\infty} dt' dz' \chi_{\alpha\beta}(z-z', t-t') E_\beta(z',t') \ , \quad (1.10)$$

where $\chi_{\alpha\beta}$ is the linear susceptibility tensor with rank two for an anisotropic medium, where the response of the medium is different for different components of the electric field. In the present thesis, the medium is isotropic and the complex susceptibility, $\chi_{\alpha\beta} \equiv \chi$, is a scalar quantity. Thus Eq. (1.10) can be written as

$$\mathcal{P}(z,t) = \int_{-\infty}^{\infty} dt' dz' \chi(z-z', t-t') E(z',t') \ . \quad (1.11)$$

We consider that the electric field amplitude $\mathcal{E}_0(z,t)$ and polarization $\mathcal{P}_0(z,t)$ vary sufficiently slowly in time and space so that the following inequalities are valid:

$$\begin{aligned} |k\mathcal{E}_0| \gg \left|k^2 \frac{\partial \mathcal{E}_0}{\partial z}\right| \gg \left|\frac{\partial {\mathcal{E}_0}^2}{\partial^2 z}\right| \quad , \quad |\omega \mathcal{E}_0| \gg \left|\omega^2 \frac{\partial \mathcal{E}_0}{\partial t}\right| \gg \left|\frac{\partial {\mathcal{E}_0}^2}{\partial^2 t}\right| \\ |k\mathcal{P}_0| \gg \left|k^2 \frac{\partial \mathcal{P}_0}{\partial z}\right| \gg \left|\frac{\partial {\mathcal{P}_0}^2}{\partial^2 z}\right| \quad , \quad |\omega \mathcal{P}_0| \gg \left|\omega^2 \frac{\partial \mathcal{P}_0}{\partial z}\right| \gg \left|\frac{\partial {\mathcal{P}_0}^2}{\partial^2 z}\right| . \end{aligned} \quad (1.12)$$

These equations define the so called *"slowly-varying amplitude approximation"* (SVAP), which plays a central role in laser physics and pulse propagation problems. It means that we consider light waves whose amplitudes vary little within the optical period and optical wavelength. Sometimes this approximation is also called the *"slowly-varying envelope approximation"* (SVEA) [4].

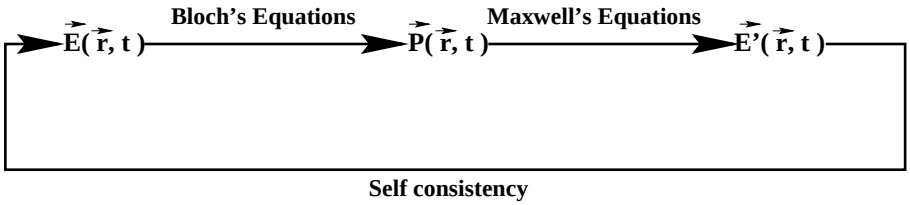

Figure 1.1: *Incident electric field $\vec{E}(\vec{r},t)$ induces polarization of the medium $\vec{\mathcal{P}}(\vec{r},t)$, which acts as a source in Maxwell's equations. The condition self-consistency then requires that the incident field $\vec{E}(\vec{r},t)$ is equal the reaction field $\vec{E}'(\vec{r},t)$.*

The SVEA leads to major mathematical simplifications as can be seen by substituting the field (1.7) and polarization (1.8) into the wave equation (1.4) and using equation (1.12) to eliminate the small contributions $\ddot{\mathcal{E}}_0$,$\ddot{\mathcal{P}}_0$,$\mathcal{E}_0{}''$,$\mathcal{P}_0{}''$ (double dot and double prime denotes second order derivative with respect to time and space respectively). We find

$$\frac{\partial \mathcal{E}_0}{\partial z} + \frac{1}{c}\frac{\partial \mathcal{E}_0}{\partial t} = 2\pi i k \mathcal{P}_0. \tag{1.13}$$

This equation tells us how light propagates through a medium and specifically how the real and imaginary parts of the polarization act. Equation (1.13) is not sufficient to describe physical problems completely, since it only tells us how a plane electromagnetic wave responds to a given polarization of the medium. Further, polarization has to be determined by using Bloch's equations of the medium. We are aware that the polarization of a medium is influenced by the field to which it is subjected. In particular for atomic gases without permanent polarization, it is the electromagnetic field itself that induces the polarization! Thus, the field drives the polarization of the medium and vice versa. This leads to the description of the interaction between the matter and field to be expressed in terms of coupled nonlinear partial differential equations which have to be solved *"self-consistently"* as depicted in Fig (1.1). Pulse propagation in a nonlinear transparent medium has been lucidly discussed by Allen and Eberly [5]. We transform to new variables

$$\tau = t - z/c, \quad \zeta = z, \tag{1.14}$$

so that

$$\partial/\partial z + c^{-1}\partial/\partial t = \partial/\partial\zeta, \quad \partial/\partial t = \partial/\partial\tau \tag{1.15}$$

and

$$\frac{\partial \mathcal{E}_0}{\partial \zeta} = 2\pi i k \mathcal{P}_0. \tag{1.16}$$

The spatio-temporal evolution of the atomic polarization $\mathcal{P}_0$ will be discussed in the subsequent section via density matrix and the numerical solution of the coupled Maxwell-Bloch equation will be addressed in the appendix.

For a steady state limit of wave equation of the type

$$\frac{\partial \mathcal{E}_0}{\partial z} = 2\pi i k \chi \mathcal{E}_0. \tag{1.17}$$

where $\mathcal{P}_0 = \chi(\omega)\mathcal{E}_0$ is the linear response of the medium to the electric field, the solution for the output field of the medium of length L can be written as

$$\vec{E}_{out}(z = L, t) = \hat{e}\mathcal{E}_0 e^{2\pi i k L \chi} e^{-i(\omega t - kz)} + c.c. \tag{1.18}$$

For $\chi \ll 1$, which is the case in the optical wavelength domain, the approximate linear value of the refractive index $\eta(\omega)$ and the extinction coefficient $\alpha(\omega)$ are given by

$$\eta(\omega) = 1 + 2\pi Re[\chi(\omega)] \tag{1.19a}$$

$$\alpha(\omega) = 4\pi k Im[\chi(\omega)] \tag{1.19b}$$

The only measurable quantity is the output intensity at the end of the medium, $I_{out} \equiv |\vec{E}_{out}|^2$. Therefore the absolute square of equation (1.18) gives Beer's Law for the intensity

$$I_{out} = I_0 e^{-\alpha L}. \tag{1.20}$$

The information about $\alpha(\omega)$ *i.e.*, the imaginary part of the complex susceptibility of the medium can be derived from the measured output intensity. Now, one can use the Kramers-Kronig relations to find the real part of the susceptibility, *i.e.,* the refractive index of the medium at all frequencies. Such relations were first introduced by them in 1926 to study the dielectric constant of a substance [6]. The measurable parameter $\alpha(\omega)$ depend upon the susceptibility of the medium which can be modified by applying strong external coherent field. In presence of a strong field, the susceptibility of the medium can be changed and this changed can be probed by a weak field (probe field). Note here that the probe field does not change the properties of the medium at the experimental time scale. The study of interaction of radiation with matter becomes important as the field incident on the atomic medium. We will use the semiclassical theory of the interaction of radiation with matter where radiation field is considered classically and the matter is treated as quantum mechanical particle with discrete energy levels.

1.2 Interaction of Radiation with Matter

The light field (em) is treated classically by Maxwell's equations while the atom is considered to have quantized energy levels and is treated by the Schrödinger equation. For simplicity, the atom is assumed to have a single electron of charge e and mass m interacting with an external electromagnetic field. The interaction between atom and field is described by the following Hamiltonian

$$\mathcal{H} = \frac{[\vec{P} - e\vec{A}(\vec{r},t)]^2}{2m} + e\Phi(\vec{r},t) + V(r), \tag{1.21}$$

where $\vec{P}$ is the momentum of the electron, $\vec{A}(\vec{r},t)$ and $\Phi(\vec{r},t)$ are the vector and scaler potentials of the external field respectively. Here $V(r)$ is a central potential experienced by the bound electron due to the presence of motionless nucleus. Quantization of the electron motion can be done by replacing the classical variable with operators, *e.g.*,

$$\vec{P} \longrightarrow -i\hbar\vec{\nabla}, \mathcal{H} \longrightarrow i\hbar\partial/\partial t. \tag{1.22}$$

Here $\hbar = h/2\pi$, where h is the Planck's constant. Therefore, the motion of electron is described by the Schrödinger equation

$$\begin{aligned} i\hbar\frac{\partial|\Psi(\vec{r},t)\rangle}{\partial t} &= \left\{\frac{[-i\hbar\vec{\nabla} - \frac{e}{c}\vec{A}(\vec{r},t)]^2}{2m} + V(r) + e\Phi(\vec{r},t)\right\}|\Psi(\vec{r},t)\rangle \\ &= (\mathcal{H}_{\mathcal{O}} + \mathcal{H}_{\mathcal{I}})|\Psi(\vec{r},t)\rangle, \end{aligned} \tag{1.23}$$

where the unperturbed Hamiltonian is given by

$$\mathcal{H}_{\mathcal{O}} = -\frac{\hbar^2}{2m}\vec{\nabla}^2 + V(r) + e\Phi \tag{1.24}$$

and the interaction Hamiltonian involves only the vector potential $\vec{A}$:

$$\mathcal{H}_{\mathcal{I}} = \frac{e}{2mc}\left[2i\hbar\vec{A}(\vec{r},t)\cdot\vec{\nabla} + i\hbar\vec{\nabla}\cdot\vec{A}(\vec{r},t)\right] + \frac{e^2}{2mc^2}\vec{A}(\vec{r},t)\cdot\vec{A}(\vec{r},t) \tag{1.25}$$

In passing we note that, the transformations $\vec{A} \longrightarrow \vec{A}' = \vec{A} + \frac{\hbar}{e}\vec{\nabla}\chi$ and $\Phi \longrightarrow \Phi' = \Phi - \frac{\hbar}{e}\frac{\partial\chi}{\partial t}$, leave the $\vec{E}$ and $\vec{B}$ as invariant quantities which are thus gauge independent. Here, χ is any arbitrary scalar function. This allows one to choose a suitable gauge to simplify a given problem. Here we are working in the radiation gauge in which $\Phi(\vec{r},t) = 0$ and $\vec{\nabla}\cdot\vec{A} = 0$. Under the radiation gauge condition, the interaction Hamiltonian becomes

$$\mathcal{H}_{\mathcal{I}} = \frac{ie\hbar}{mc}\vec{A}(\vec{r},t)\cdot\vec{\nabla} + \frac{e^2}{2mc^2}\vec{A}(\vec{r},t)\cdot\vec{A}(\vec{r},t) \tag{1.26}$$

The dipole moment approximation is often used in quantum optics, which simplifies the interaction Hamiltonian term [7]. This approximation assumes that the whole atom is submerged in a plane em wave described by a vector potential, $\vec{A}(\vec{r}+\vec{r}_0,t)$, which is assumed to have no spatial variation in the vicinity of the atom whose nucleus is located at $\vec{r}_0$. For such a case,

$$\begin{aligned}\vec{A}(\vec{r}+\vec{r}_0,t) &= \vec{A}(t)exp\left[i\vec{k}\cdot(\vec{r}+\vec{r_0})\right] \\ &= \vec{A}(t)exp(i\vec{k}\cdot\vec{r}_0)(1+i\vec{k}\cdot\vec{r}+\cdots)\end{aligned} \tag{1.27}$$

Taking $\vec{k}\cdot\vec{r}\ll 1$, we obtain

$$\vec{A}(\vec{r}+\vec{r}_0,t)\approx\vec{A}(t)exp(i\vec{k}\cdot\vec{r}_0). \tag{1.28}$$

Using the unitary transformation $|\Psi(\vec{r},t)\rangle = e^{\frac{ie}{\hbar}\vec{r}\cdot\vec{A}_0}|\psi(\vec{r},t)\rangle$ in Eq. (1.23), we get

$$\begin{aligned}i\hbar\frac{\partial|\psi(\vec{r},t)\rangle}{\partial t} &= \left\{\frac{\hbar^2}{2m}\vec{\nabla}^2+V(r)-e\vec{r}\cdot\vec{E}(t)\right\}|\psi(\vec{r},t)\rangle \\ &= (\mathcal{H}_{\mathcal{O}}+\mathcal{H}_{\mathcal{I}})|\psi(\vec{r},t)\rangle\end{aligned} \tag{1.29}$$

The atom-field interaction Hamiltonian in the semiclassical picture is given by

$$\mathcal{H}_{\mathcal{I}} = -e\vec{r}\cdot\vec{E} = -\vec{d}\cdot\vec{E} \tag{1.30}$$

where the dipole moment operator $\vec{d}$ is $e\vec{r}$. A significant contribution towards understanding radiation-matter interaction was given by Einstein. He employed the basic ideas of quantum mechanics to lay the foundation for the quantitative analysis of the absorption and emission of light by atoms [8]. Later this simple theory has been extensively verified by rigorous quantum mechanical calculations.

For illustration, it is simpler to consider two energy states of an atom, namely, the excited state $|1\rangle$ and ground state $|2\rangle$. Phenomenologically, Einstein introduced three processes underlying radiation-matter interactions:

Stimulated absorption: In the presence of radiation, the transition rate for absorption $|2\rangle \longrightarrow |1\rangle$ is proportional to the radiative energy density and the probability per unit time for the stimulated absorption is given by $\mathcal{B}_{21}$.

Stimulated emission: In the presence of radiation, the transition rate for emission $|1\rangle \longrightarrow |2\rangle$ is proportional to the radiative energy density and the probability per unit time for the stimulated emission is denoted by $\mathcal{B}_{12}$.

Spontaneous emission: In the absence of radiation fields, there is a finite probability that the atom in the excited state $|1\rangle$ decays into the ground state $|2\rangle$ by emitting a photon of energy $\hbar\omega_{12}$. The probability per unit time for occurrence of this spontaneous emission is denoted by $\mathcal{A}_{12}$.

The above coefficients $\mathcal{A}$ & $\mathcal{B}$ are independent of the radiative energy density, depending only on the property of the atomic states. The interrelation of these three probabilities at thermal equilibrium is given by

$$\mathcal{A}_{12} = \frac{\hbar\omega_{12}^3}{\pi^2 c^3}\mathcal{B}_{12} \tag{1.31a}$$

$$\mathcal{B}_{12} = \frac{g_2}{g_1}\mathcal{B}_{21}. \tag{1.31b}$$

Here $g_1(g_2)$ is the degeneracy of the ground state (excited state) and ω_{12} is the atomic transition frequency. A full quantum mechanical treatment for the two level atom relates the above probabilities to atomic properties:

$$\mathcal{A}_{12} = \frac{4|\vec{d}_{12}|^2\omega_{12}^3}{3\hbar c^3}, \tag{1.32a}$$

$$\mathcal{B}_{12} = \frac{4\pi^2|\vec{d}_{12}|^2}{3\hbar^2}. \tag{1.32b}$$

Here $\vec{d}_{12}$ is the dipole moment matrix element of the relevant transition. It is clear from the above that the spontaneous emission rate $\mathcal{A}_{12}$ increases with the increase in the atomic transition frequency ω_{12}. At this point a natural question arises on the possibility of controlling the spontaneous emission rate. With using the Fermi golden rule it can be shown that the transition rate from a discrete atomic state to a continuum of electromagnetic modes is given by

$$\mathcal{A}_{12} = \frac{2\pi}{\hbar}|V_{12}|^2\rho(\omega) \tag{1.33}$$

where $|V_{12}|^2$ is the transition matrix element; it connects the initial and final states of an atomic system and $\rho(\omega)$ is the density of the mode of the final radiation states [9]. Therefore, the spontaneous emission rate can be changed by changing the density of modes or the coupling strength of the incident radiation. The semiclassical treatment is widely used in laser physics and in non-linear optical phenomena, since the exact study of the radiation-matter interaction is an extremely difficult problem.

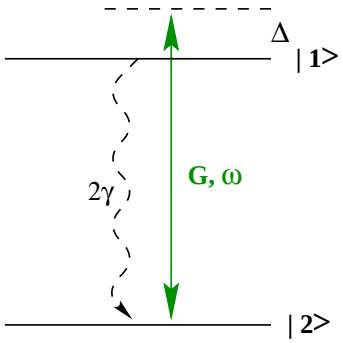

Figure 1.2: *Two level atomic system coupled to a control field with Rabi frequency* $2G$.

1.3 Induced Atomic Coherences in Two Level Atomic Systems

The coherent interaction of the external laser fields and atoms induces atomic coherence among the atomic states. In recent years, atomic coherence has played a central role in the precise control over the optical property of the medium. Next, we will show how this atomic coherence is created and manipulated using the density matrix formalism.

The simplest nontrivial problem involving atom-field interaction is the coupling of a two level atom with a quasi-monochromatic radiation field. In nature, real two level atoms do not exist. A two level description is found to be useful in explaining phenomena where two levels involved are in resonance (or near resonance) with the external radiation field, while all other levels are highly detuned. In this two level atomic system, we will introduce certain realistic approximations which bring the problem to a tractable form.

Let $|1\rangle$ and $|2\rangle$ represent the excited and ground states of the atom as shown in Fig (1.2). The respective eigenvaules of the states $|1\rangle$ and $|2\rangle$ are $\hbar\omega_1$ and $\hbar\omega_2$ for the unperturbed Hamiltonian $\mathcal{H}_0$. By using the completeness relation $|1\rangle\langle 1| + |2\rangle\langle 2| = 1$, we write the Hamiltonian $\mathcal{H}_0$

$$\mathcal{H}_0 = \hbar\omega_1|1\rangle\langle 1| + \hbar\omega_2|2\rangle\langle 2| \tag{1.34}$$

and the wave function in the Schrödinger picture is as fellow:

$$|\psi\rangle = C_1|1\rangle + C_2|2\rangle, \tag{1.35}$$

where C_i $(i = 1, 2)$ is the probability amplitude of being in a state $|i\rangle$. Then the density

matrix operator is defined as the projector $\rho = |\psi\rangle\langle\psi|$, which is given by in matrix form as

$$\begin{pmatrix} \rho_{11} & \rho_{12} \\ \rho_{21} & \rho_{22} \end{pmatrix} \tag{1.36}$$

where the matrix elements are given by

$$\rho_{11} = C_1 C_1^*, \text{ probability of being in upper level} \tag{1.37a}$$

$$\rho_{22} = C_2 C_2^*, \text{ probability of being in lower level} \tag{1.37b}$$

$$\rho_{12} = \rho_{21}^* = C_1 C_2^*, \quad \text{atomic coherence} \tag{1.37c}$$

An atomic coherence depends on the phase difference between C_1 and C_2. These can be related to the macroscopic property of the atomic medium. The dipole moment operator can be written as

$$\vec{d} = \vec{d}_{12}|1\rangle\langle 2| + \vec{d}_{21}|2\rangle\langle 1| \tag{1.38}$$

where the diagonal element $\vec{d}_{11}$ and $\vec{d}_{22}$ are zero as the dipole operator $\vec{d}$ has odd parity. Therefore, the elements of the dipole operator $\vec{d}$ will be non zero if and only if the states $|1\rangle$ and $|2\rangle$ have different parity. The two level atomic system is driven by a plane monochromatic laser field

$$\vec{E} = \hat{e}\mathcal{E}_0 e^{-i(\omega t - \vec{k}.\vec{r})} + \text{c.}c., \tag{1.39}$$

where $\hat{e}$ and $\mathcal{E}_0$ are respectively the direction of polarization and constant amplitude for the continuous wave (cw) respectively. The carrier frequency ω of the cw is very close to the atomic transition frequency, ω_{12}, $(= \omega_1 - \omega_2)$ of the two level atomic system and is highly detuned with all other levels. The interaction Hamiltonian of the two level atom in the dipole moment approximation can be written as :

$$\begin{aligned} \mathcal{H}_I &= -\vec{d}\cdot\vec{E} \\ &= -(\vec{d}_{12}|1\rangle\langle 2| + \vec{d}_{21}|2\rangle\langle 1|)\cdot\vec{E}. \end{aligned} \tag{1.40}$$

Therefore the total Hamiltonian of the atom is given by

$$\mathcal{H} = \hbar\omega_{12}|1\rangle\langle 1| - (\vec{d}_{12}|1\rangle\langle 2| + \vec{d}_{21}|2\rangle\langle 1|)\cdot\vec{E}, \tag{1.41}$$

where the energy of the ground state level $|2\rangle$ is taken to be zero. We now make use of the unitary transformation :

$$|\psi(t)\rangle = e^{-i\omega|1\rangle\langle 1|t}|\phi(t)\rangle; \tag{1.42}$$

to write the Schrödinger equation written as

$$i\hbar\frac{\partial|\phi(\vec{r},t)\rangle}{\partial t} = \mathcal{H}_{eff}|\phi(t)\rangle. \tag{1.43}$$

Here the effective Hamiltonian is

$$\mathcal{H}_{eff}/\hbar = -\Delta|1\rangle\langle 1| - (G|1\rangle\langle 2| + \mathrm{h.c.}) - (\mathrm{G^{'}e^{-2i\omega t}}|1\rangle\langle 2| + \mathrm{h.c.}), \tag{1.44}$$

where $\Delta = \omega - \omega_{12}$, is the detuning of the control field from the atomic transition frequency. The coupling strengths G and $G^{'}$ are given by

$$G = \frac{\vec{d}_{12}\cdot\vec{\mathcal{E}}_0}{\hbar}e^{i\vec{\mathrm{k}}\cdot\vec{r}}, \quad G^{'} = \frac{\vec{d}_{12}\cdot\vec{\mathcal{E}}_0}{\hbar}e^{-i\vec{\mathrm{k}}\cdot\vec{r}} \tag{1.45}$$

It should be noted that the effective Hamiltonian contains d.c terms; $-\Delta|1\rangle\langle 1| - (G|1\rangle\langle 2| + G^{*}|2\rangle\langle 1|)$ and a highly oscillating term (oscillating at frequency $2\omega_c$) related to $G^{'}$. The value of $G^{'}$ becomes important only when $G^{'} \approx \omega$. Therefore, the term $G^{'}$ can be neglected at optical frequency domain where $G^{'} \ll 2\omega$. This approximation is known as the *rotating wave approximation* (RWA) which is used frequently in this thesis [10]. Therefore, the effective Hamiltonian becomes

$$\mathcal{H}_{eff}/\hbar = -\Delta|1\rangle\langle 1| - (G|1\rangle\langle 2| + G^{*}|2\rangle\langle 1|). \tag{1.46}$$

In writing Eq. (1.46) the RWA has been made to remove the explicit time dependence of $\mathcal{H}_{eff}$. The coupling strength $2G$ is called the Rabi frequency [11]. To obtain the dynamics of the density matrix equation using the Liouville equation [1]:

$$\dot{\rho} = -\frac{i}{\hbar}[H_{eff},\rho]. \tag{1.47}$$

The dynamics of population and polarization of the atoms in the two-level configuration is given by

$$\dot{\rho}_{11} = -\dot{\rho}_{22} = iG\rho_{21} - iG^{*}\rho_{12}, \tag{1.48a}$$

$$\dot{\rho}_{12} = \dot{\rho}^{*}_{21} = i\Delta\rho_{12} + iG(\rho_{22} - \rho_{11}), \tag{1.48b}$$

where dot denotes $\partial/\partial t$. The density-matrix elements in the original frame are given by $\rho_{12}e^{-i\omega t}, \rho_{11}$, and ρ_{22}. These equations are known as the optical Bloch equations (OBE),

[1] The Liouville equation is a more general compared to the Schrödinger equation because it has both satistical and quantum mechanical information of the system

in analogy to the Bloch equations in nuclear magnetic resonance. Note that $\dot{\rho}_{11} = -\dot{\rho}_{22}$, in accordance with the requirement of a closed two-level system [2], where the total population is conserved ($\rho_{11}+\rho_{22} = 1$). Let us assume that initially all the atoms are in the ground state $|2\rangle$ and thus $\rho_{22}(0) = 1$ with all other density-matrix elements beings zero. The solutions for the atomic population and atomic polarization can be obtained by solving the set of density matrix equations (1.48) and can be written as

$$\rho_{22} = \cos^2\left(\frac{\Omega t}{2}\right) + \frac{\Delta^2}{\Omega^2}\sin^2\left(\frac{\Omega t}{2}\right) \tag{1.49}$$

$$\rho_{12} = \frac{2G}{\Omega^2}\sin\left(\frac{\Omega t}{2}\right)\left\{\Delta\sin\left(\frac{\Omega t}{2}\right) + i\Omega\cos\left(\frac{\Omega t}{2}\right)\right\} \tag{1.50}$$

where $\Omega = \sqrt{(\Delta^2 + 4|G|^2)}$ is called the generalized Rabi frequency. For the zero detuning case, with $\omega = \omega_{12}$, Eq. (1.49) reduces to

$$\rho_{22} = \cos^2\left(\frac{\Omega t}{2}\right); \tag{1.51}$$

the atom oscillates symmetrically between its ground and excited states with an angular frequency Ω. The increase in the detuning of the field results in the increase of the Rabi oscillation with a reduced amplitude. The two level atom interacting with a classical electromagnetic field has been beautifully discussed in the book by Allen and Eberly [5].

The above calculation does not include spontaneous emission. To include the same it is necessary to generalize these Bloch equations by inclusion of the effects of the spontaneous emission [12]. In the presence of spontaneous emission, the Bloch equations are modified to

$$\begin{aligned}
\dot{\rho}_{11} &= -2\gamma\rho_{11} + iG\rho_{21} - iG^*\rho_{12} \\
\dot{\rho}_{22} &= 2\gamma\rho_{11} - iG\rho_{21} + iG^*\rho_{12} \\
\dot{\rho}_{12} &= -[\gamma - i\Delta]\rho_{12} + iG(\rho_{22} - \rho_{11}) \\
\dot{\rho}_{21} &= -[\gamma + i\Delta]\rho_{12} + iG^*(\rho_{11} - \rho_{22})
\end{aligned} \tag{1.52}$$

where 2γ $(1/T_1)$ describes the decay rate of the atomic excited state $|1\rangle$ and γ $(1/T_2)$ is the decay rate of the atomic coherence. However, in cases where the collision between atoms play a significant role, the decay of the coherences and the populations are described by

[2] A driven system is said to be a closed system when the excited state decays only to the ground state. If the excited state decays not only to the ground state but also to the environment then the system is called an open system. For an open system the total population is not conserved

different decay parameters, and in those cases the parameters T_2 and T_1 are introduced to account for this difference. This will be discussed in chapter 4.

The solution of the above equations are no longer purely oscillatory, as in the cases of Eqs. (1.49) and (1.50). The system now settles down into a steady state after a sufficiently long time ($t \gg 1/\gamma$). Then all time derivatives in Eqs. (1.52) are set equal to zero; it is then reduced to linear algebraic equations. The simultaneous equations for steady state density matrix elements are readily solved to give

$$\begin{aligned} \rho_{11} &= \frac{|G|^2}{(\gamma^2+\Delta^2)+2|G|^2} \\ \rho_{12} &= \frac{iG(\gamma+i\Delta)}{(\gamma^2+\Delta^2)+2|G|^2}. \end{aligned} \tag{1.53}$$

The induced polarization, say at frequency ω, is expressed in terms of the non-diagonal elements of the density matrix ρ_{12} and ρ_{21}:

$$\vec{\mathcal{P}} \equiv \mathcal{N}\langle\vec{d}\rangle \equiv \mathcal{N}\mathrm{T}r(\vec{d}\rho) \equiv \mathcal{N}(\vec{d}_{21}\rho_{12} + \mathrm{h.}c.). \tag{1.54}$$

Here $\mathcal{N}$ is the atomic density of the medium. Using the steady state value of ρ_{12}, one can easily calculate the susceptibility of the medium

$$\chi = \frac{\mathcal{N}|d_{12}|^2}{\hbar}\frac{i(\gamma+i\Delta)}{(\gamma^2+\Delta^2)+2|G|^2} \tag{1.55}$$

This is no longer a linear susceptibility because the strength of the field $\mathcal{E}_0$ is contained in the quantity G that appears in the denominator. These contributions are related to the nonlinear susceptibility [13], which controls varieties of higher-order processes that occur in nonlinear optics. Note that the imaginary part of the above susceptibility, which gives the absorption profile of the medium, is of the Lorentzian type. The full width at half maximum (FWHM) of the Lorentzian profile is $\gamma_c = \sqrt{\gamma^2+2|G|^2}$. Therefore, the width depends on the intensity of the applied field as shown in Fig. (1.3)(red-long dashed). The additional contribution to the line width is known as *power or saturation broadening* . The linear susceptibility expression can be obtained from Eq. (1.55) after dropping the $2|G|^2$ term in the denominator:

$$\chi = \frac{\mathcal{N}|d_{12}|^2}{\hbar}\frac{i}{(\gamma-i\Delta)}. \tag{1.56}$$

In the presence of a weak field, Re $[\chi]$ has a standard dispersive line shape i.e., the dispersion is anomalous, Im $[\chi]$ has also a Lorentzian shaped with natural line-width 2γ as

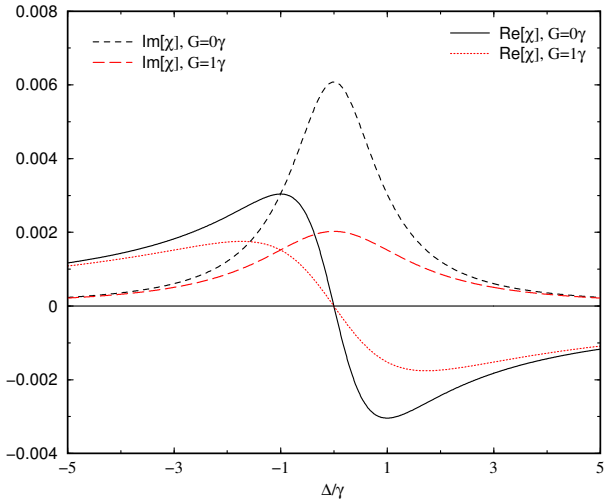

Figure 1.3: *Real* $[\chi]$ *and imaginary* $[\chi]$ *parts of the susceptibility of a two-level atom as a function of the atom-field detuning* $\Delta = \omega - \omega_{12}$ *in units of* γ *for two different field G=0,* 1γ*. The parameters of the above graph for* ^{87}*Rb vapor are chosen as density* $\mathcal{N} = 2 \times 10^{12}$ *atoms/cc,* $\gamma = 3\pi \times 10^6$ *rad/sec .*

shown in the Fig. (1.3) (black-dashed) . However, as can be seen from Fig. (1.3) for the case of a two-level system, in usual the medium the light pulses experience very large absorption in the vicinity of the sharp atomic resonance that prevents a clear observation of high anomalous dispersion. We next show that this susceptibility behavior can be drastically modified by applying an additional control field which will extend two level system to three level atomic configuration.

1.4 Control of Susceptibility in Multilevel Systems

The three level system interacting with two monochromatic fields is considered as a natural extension of the two level atomic system. The atomic coherence effects in a three level system are greatly enhanced compared to the two level system which can change the absorption and dispersion of the system drastically. Depending on the level structure and the dipole allowed transitions involved in the atom-field interaction, there are three types of three level configurations as shown in Fig (1.4). A strong field, coupling the states $|1\rangle$ and $|2\rangle$ at frequency ω_c, with the potential to modify the property of the system, is called the *control* field. A weak field at frequency ω_p used to couple $|1\rangle \longleftrightarrow |3\rangle$ is called a *probe* field which measures the changes of the atomic system due to the control field. The detuning Δ_c, Δ_p and the coupling constant $2g$ and $2G$ are defined by

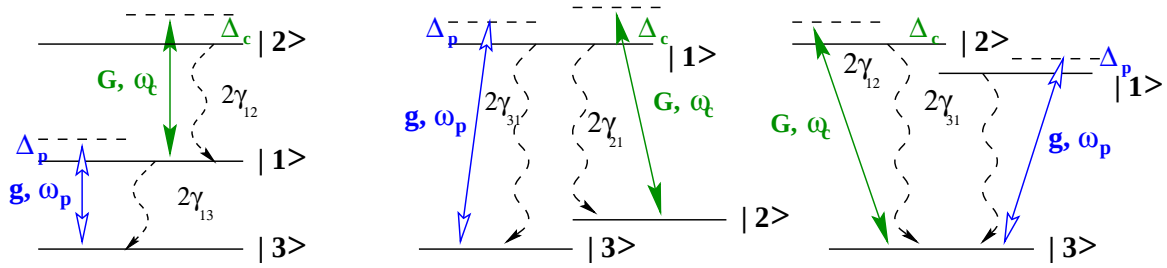

Figure 1.4: *Three possible configurations in three level atomic system with two laser fields of Rabi frequency* $2G$ *and* $2g$*:* Ξ*,* Λ*,* V*.*

$$\Delta_c = \omega_c - \omega_{12}\ ,\ \Delta_p = \omega_p - \omega_{13}\ ,\ 2g = \frac{2\vec{d}_{13}\cdot\vec{\mathcal{E}}_p}{\hbar}\ ,\ 2G = \frac{2\vec{d}_{12}\cdot\vec{\mathcal{E}}_c}{\hbar} \tag{1.57}$$

Here we will the concentrate on a Λ-system because it is a much more robust system than the other two systems. The reason behind robustness is that the two lower metastable states present in a Λ-system have longer life time. Most of the work of this thesis is concentrated on Λ-systems. The total Hamiltonian for a Λ-system is given by

$$\mathcal{H}/\hbar = \omega_{13}|1\rangle\langle 1| + \omega_{12}|2\rangle\langle 2| - \left(G|1\rangle\langle 2|e^{-i\omega_c t} + g|1\rangle\langle 2|e^{-i\omega_p t} + \text{h.}c.\right), \tag{1.58}$$

where the state $|3\rangle$ is considered as a ground state. Making a unitary transformation $|\Psi(t)\rangle = e^{[i\omega_p|1\rangle\langle 1|t + i(\omega_p-\omega_c)|2\rangle\langle 2|t]}|\psi(t)\rangle$ in the Schrödinger Eq. (1.23), the effective Hamiltonian under the RWA is given by

$$\mathcal{H}_{\text{eff}}/\hbar = -\Delta_p|1\rangle\langle 1| + (\Delta_c - \Delta_p)|2\rangle\langle 2| - (G|1\rangle\langle 2| + g|1\rangle\langle 3| + \text{h.}c.). \tag{1.59}$$

Using the Liouville equation, we obtain the corresponding density matrix equations:

$$\dot{\sigma}_{11} = iG\sigma_{21} + ig\sigma_{31} - iG^*\sigma_{12} - ig^*\sigma_{13} - 2(\gamma_{21}+\gamma_{31})\sigma_{11}\ , \tag{1.60a}$$

$$\dot{\sigma}_{22} = iG^*\sigma_{12} - iG\sigma_{21} + 2\gamma_{21}\sigma_{11}\ , \tag{1.60b}$$

$$\dot{\sigma}_{12} = -[\gamma_{21}+\gamma_{31} - i\Delta_p]\sigma_{12} + iG\sigma_{22} + ig\sigma_{32} - iG\sigma_{11}\ , \tag{1.60c}$$

$$\dot{\sigma}_{13} = -[\gamma_{21}+\gamma_{31} - i\Delta_c]\sigma_{13} + iG\sigma_{23} + ig\sigma_{33} - ig\sigma_{11}\ , \tag{1.60d}$$

$$\dot{\sigma}_{23} = -(\Gamma_{23} - i(\Delta_p - \Delta_c))\sigma_{23} + iG^*\sigma_{13} - ig\sigma_{21}\ , \tag{1.60e}$$

where the following transformations have been used

$$\rho_{13} = \sigma_{13}e^{-i\omega_p t},\ \ \rho_{23} = \sigma_{23}e^{-i(\omega_p-\omega_c)t},\ \ \rho_{12} = \sigma_{12}e^{-i\omega_c t}\ \text{ and }\ \rho_{ii} = \sigma_{ii} \tag{1.61}$$

Let the spontaneous emission rates from the states $|1\rangle$ to the state $|3\rangle$ and $|2\rangle$ be denoted by $2\gamma_{31}$ and $2\gamma_{21}$, respectively and Γ_{23} be the decay rate of the ground state atomic coherence

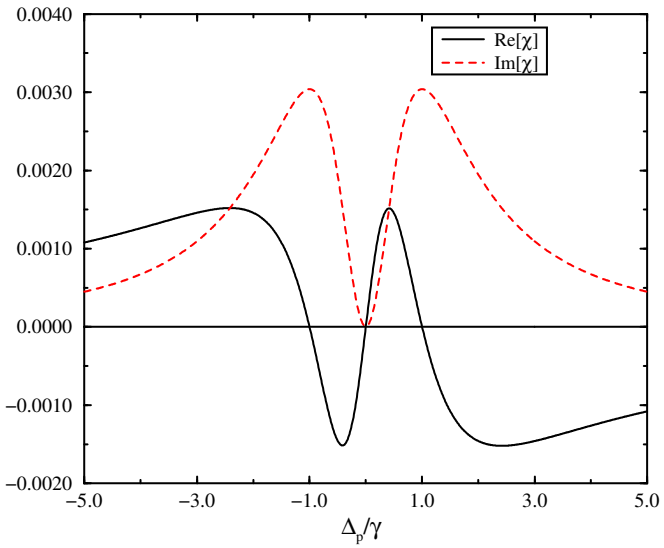

Figure 1.5: *Real* $[\chi]$ *and imaginary* $[\chi]$ *parts of the susceptibility versus the probe detuning* Δ_p/γ *for the three level* Λ*-system in the presence of control field. The parameters of the above graph for* ^{87}*Rb vapor are chosen as density* $\mathcal{N}= 2 \times 10^{12}$ *atoms/cc,* $G= 1\gamma$*,* $\Delta_c = 0$*,* $\Gamma_{23} = 0$*,* $\gamma = 3\pi \times 10^6$ *rad/sec .*

σ_{23}. The explicit expressions of the decay terms can be obtained by using the master equation approach [14]. All the three level configurations are equivalent unless the decay terms are included. In the absence of any field, we assume that the population is in the ground state $|3\rangle$. The induced atomic coherence by the probe field for the transition $|1\rangle \longleftrightarrow |3\rangle$ can be calculated to the lowest order in the probe field at steady state limit

$$\sigma_{13} = \frac{ig(\Gamma_{23} - i(\Delta_p - \Delta_c))}{|G|^2 + (\gamma_{21} + \gamma_{31} - i\Delta_p)(\Gamma_{23} - i(\Delta_p - \Delta_c))}. \tag{1.62}$$

From this equation, we obtain the susceptibility expression for the probe field by means of the polarization expression $\mathcal{P} = \mathcal{N} d_{13}\sigma_{13} = \chi E$, which yields

$$\chi = \frac{i\mathcal{N}|d_{13}|^2}{\hbar} \frac{1}{\frac{|G|^2}{(\Gamma_{23} - i(\Delta_p - \Delta_c))} + (2\gamma - i\Delta_p)}, \tag{1.63}$$

where $\gamma_{31} = \gamma_{21} = \gamma$ has been used. In the absence of the applied control field ($|G|^2 = 0$), the above expression gives the same result as in the two level system where the absorption is large as shown in Fig. (1.3). By applying a suitable control field, the absorption of the probe field by the medium can become zero as shown in the Fig .(1.5). This effect can be understood by using the quantum interference theory. It has been well known in quantum

mechanics from the time of Fano [15] that if states of atom are coupled via several possible alternative transition processes, interference between the amplitudes of these processes leads to either constructive or destructive interferences of the total transition probability. These effects arise because of probability amplitudes which can be either positive or negative in sign. This type of interference effect can be precisely found in the laser control of the atomic media. The external control field creates a new path for the electron to reach the same final state. For suitable field parameters, a destructive interference created by the external control field permits the propagation of a weak probe pulse through an opaque atomic medium. This phenomenon is know as *"Electromagnetically Induced Transparency"* (EIT).

The possibility of modifying the linear optical properties of the atomic medium using external auxiliary field was first demonstrated by Tewari and Agarwal [16] and much later by Harris and coworkers [17]. EIT was first coined to by Stevan Harris in his paper (1990) where the enhancement of nonlinear effects based on EIT was proposed [17]. EIT was demonstrated for the first time by Harris and his coworker in a Λ-system in strontium vapor [18]. This experiment showed that the transmittance of the weak probe field, which couples a ground state and an autoionising state, could be increased from e^{-20} (in the absence of a control field) to e^{-1} (in presence of a control field). The important point is that large increment in probe transmission is possible because of the presence of quantum interference as otherwise the transmittance would only have increased to e^{-7} due to the presence of strong saturating field. This implies that the observed phenomenon is not a sort of *hole-burning* or *saturation effect* [19, 20, 21, 22, 23], it is due purely to quantum interference phenomena. One could also imagine that if somehow the population of the ground probe level was removed then there would be a large transmission of the probe field. This is not a true realization of the experimental situation since the probe field is kept sufficiently weak to prevent significant population movement. The EIT can be observed even on the reduction of the Rabi frequency of the control field below the spontaneous decay rate of the common excited state so that there is no Aulter-Townes splitting [24]. This clearly demonstrates that the reduction of probe absorption at low intensity of the control field is possible due to the presence of quantum interference between the dressed states, and not due to the ac-stark shift of the atomic levels [25]. Many review articles on EIT exist in literature [26, 27, 28].

So far we have discussed that one can manipulate the required dispersive property of the medium by the application of coherent control fields of suitable intensity. Next, we will show that the precise control of the group velocity of the light pulse through the atomic medium can be obtained by manipulating the dispersive property of the medium.

1.5 Group Velocity and its Kinematics

Light pulses in a dispersive media are characterized by various velocities, which was first pointed out by Brillouin in his famous book; *Wave propagation and group velocity* [2]. For an absorptive, dispersive medium, he found it necessary to demarcate velocities into five different kinds:

the *phase* velocity, at which the zero-crossing of the carrier wave moves,
the *group* velocity, at which the peak of the envelope of a wave packet moves,
the *energy* velocity, at which energy is transported by the wave,
the *signal* velocity, at which the half-maximum wave amplitude moves, and
the *front* velocity, at which the first appearance of the discontinuity moves.

These five velocities can differ from each other in the anomalous dispersion region near the line center. The group velocity may be faster than c (in fact it may become infinite or even negative), but the energy and signal velocities are always less than c. In a normal dispersive medium, the last four mentioned velocities coincide and usually are less than the phase velocity.

In the first section we derive a basic equation that governs the propagation of optical pulses through the medium. We start with Maxwell's equation for the applied electric field E

$$\vec{\nabla}^2\vec{E} - \frac{1}{c^2}\frac{\partial^2\vec{E}}{\partial t^2} = \frac{4\pi}{c^2}\frac{\partial^2\vec{\mathcal{P}}}{\partial t^2}, \tag{1.64}$$

where induced polarization $\mathcal{P}$ is usually a complicated nonlinear function of E as in Eq. (1.9). In the linear case, however, induced macroscopic polarization $\mathcal{P}$ can be expressed in terms of susceptibility by the relation

$$\mathcal{P}(z,t) = \int_{-\infty}^{\infty} \chi(\omega)E(z,\omega)e^{-i\omega t}d\omega \tag{1.65}$$

where the electric field $E(z,\omega)$ and susceptibility $\chi(\omega)$ are related with $E(z,t)$ and $\chi(t-t')$

by Fourier transformations as given below:

$$E(z,t) = \int_{-\infty}^{\infty} E(z,\omega)e^{-i\omega t}d\omega \tag{1.66}$$

$$\chi(t-t') = \int_{-\infty}^{\infty} \chi(\omega)e^{-i\omega(t-t')}d\omega. \tag{1.67}$$

The susceptibility $\chi(\omega)$ can be expanded in Taylor series as

$$\chi(\omega) = \chi(\omega_0) + (\omega-\omega_0)\left[\frac{\partial\chi}{\partial\omega}\right]_{\omega_0} + \cdots \tag{1.68}$$

and we obtain the expression for the induced polarization (keeping terms only upto first order in $(\omega-\omega_0)$),

$$\mathcal{P}(z,t) = \left[\chi(\omega_0)\mathcal{E}_0(z,t) + i\frac{\partial\chi(\omega_0)}{\partial\omega}\frac{\partial\mathcal{E}_0}{\partial t}\right]e^{-i(\omega_0 t - k_0 z)}. \tag{1.69}$$

Substituting the expression for the field (1.66) and polarization (1.69) into the wave equation (1.64) and using the slowly varying envelope approximation, we can obtain the wave equation in a simplified form

$$\frac{\partial\mathcal{E}_0}{\partial z} + \frac{1}{c}\frac{\partial\mathcal{E}_0}{\partial t} = 2\pi i k_0\left[\chi(\omega_0)\mathcal{E}_0(z,t) + i\frac{\partial\chi(\omega_0)}{\partial\omega}\frac{\partial\mathcal{E}_0}{\partial t}\right]. \tag{1.70}$$

Subsequent rearrangement of the above equation gives

$$\frac{\partial\mathcal{E}_0}{\partial z} + \frac{1}{v_g}\frac{\partial\mathcal{E}_0}{\partial t} = 0, \tag{1.71}$$

where the group velocity of the light pulse is expressed as:

$$v_g \equiv \mathrm{Re}\frac{d\omega}{dk} = \mathrm{Re}\left[\frac{c}{1+2\pi\chi(\omega_0)+2\pi\omega_0\left.\frac{\partial\chi}{\partial\omega}\right|_{\omega_0}}\right]. \tag{1.72}$$

It is clear from the above group velocity expression that when the light pulses, propagate through the medium it has mastery over temporal dispersion of the refractive index given by

$$n(\omega) = \sqrt{1+4\pi\chi(\omega)}, \tag{1.73}$$

where $\chi(\omega)$ is the complex susceptibility of the medium. The real part of the susceptibility (denoted as χ') gives the dispersive nature of the medium, while the imaginary part (denoted as χ'') leads to the absorption by medium. In our expression of group velocity Eq. (1.72), we have assumed absorption or gain of the medium to be very small. Otherwise

the group velocity loses its own identity as strong absorption prevents the propagation of light through the medium. The third term in denominator of Eq. (1.72) is due to frequency dispersion and v_g can be expressed as

$$v_g = \mathrm{R}e\left[\frac{c}{1+2\pi\chi(\omega_0)+2\pi\omega_0\left.\frac{\partial\chi}{\partial\omega}\right|_{\omega_0}}\right] = \mathrm{R}e\left[\frac{c}{n_g}\right], \tag{1.74}$$

where group index $n_g = n + \omega\,\partial n/\partial\omega$. Note that the group index (n_g) is totally different from the refractive index n of the medium. The control of group velocity of the light pulses through the material medium is possible by two distinct ways as inferred from Eq. (1.72).

First, one can change the group velocity by enhancing of the refractive index $n \gg 1$. In general, the index of refraction, n can be made large by working in the neighborhood of an optical resonance. Usual dispersion-absorption relations tell us that the absorption of the light pulses will be large at the same detuning at which the resonant refractive index is large. Naturally, an important question is whether it is possible to make large refractive index associated with very small absorption at resonance condition. It was demonstrated that vanishing absorption can be achieved when the atoms are prepared in coherent superposition states called "phaseonium" [29]. In a "phaseonium" gas without population in the excited states, the zero absorption is always accompanied by vanishing refractive index. However, with a small population in the excited states, absorption vanishes at slightly off resonance, where the refractive index has a non zero value. This is the idea to get a large refractive index in a nonabsorbing medium [30, 31, 32, 33, 34, 35]

The second way of changing group velocity is to change the slope of the temporal dispersion $\partial n/\partial\omega$. For normal dispersive medium; $\partial n/\partial\omega > 0$ it leads to light propagating through the medium with *subluminal* velocity (light traveling slower in the medium than in vacuum). For the case of anomalous dispersion: $\partial n/\partial\omega < 0$ implies that $n + \partial n/\partial\omega < 1$. This results in light pulse propagation at a *superluminal* velocity (light traveling at a velocity faster than in the vacuum). One example of this case is $v_g = \infty$ when the condition of $n + \partial n/\partial\omega = 0$ is satisfied. This corresponds a rare situation; here the response of the medium to the applied field is local.

All these indicate that the precise control of the velocity of the light pulses through the medium is made possible by manipulating its dispersive property. As mentioned in an earlier section, one can manipulate the dispersive property of the medium by applying the

control field. Therefore, the external control fields act as key tools for precise control of the group velocity of light pulses through the atomic medium.

1.6 Subluminal Pulse Propagation

Two level atomic system is able to slow light pulse propagation. However, two level atomic systems show large absorption, which prevents the propagation of pulse inside the medium. One can get rid of this large absorption by using a very strong field which takes the medium into a saturating condition. Using this technique, Mossberg observed a group velocity of c/60 [36]. McCall and Hahn demonstrated that light pulses energies of a certain profile (called Π- pulses) can be transmitted even through strongly absorbing two level medium without any change in its shape and energy [37]. In this case, the leading edge of the pulse is absorbed producing inversion in the medium. This inversion amplifies the trailing part of the pulse and thus the energy is conserved for the pulse. This phenomenon is called *self induced transparency* (SIT) [38, 39, 40]. The absorption of leading edge and amplification of trailing edge results in a delay and thus light pulses move with a slower velocity as compared to free space. Note that the pulse duration is much shorter than the inverse of the homogeneous linewidth. The experimentally observed lowest group velocity for SIT is about $c/10^4$ [41, 42, 43]. Recently, Bennink *et al.* have predicted that a simple two-level system driven by a strong control field can display a very sharp normal dispersion which leads to dramatically reduce the value of the group velocity [44].

In a multilevel system *i.e.*, a system with more than two levels, coherent coupling of more than one transition can dramatically alter the group velocity. For a medium that can be modelled as a set of atoms with relevant energy level in Λ-configuration, the group velocity expression in Eq. (1.74) can be written as:

$$v_g = \frac{c}{1 + \frac{2\pi\omega_{13}\mathcal{N}|d_{13}|^2\left(G^2-\Gamma_{23}\right)}{\hbar\left(G^2+2\gamma\Gamma_{23}\right)^2}}, \tag{1.75}$$

where $\Delta_p = \Delta_c = 0$. For the intensity of the control field $|G|^2 \gg \gamma\Gamma_{23}$, the group index expression will be $n_g = \frac{2\pi\omega_{13}\mathcal{N}|d_{13}|^2}{\hbar|G|^2}$. This implies that group velocity of the light pulse is very much sensitive to the intensity of the applied control field. For ultra slow group velocity one requires a large group index. This is made possible when the dephasing rate of the ground state atomic coherence is reduced significantly, thereby, narrowing the width

of the EIT window. The slope of the refractive index become very steep which results in the group velocity getting reduced to a very small value. Thus group velocity can be controlled using the coherent manipulation of dispersion.

In 1992, Harris *et al.* theoretically studied the EIT dispersive property, and found that there is a steep normal dispersion in the line center of the transparency window in which the group velocity of the light pulse can be slowed $[c/v_g = 250]$ [45]. From then on, researchers focused their attention on slowing down the light speed in highly dispersive EIT media. Min Xiao *et al.*, for the first time observed the normal dispersion slope corresponding to a group velocity $c/v_g = 13.2$ in the region of the transparency window in hot Rb vapour in a ladder configuration [46]. Soon thereafter, Kasapi *et al.* measured the subluminal group velocity of $c/v_g = 165$ in a 10 cm Pb vapor cell in EIT configuration [47]. Schmidt *et al.* measured simultaneously the absorption and dispersion in the vicinity of an EIT resonance in a cesium vapor cell. They found steep dispersion corresponding to group velocity of $c/v_g = 3000$, associated with low absorption [48]. The light pulse can propagate with extremely slow group velocity in three level Λ-systems at two photon Raman resonance condition [49]. Paspalakis and Knight have shown how the group velocity of the probe pulse can also be controlled in a multilevel EIT system [50]. Slow light has also been observed in far-off-resonance Raman systems [51].

Electromagnetically induced transparency in a Bose-Einstein condensate is an excellent environment for studying the ultra slow group velocity of light pulses. By using this technique, Hau and her coworkers demonstrated the ultra slow group velocities of 17 m/s in an ultra cold gas of sodium atoms. In ultra cold atoms, extremely narrow transparency dip due to quantum interference can be induced by using very low intensity of the control field. A very rapid variation in the refractive index is present at the line center of the low absorption region. This steep slope together with high density ultra cold atoms leads to ultra-slow group velocity [52]. A model was proposed by Morigi and Agarwal to explain the temperature dependence of the group velocity as observed by Hau *et al.* in a Bose-Einstein condensate [53]. Kash *et al.* have reported ultra-slow light in coherently driven hot Rb atoms. By a suitable choice of experimental parameters such as the control field intensity and atomic density, a group velocity of 90 m/s was observed [54]. Budker *et al.* performed the ultra-slow group velocity experiment on rubidium vapor in a cell with anti-relaxation parafin wall coating [55]. This coating suppresses inelastic collisions of atoms

with the walls of the vapour cell. They observed the group delay of 13 ms, corresponding to 8 m/s group velocity of light. However, the density of the Rb atoms in such experiment is modest i.e., $\sim 10^{12}$ atoms/cm^3. It is of considerable interest to produce ultra-slow light in solid state material, where the atomic density is a million times larger than in gases. Ultra-slow light in a solid state material like Pr^{3+} doped Y_2SiO_5 crystal at a cryogenic temperature was first demonstrated by Turukhin *et al.*. In their experiment, they were able to slow down the group velocity of light pulses to 45 m/s [56]. Bigelow *et al.* demonstrated the propagation of ultra-slow light with a velocity 57.5 m/s in a ruby crystal at room temperature [57].

Ultra-slow light offers many newer applications in quantum and non-linear optics. A very interesting and exciting application of ultra-slow light in optical "black hole". This idea was put forward by Leonhardt and Piwnicki [58, 59, 60]. They pointed out that for a highly dispersive medium, a vortex can create a long-range Aharonov-Bhom effect [61, 62, 63, 64] on incident light and at shorter ranges the vortex can behave like a black hole *i.e.,* as if the light is being trapped into the vortex in a way that matter is trapped into a black hole in space. Further, applications of slow light in moving media was demonstrated in nonlinear interactions at very low levels [65, 66]. Slow light has found application in quantum networks and quantum information processing. Quantum entanglement of slow photons [67], non-classical and entangled atomic ensembles [68], and quantum memories [69] are other interesting areas needing further research.

Freezing of Light

The ultimate control over the velocity of light pulse can be obtained by reducing the group velocity to zero. For a temporally dispersive medium, the minimum value of the group velocity is written as

$$v_g = \frac{2\pi\Gamma_{23}}{3\mathcal{N}\lambda^2} \tag{1.76}$$

when $G^2 \approx \gamma\Gamma_{23}$. The above equation implies that the group velocity attains its minimum value but it will never be equal to zero, since $\Gamma_{23} \neq 0$, which prevents the stoppage of light inside the medium. This is the main constraint of a temporally dispersive medium. One can overcome this limitation by considering the spatial as well as the temporal dispersion of the medium *i.e.,* by using the dependence of refractive index on the frequency ω_0 and wave vector $\vec{k}_0$. It has been shown both theoretically and experimentally how the control

fields can produce spatially varying refractive index profiles [70]. Therefore, the group velocity can be expressed in the following form

$$v_g \equiv \mathrm{R}e\frac{d\omega}{dk} = \mathrm{R}e\left[\frac{c\,(1-2\pi k_0\partial\chi/\partial k)}{1+2\pi\chi+2\pi\omega_0\partial\chi/\partial\omega}\right]. \tag{1.77}$$

This equation suggests that the stoppage of light is possible by making the numerator to zero instead of increasing the dominator to a very large value, which is rather impossible. This idea was proposed by Kocharovskaya *et al.* and they proved it in a coherently driven Doppler broadened atomic medium via EIT [71].

1.7 Storage and Retrieval of Light Pulses

Over the past couple of years, storage and retrieval of light pulses in an atomic medium, have received serious attention in the field of quantum information due to the fact that photons are the most suitable candidates to carry information. In general, photons are difficult to store and retrieve without any destruction. In this context, matter can be used to serve as the storage element of the light pulse. The faithful map of the quantum state of the light pulse onto matter with less dissipation is made feasible by using the technique of electromagnetically induced transparency. Accompanied with the transparency, is a drastic modification of the dispersive property of the medium. This modification can result in ultraslow velocity of light pulses which is the basic principle of the light storage technique.

Classical storage of optical information in time domain based on the phenomenon of photon echo experiments in two level systems [72] and multilevel media [73, 74], has a long history. However, in this promising technique for high capacity storage of classical optical information, the storage time is very short because of shorter transverse relaxation time. Storage time can be increased by using the stimulated photon echo combined with the long lifetime of the ground-state hyperfine levels [73, 75, 76]. Usually the photon echo technique does not provide complete information about the signal because the retrieved pulse has a different shape compared to the input pulse shape. Non-linear optical effects at low light levels [65, 77, 78] give rise to an opportunity to store and retrieve light pulse without loss of generality [79, 69, 80].

A weak probe pulse moves with a substantially reduced velocity in a EIT configured three-level Λ-system in the presence of control field. The propagation velocity of the weak

probe pulse is reduced very much due to the formation of a dark state polariton, which is a mixture of atomic coherence and the field. The characteristic of the dark polariton depends on the intensity of the control field. Dynamically reducing the intensity of the control field decelerates the polariton and this can effectively bring to halt the light pulse inside the medium. When this happens, the polariton develops a purely atomic character and the information about the weak probe pulse is mapped onto the atomic coherence. Therefore, the weak probe pulse can be stored inside an atomic ensemble in the form of atomic coherence. The atomic coherence can be transferred back to a input probe pulse by reaccelerating the polariton. The EIT Polaritons were first considered theoretically by Mazets and Matisov [81], and later by Fleischhauer and Lukin [69, 82] who proposed storage and retrieval of the weak probe pulses in an atomic medium by switching off the control field adiabatically. The role of adiabaticity for the light storage technique has been relaxed in the discussion of Matsko *et al.*. They have shown that almost perfect light storage is possible by using adiabatic as well as non-adiabatic switching of the control field [83]. Juzeliunas and Carmichael formulated a theory of slow EIT polaritons in BEC model with a Λ-configuration for storage and retrieval of laser pulse [84]. These effects have also been observed in a double Λ-system [85]. In the presence of the detunings of the weak probe pulse and control field, storage of light has also been investigated [86]. Storing and releasing light pulses can now be achieved in a gas of moving atoms by using a pair of stationary and spatially separated control fields, *i.e.*, there is no need to switch off and on a control field at precise times [87].

Using the EIT technique, Phillips *et al.* [88] have experimentally demonstrated a method of storage and retrieval of light pulses in a hot Rb vapour by changing the intensity of the control field. In their experiment, light can be stored inside the medium only upto ~ 0.5 ms due to the short lifetime of the atomic coherence. Almost at the same time, Hau *et al.* [89] have performed the light storage experiment in a laser cooled atomic sodium vapour near the temperature for Bose-Einstein condensation. Both experiments have been carried out with orthogonally polarized weak probe and control fields. Gao *et al.* have shown that the weak probe pulse with arbitrary polarization can be stored in a hot Rb vapour [90]. In a different development, Bajcsy *et al.* have been demonstrated that storage of light in a Rb vapour is possible via the simultaneous application of a pair of counter propagating control field. These two counter propagating control fields create a standing wave interference

pattern of dark and bright regions inside the medium. The bright regions of the standing wave pattern diminish the EIT, causing the atoms to absorb photons. But, by tuning the two control fields to make the bright region very narrow, one can force the region to reflect rather than absorb light pulse. This results in trapping of light pulse inside the medium. The trapped light can be retrieved only after one of the control beams is turned off and the properties of the released light will then depend on the remaining control field [91].

The released light can be modified in a controlled way by processing the atomic medium during the storage stage. On this issue, Zibrov *et al.* applied an additional control field which is scattered by the ground state Zeeman coherence and is released as a new field [92]. The property of the new field depends solely on the characteristics of the additional control field. Another successful experimental demonstration was made by Mair *et al.* regarding this issue. They applied an additional magnetic field during the light storage stage in order to change the phase of the atomic coherence which results in a phase shift of the retrieved pulse [93]. The effect of detuning in the light storage experiment has been reported experimentally (as well as theoretically) by Payne *et al.* [94, 95]. Recently, Hemmer and his coworkers reported the storage of light in solid state material at a cryogenic temperature [56]. Storage and retrieval of light will have profound implication in the area of quantum information processing [96, 97]. The possible application of the light storage technique to generate continuous beams of atoms in nonclassical or entangled quantum states has also been proposed [98]. Storage of light can fulfill the dream of creating superfast computers that manipulate the quantum states of light beams rather than the classical states of electrons as in today's computers. A comprehensive reviews of this subject have been carried out recently [99, 100, 101].

1.8 Superluminal Pulse Propagation

Sommerfeld and Brillouin first demonstrated that the group velocity of light pulses could exceed c in a media exhibiting anomalous dispersion near the absorption line center [102, 2]. In their classic paper, a rectangular shaped light pulse where the sharply vanishing amplitude of pulse gives rise to the front of the pulse was considered. Interestingly they found that the speed of the front of the pulse is equal to the speed of light in vacuum even in the case of anomalously dispersive region, where the group velocity $v_g > c$ or $v_g < 0$ and

the pulse gets sufficiently distorted. Much later, in 1969, a theoretical paper by Aharonov *et al.* pointed out the possibility of superluminal group velocities in a non-optical context which involve an unstable configuration and do not violate causality [103]. In 1966 Basov *et al.* first demonstrated that the group velocity of a laser pulse in an amplifier (population-inverted two level medium) could exceed c [104]. This phenomenon comes from the fact that the amplification of the front portion of the pulse leaves less gain available for the back portion, resulting in an advancement of the peak of the pulse. This advancement comes solely from the pulse reshaping process. In a subsequent paper, Icsevgi and Lamb [105] argued that Basov *et al.* [104] considered an unphysical input pulse extending to infinity at both ends resulting in an apparent violation of causality. Propagation of light pulses with group velocity v_g greater than speed of light c, which results from amplification, is now known as superluminal propagation [106, 107].

In 1970, Garrett and McCumber [108] made an important contribution towards superluminal propagation. They investigated theoretically the propagation of sufficiently smooth pulses, such as Gaussian pulses through either an amplifying or absorbing medium under the conditions that the pulse bandwidth is much smaller than the width of the absorption line and the medium is sufficiently short for distortion-free propagation. In 1981, Chu and Wong established the predictions of Garrett and McCumber [108] by measuring the transmission time of a resonant picosecond laser pulse in GaP:N [109]. Later, Segard and Macke [110] also confirmed experimentally (as well as numerically) the theoretical predications made by Garrett and McCumber [108]. They used millimeter wave pulses through a linear resonant molecular absorber and observed significant pulse advancement and negative group velocities with no pulse distortion.

The study on superluminal propagation has received considerable boost from the work of Raymond Y. Chiao and coworkers [111, 112, 113, 114, 115, 116, 117, 118, 119]. By using two closely spaced Raman gain lines which induces a transparenency in the anomalous dispersion region where the group velocity exceeds c without any significant pulse distortion was initially proposed by Steinberg and Chiao [115]. The idea of Chiao *et al.* has been experimentally verified by Wang and his coworkers [120, 121]. Wang *et al.* used two intense cw pumps with a slight frequency separation of 2 MHz. They were sufficiently detunned from a particular Zeeman component of the cesium resonance line to create the Raman gain doublet. These Raman gain doublet results in a lossless anomalous dispersion

region and therefore the group velocity of a pulse in this anomalous dispersion is greater than c and can even become negative while the shape of the pulse remains same. They measured a negative group velocity $v_g = -c/315$ which means that a light pulse propagating through atomic vapor cell exits early as compared to the propagation through the same length in free space. Therefore, the peak of the pulse leaves the cell before it enters. This counterintuitive phenomenon about light pulses is a consequence of classical interference between its different Fourier components in the anomalously dispersion region and does not violate causality [122].

Akulshin and his coworkers have demonstrated that extraordinarily steep anomalous dispersion can be obtained in two level atomic systems by using electromagnetically induced absorption [123, 124, 125]. They observed a value of anomalous dispersion corresponding to a negative group velocity $v_g \simeq -c/23000$ with large absorption. Steep anomalous dispersion in the absence of absorption has been shown both theoretically and experimentally in a two level atomic system strongly driven by a resonant pump [126, 127, 128, 129], for both weak and moderately strong probes [126]. The superluminal propagation of pulses has also been studied inside diffractive structures [130], photonic band gap materials [131, 132], active plasma medium [107, 133], and nonlinear coherent medium [134]. In a Raman scheme, Payne and Deng theoretically demonstrated how light pulse moves with superluminal velocity when two-photon detuning is large [49].

There have been a few attempts to realize both subluminal and superluminal pulse propagation in a single atomic system. Talukder *et al.* [135] have shown femtosecond laser pulses propagating from superluminal to subluminal velocities in an absorbing dye with change in dye concentrations. The group velocity of the weak pulse can be switched from subluminal to superluminal by manipulating the phases of the two weak optical fields applied to a V-shaped three level system [136]. Budker *et al.* demonstrated that propagation can be changed from subluminal to superluminal by using, say, a static magnetic field of the order of a few microgauss [55]. The experimental demonstration of the change of the group velocity from superluminal to subluminal can be obtained by changing the power of the coupling intensity in the single atomic transition [137]. Bigelow *et al.* have demonstrated that ultraslow and superluminal propagation can be obtained in the same solid state material at room temperature by changing the excitation wavelength [138].

Superluminal group velocity has restarted the debate about the definition of informa-

tion velocity. On this issue, Diener has clarified that the information velocity, *i.e.*, the speed of a point of non-analyticity, can never exceed in vacuum speed of light, not even in the case of superluminal group velocity [139, 140]. This preserves causality. The propagation pulse, consists of a few photons, through an anomalous dispersion media where quantum fluctuations in the photon numbers impose severe restrictions on the observation of superluminal phenomena [141, 142, 143]. Very recently, Stenner and his coworkers have experimentally shown that the time to detect information propagation through a gain assisted anomalous dispersive medium is slightly longer than the time required to detect the information travelling the same distance in vacuum, even though superluminal group velocity exceeds the speed of light c [144]. Many reviews on this superluminal propagation now exist in the literature [101, 145].

The possible application of superluminal light propagation can be found in optical communication, optical networks, opto-electronic devices and wave guides where smooth pulse are used. As we know, time synchronization of differently routed pulses decide the clock speed of computer chips. If different pulses are routed through different paths, they will arrive at different times at the final logic gate. Therefore, the time synchronization at final gate can be achieved by adding extra time delay to pulses arriving early. As a result, the clock speed of the computer chip becomes slower and it reduces the performance of computers. By using the principle of superluminality one can speed up the clock of a computer chip [146].

CHAPTER 2

From Subluminal to Superluminal Propagation

Light pulse travels at an enormous speed of 300,000 kilometers per second in vacuum. Recent research has established the possibility of controlling the speed of light in a medium by manipulating the dispersive property of the medium. It is well understood as to how the dispersion of a medium can be manipulated by the use of control laser fields which precisely controls the speed of the light pulses. When a well-defined light pulse of angular frequency, ω_1, propagates in a highly dispersive linear medium of optical refractive index $n(\omega_1)$, the light pulse propagates at a group velocity, given by

$$v_g = \frac{c}{n_g}, \tag{2.1}$$

where $n_g = n(\omega_1) + \partial n(\omega_1)/\partial\omega_1$ is the group-velocity index. We assume that the absorption or gain of the medium is very small *i.e.,* imaginary part of the refractive index, $n(\omega_1)$, vanishes. Group velocity is the velocity with which the peak of a light pulse propagates through the dispersive medium. The expression of Eq. (2.1) indicates that the functional form of the real part of the refractive index, $n(\omega_1)$, and its derivative, $\partial n(\omega_1)/\partial\omega_1$, determine the group velocity, v_g. In the normal dispersion region where the refractive index changes sharply and $\partial n(\omega_1)/\partial\omega_1 \gg 1$, the group velocity become subluminal i.e., $v_g < c$. Furthermore, it may be noted from Eq. (2.1) that for the anomalous region, where $\partial n(\omega_1)/\partial\omega_1 \ll 0$, the group velocity can be superluminal (e.g. $v_g > c, \infty$ or even -ve). A negative group velocity corresponds to the situation where the peak of the pulse arrives at the output end of the medium before it has entered the medium. In this chapter, we demonstrate how the application of the coupling field connecting two lower level

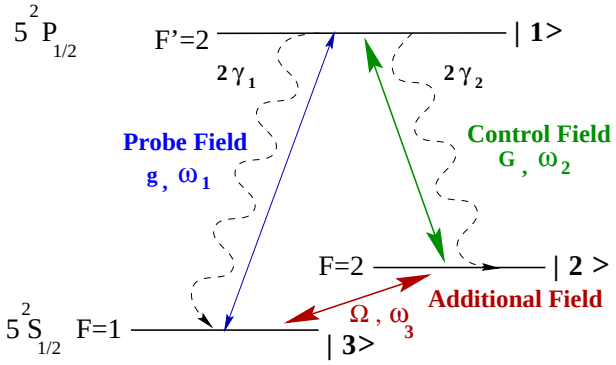

Figure 2.1: *Schematic diagram of three level Λ-system.*

metastable states of a Λ-system, allows one to change the dispersion at line center such that it can switch from normal to anomalous and again back to normal region. In particular, we show how the light pulse propagates with superluminal velocity through a gain assisted anomalous dispersive medium with very little pulse distortion. The distortion of the light pulse solely comes from the group velocity dispersion which will be discussed later. The effect of Doppler broadening on the group velocity calculation will also be discussed.

2.1 Model System and Its Basic Equations

The atomic system we investigate here is a Λ-shaped closed three level system as depicted in Fig (2.1). Here we define all fields as

$$\vec{E}(z,t) = \vec{\mathcal{E}}(z,t)\, e^{-i(\omega t - kz)} \; + \; c.c., \tag{2.2}$$

where $\vec{\mathcal{E}}$ is the slowly varying envelope of the field. We consider the propagation of a weak probe pulse whose central frequency ω_1 is close to the frequency of the atomic transition $|1\rangle \leftrightarrow |3\rangle$. we apply a control field on the optical transition $|1\rangle \leftrightarrow |2\rangle$. The transition $|2\rangle \leftrightarrow |3\rangle$ is generally an electric dipole forbidden transition. The states $|2\rangle$ and $|3\rangle$ are metastable states. An additional control field, referred to as lower level (LL) coupling field, acts on the transition $|2\rangle \leftrightarrow |3\rangle$. The application of lower level coupling field can produce regions in the optical response with an appropriate dispersion profile. The dispersion can change from normal to anomalous depending on the intensity of the lower level coupling field. The model of Λ atomic configuration can be found for example in energy levels of ^{87}Rb where the hyperfine levels $|5^2S_{1/2}; F = 1\rangle$ as $|3\rangle$, $|5^2S_{1/2}; F = 2\rangle$ as $|2\rangle$, and $|5^2P_{1/2}; F' = 2\rangle$

as $|1\rangle$ as shown in Fig. (2.1). The nature of LL field, which will couple to $|2\rangle(5^2S_{1/2}; F = 2)$ $\leftrightarrow |3\rangle$ $(5^2S_{1/2}; F = 1)$, depends on the level structure of the atom. The frequency difference between hyperfine levels $|5^2S_{1/2}; F = 1\rangle$ and $|5^2S_{1/2}; F = 2\rangle$ is 6.8 GHz which corresponds to the microwave field in the case of ^{87}Rb. It could be an infrared field in case of ^{208}Pb atom. Moreover, it could be a dc field if one is considering transparency with Zeeman sublevels. The total Hamiltonian for such a closed Λ-system coupled with the probe and control fields can be written as

$$\mathcal{H} = \hbar\omega_{_{13}}|1\rangle\langle 1| + \hbar\omega_{_{13}}|2\rangle\langle 2| - \hbar G e^{-i\omega_2 t}|1\rangle\langle 2| - \hbar\Omega e^{-i\omega_3 t}|2\rangle\langle 3| - \hbar g e^{-i\omega_1 t}|1\rangle\langle 3| + h.c., \quad (2.3)$$

where the Rabi frequencies $2g$, $2G$ and 2Ω are defined by

$$2g = \frac{2\vec{d}_{13}.\vec{\mathcal{E}}_p}{\hbar}, \;\; 2G = \frac{2\vec{d}_{12}.\vec{\mathcal{E}}_c}{\hbar}, \;\; 2\Omega = \frac{2\vec{\mu}_{23}.\vec{\mathcal{B}}}{\hbar}, \quad (2.4)$$

for the probe transition $|1\rangle \leftrightarrow |3\rangle$, the pump transition $|1\rangle \leftrightarrow |2\rangle$ and the additional coupling transition $|2\rangle \leftrightarrow |3\rangle$, respectively. The electric and magnetic dipole-matrix element are represented by $\vec{d}_{_{ij}}$ and $\vec{\mu}_{_{ij}}$, respectively. Note that magnetic dipoles are much weaker than electric dipoles this has serious implications for the power requirements of the LL coupling field. In writing Eq. (2.3), we have made RWA to neglect the rapidly oscillating term. The state $|1\rangle$ decays to the states $|3\rangle$ and $|2\rangle$ at the rates $2\gamma_1$ and $2\gamma_2$, respectively. For simplicity we ignore all collisional effects though they could be easily included. By making a unitary transformation from the density matrix ρ to σ via

$$\rho_{12} = \sigma_{12}e^{-i\omega_2 t} \;\; ; \;\; \rho_{13} = \sigma_{13}e^{-i(\omega_2+\omega_3)t} \;\; ; \;\; \rho_{23} = \sigma_{23}e^{-i\omega_3 t} \;\; , \quad (2.5)$$

we have the relevant density matrix equations

$$\begin{aligned}
\dot{\sigma}_{11} &= iG\sigma_{21} + ige^{-i\Delta_4 t}\sigma_{31} - iG^*\sigma_{12} - ig^*e^{i\Delta_4 t}\sigma_{13} - 2(\gamma_1+\gamma_2)\sigma_{11} \, , \\
\dot{\sigma}_{22} &= iG^*\sigma_{12} + i\Omega\sigma_{32} - iG\sigma_{21} - i\Omega^*\sigma_{23} + 2\gamma_2\sigma_{11} \, , \\
\dot{\sigma}_{12} &= -[\gamma_1+\gamma_2+\Gamma_{12} - i\Delta_2]\sigma_{12} + iG\sigma_{22} + ige^{-i\Delta_4 t}\sigma_{32} - iG\sigma_{11} - i\Omega^*\sigma_{13} \, , \\
\dot{\sigma}_{13} &= -[\gamma_1+\gamma_2+\Gamma_{13} - i(\Delta_2+\Delta_3)]\sigma_{13} + iG\sigma_{23} + ige^{-i\Delta_4 t}\sigma_{33} - ige^{-i\Delta_4 t}\sigma_{11} - i\Omega\sigma_{12} \, , \\
\dot{\sigma}_{23} &= -(\Gamma_{23} - i\Delta_3)\sigma_{23} + iG^*\sigma_{13} + i\Omega\sigma_{33} - ige^{-i\Delta_4 t}\sigma_{21} - i\Omega\sigma_{22} \, ,
\end{aligned} \quad (2.6)$$

with $\sigma^*_{ij} = \sigma_{ij}$ and $\sigma_{11} + \sigma_{22} + \sigma_{33} = 1$. Here Γ's give collisional dephasings, the detunings $\Delta_1, \; \Delta_2, \; \Delta_3$, and Δ_4 are defined by

$$\Delta_1 = \omega_1 - \omega_{13} \; ; \; \Delta_2 = \omega_2 - \omega_{12} \; ; \; \Delta_3 = \omega_3 - \omega_{23} \; ; \; \Delta_4 = \Delta_1 - \Delta_2 - \Delta_3 \;\; . \quad (2.7)$$

We are interested in calculating the group velocity of the probe pulse for transparent medium, i.e., systems, which have very low probe absorption or gain. The group velocity of the probe pulse is given by

$$v_g = \frac{c}{1 + 2\pi\chi_{13}^{'}(\omega_1) + 2\pi\omega_1 \frac{\partial\chi_{13}^{'}(\omega_1)}{\partial\omega_1}} \ , \tag{2.8}$$

where $\chi_{13}^{'}(\omega_1)$ is the real part of the probe susceptibility $\chi_{13}(\omega_1)$. We are working under conditions such that $Im[\chi_{13}(\omega_1)] = \chi_{13}^{''}(\omega_1) \approx 0$. The susceptibility $\chi_{13}(\omega_1)$ will depend strongly on the intensities and the frequencies of the control and the LL coupling field. The susceptibility χ_{13} can be obtained by considering the steady state solution of Eq. (2.6) to first order in the probe field on the transition $|1\rangle \leftrightarrow |3\rangle$. For this purpose we assume that $\gamma_1 = \gamma_2 = \gamma$ and write the solution as

$$\sigma = \sigma^0 \ + \ \frac{g}{\gamma} \, e^{-i\Delta_4 t} \, \sigma^+ \ + \ \frac{g^*}{\gamma} \, e^{i\Delta_4 t} \, \sigma^- + ... \tag{2.9}$$

The $13-$ element of σ^+ will yields the susceptibility at the frequency ω_1 which can be seen by combining Eqs. (2.5) and (2.9)

$$\chi_{13}(\omega_1) = \frac{\mathcal{N}|d_{13}|^2}{\hbar\gamma}\sigma_{13}^{+} \ , \tag{2.10}$$

where $\mathcal{N}$ is the density of atoms. The group velocity can be obtained by substituting Eq. (2.10) in Eq. (2.8). Another important quantity is time delay T_d with respect to propagation in the vacuum over the same distance is given by

$$T_d = L(\frac{1}{c} - \frac{1}{v_g}), \tag{2.11}$$

where L is the length of the medium. In presence of the LL coupling field it is difficult to obtain algebraically simple expressions for χ_{13}, however Eqs. (2.6) can be solved numerically in the steady state limit.

2.2 Numerical Results and Discussion

Here, we present a number of numerical results obtained from the study of the steady state response of the medium described in the above section. We have used the parameters for ^{87}Rb vapor with the natural decay rate of the excited state $|1\rangle$ ($\gamma = 3\pi \times 10^6$ rad/sec), the

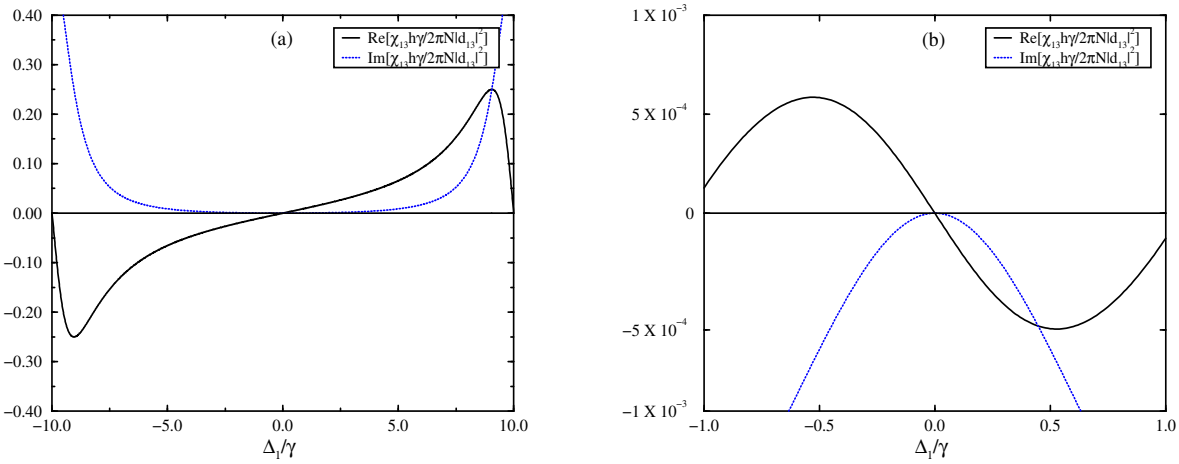

Figure 2.2: *(a) and (b) Real and imaginary parts of the susceptibility [Eq. (2.10) ; $\chi_{13}\hbar\gamma/\mathcal{N}|d_{13}|^2$] versus the probe detuning Δ_1/γ for the three level Λ-system in the presence of control field, for (a) LL coupling field $\Omega = 0$ and (b) LL coupling field $\Omega = 5\gamma$. The parameters of the above two graphs for ^{87}Rb vapor are chosen as density $\mathcal{N}= 2 \times 10^{12}$ atoms/cc, G= 10γ, $\Delta_2 = \Delta_3 = 0$, $\Gamma_{12} = \Gamma_{13} = \Gamma_{23} = 0$, $\gamma = 3\pi \times 10^6$ rad/sec .*

wavelength for the ground to excited state transition ($\lambda_1 = 7950\mathring{A}$), and density of atoms in the medium ($\mathcal{N}$ = 2×10^{12} atoms cm^{-3}). Fig. (2.2) shows the dispersive behavior of the medium in the absence and presence of the additional control field (LL), respectively. We plot absorption Im$[\chi_{13}\hbar\gamma/\mathcal{N}|d_{13}|^2]$ and refraction Re$[\chi_{13}\hbar\gamma/\mathcal{N}|d_{13}|^2]$ as a function of the dimensionless probe detuning Δ_1/γ. Fig. (2.2a) shows a normal dispersion accompanied with a transparency window (EIT window) in the absence of the LL coupling field i.e., $\Omega = 0$. The dispersion becomes zero at the line center $\Delta_1 = 0$, and its slope around this point is positive and steep. This can lead to the subluminal group velocity. The dispersion slope is very sensitive to the intensity of the control field. By suitable application of the LL coupling field, the dispersive nature of the medium can be modified dramatically. As shown in Fig. (2.2b), the real part of χ_{13} exhibits anomalous dispersion whereas the imaginary part of χ_{13} is fairly flat and negative, vanishing exactly at line center, i.e., $\Delta_1 = 0$. The anomalous dispersion along the negative flat region in the imaginary part of χ_{13} is especially fascinating for superluminal propagation. In the experiment of Wang *et al.* similar regions of χ_{13} were used to produce superluminal propagation [120]. To clarify further, we have plotted the group index n_g as a function of the intensity of LL coupling field. We notice from the Fig. (2.3), how the group index n_g changes from large positive values to

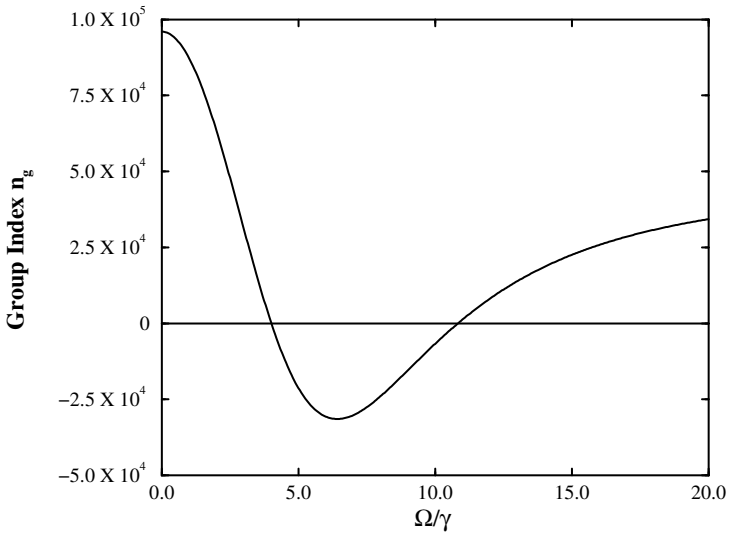

Figure 2.3: *Variation of group index with the Rabi frequency of LL coupling field. We have used the same parameters as in Fig. (2.2).*

large negative values and back to positive values as the intensity of the LL coupling field is increased. Thus, LL coupling field is like a knob which can be used to change light pulse propagation from subluminal to superluminal. We note that the production of superluminal propagation depends very much on the nature of the atomic transitions within the system under study and the choice of a large number of parameters such as the powers of the control and coupling fields. From our numerical results it is clear that we need a large coupling between $|2\rangle$ and $|3\rangle$. For a magnetic dipole transition between the states $|2\rangle$ and $|3\rangle$ the requirement of power of the LL coupling field is large and, in principle, this can be met by using pulsed fields with a pulse width $\gtrsim \mu$ sec. However, if $|2\rangle$ and $|3\rangle$ are chosen to be Zeeman levels, then the available dc magnetic field can be utilized to change propagation from subluminal to superluminal. Note that for ^{87}Rb, a Rabi frequency of 100γ implies a magnetic field of the order of 99.3 Gauss. Another possibility would be to consider an effective interaction between $|2\rangle$ and $|3\rangle$ via Raman transition using two other laser fields. The choice of the system is quite open and we have essentially shown the "in principle" possibility of subluminal to superluminal light propagation.

2.3 Distortion Free Superluminal Pulse Propagation

To verify the above result, we consider the propagation of a Gaussian shaped probe pulse through the transparent anomalous dispersing medium of length L. The envelope of the Gaussian pulse in the frequency domain is given by

$$\mathcal{E}_{in}(\omega) = \frac{\mathcal{E}_0}{\sqrt{\pi\Gamma^2}} \exp\left[-(\omega-\omega_0)^2/\Gamma^2\right], \tag{2.12}$$

where Γ is the spectral width of the pulse. In the time domain the Fourier counterpart can be written as

$$\mathcal{E}_{in}(z,t) = \int_{-\infty}^{\infty} d\omega \mathcal{E}_{in}(\omega) e^{-i(\omega t - kz)}. \tag{2.13}$$

Therefore, at the entrance point of the medium i.e., at $z = 0$, we can rewrite the above equation

$$\begin{aligned} \mathcal{E}_{in}(0,t) &= \int_{-\infty}^{\infty} d\omega \mathcal{E}_{in}(\omega) e^{-i\omega t} \\ &= \frac{\mathcal{E}_0}{2\pi} e^{-\frac{(t\ \Gamma)^2}{4}} e^{-i\omega_0 t}, \end{aligned} \tag{2.14}$$

where ω_0 is the carrier frequency of the light pulse. At the exit point of the medium, i.e., at $z = L$, the form of the output pulse is given by

$$\mathcal{E}_{out}(t) = \int_{-\infty}^{\infty} d\omega \mathcal{E}_{in}(\omega) e^{-i\left(\omega t - \frac{\omega L}{c} n(\omega)\right)} \tag{2.15}$$

The limited spectral bandwidth of the input pulse allows us to approximate $\omega n(\omega)$ by the first few terms of the Taylor series:

$$\begin{aligned} \omega n(\omega) &= \omega_0 n(\omega_0) + (\omega-\omega_0) \left.\frac{\partial(\omega n(\omega))}{\partial\omega}\right|_{\omega=\omega_0} + \frac{(\omega-\omega_0)^2}{2!} \left.\frac{\partial^2(\omega n(\omega))}{\partial\omega^2}\right|_{\omega=\omega_0} + \cdots \\ &= \omega_0 n(\omega_0) + (\omega-\omega_0) \left.\frac{c}{v_g}\right|_{\omega=\omega_0} + \frac{(\omega-\omega_0)^2}{2!} \left.\frac{\partial^2(\omega n(\omega))}{\partial\omega^2}\right|_{\omega=\omega_0} + \cdots \end{aligned} \tag{2.16}$$

where the expansion is carried out upto the quadratic term. Nonlinear term in the expansion of Eq. (2.16) are often associated with "group velocity dispersion" which causes pulse distortion. Thus after integration, we can obtain the output pulse

$$\mathcal{E}_{out}(t) = \frac{\mathcal{E}_0}{\sqrt{1-i\kappa L}} e^{-i\omega_0\{t-\frac{z}{c}-\frac{z}{c}n(\omega_0)\}} e^{-\frac{\left[\Gamma(t-L/v_g)\right]^2}{4(1-i\kappa L)}}, \tag{2.17}$$

with

$$\kappa = \frac{\Gamma^2}{2c}\left[\frac{\partial^2}{\partial\omega^2}(\omega n(\omega))\right]\Big|_{\omega=\omega_0} = \frac{\Gamma^2}{2c}\left[\frac{\partial^2}{\partial\omega^2}(\omega\left(1+2\pi\chi(\omega)\right))\right]\Big|_{\omega=\omega_0}. \tag{2.18}$$

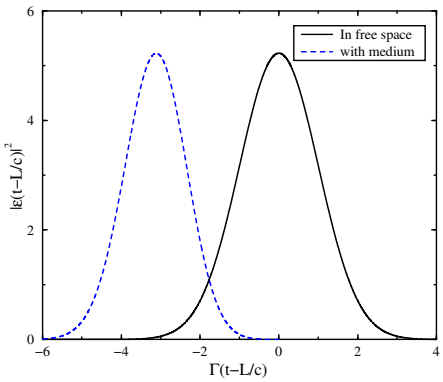

Figure 2.4: *The pulse is taken to have a central frequency in resonance with the transition* $|1\rangle \leftrightarrow |3\rangle$. *The solid curve of (d) shows light pulse propagating at speed* c *through 6 cm of vacuum. The dotted curve shows same light pulse propagation through* ^{87}*Rb vapour with density* 2×10^{12} *atom/cm*^{3} *of length 6 cm with a time delay* -4.39μ*sec in the presence of a LL coupling field with Rabi frequency* $\Omega = 5\gamma$. *The pulse width* Γ *is 120KHz. Other parameters are chosen as G=* 10γ, $\Delta_1 = \Delta_2 = \Delta_3 = 0$, $\Gamma_{12} = \Gamma_{13} = \Gamma_{23} = 0$, $\gamma = 3 \times \pi \times 10^6$ *rad/sec.*

where $\chi(\omega)$ is the complex susceptibility of the dilute atomic gas, such that $|4\pi\chi| \ll 1$. We are working in the region such that $\text{Im}[\chi(\omega_0)] \approx 0$, i.e., first exponential part of the Eq. (2.17) does not have any contribution on the amplitude reduction or gain. Therefore, the change in the amplitude and width of the pulse solely comes from the imaginary part of the group velocity dispersion. The broadening and narrowing of the pulse respectively depend on whether Im $[z\kappa] > 0$ or Im $[z\kappa] < 0$.

The effect of superluminality in course of the probe pulse propagation has been shown in Fig (2.4). In this Fig (2.4) we also show the pulse at the output in absence of the medium. The advancement of the pulse due to the superluminality medium is seen. The time delay of the probe pulse, calculated from the relative delay between the peak positions of the reference pulse and output pulse, is $-4.39\mu s$. This result is in very good agreement with the results of the Eq. (2.11). For our numerical simulation, we have considered 6 cm long ^{87}Rb atomic vapour at atomic density $\mathcal{N} = 2 \times 10^{12}$ atom/cm^3. We have used pulse width $\Gamma = 120$ KHz to avoid any severe absorption of the pulse and in order that it is well contained within the transparency window of the medium. We also note that the output pulse gets narrowed as compared to the input pulse. This narrowing is related to the second order of the susceptibility, i.e., the group velocity dispersion as discussed earlier.

Next, we have investigated the pulse width change factor (Im$[\kappa L]$). Fig. (2.5) depicts

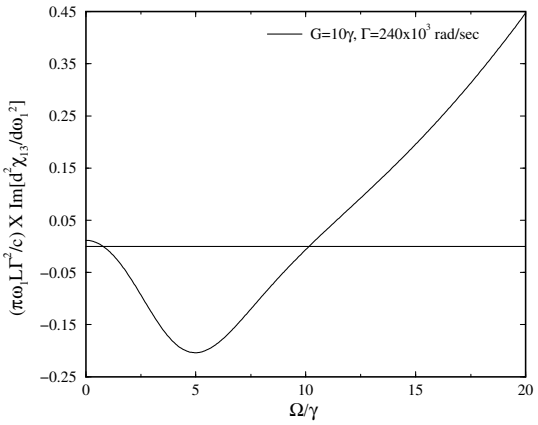

Figure 2.5: *Variation of the pulse width change factor Im$[\kappa L]$ with the Rabi frequency of the LL coupling field. We get narrowing of the pulse by ∼20.37% for the chosen parameters as in Fig. (2.4).*

the imaginary part of the group velocity dispersion as function of the intensity of the LL coupling field. The narrowing of the pulse as shown in the Fig. (2.4) is in conformity with the pulse width change factor Im$[\kappa L]$ by about 20% for the chosen parameters.

2.4 Doppler Effect on Group Index Calculation

In this section, we determine the influence of the Doppler broadening on the superluminal group velocity calculation. For a single atom, moving with a velocity v along the z-axis, the probe frequency $\omega_1(v)$ as seen by the atom, is given by

$$\omega_1(v) = \omega_1 \pm k_1 v \tag{2.19}$$

where the negative (positive) sign corresponds to co-propagating (counter - propagating) atom and probe respectively. In our model system we consider probe and control fields are copropagating with atom. Hence, the control field frequency $\omega_2(v)$ and LL coupling field frequency $\omega_3(v)$, as seen by the atom are given by

$$\omega_2(v) = \omega_2 - k_2 v, \quad \omega_3(v) = \omega_3 - k_3 v. \tag{2.20}$$

Note that the velocity dependence of the LL coupling field frequency ω_3 is insignificant and hence we can ignore it. The detunings of the probe and control fields from their respective transitions are given by

$$\delta_1(v) = \omega_1(v) - \omega_{13} = \Delta_1 - k_1 v, \;\; \delta_2(v) = \omega_2(v) - \omega_{12} = \Delta_2 - k_2 v. \tag{2.21}$$

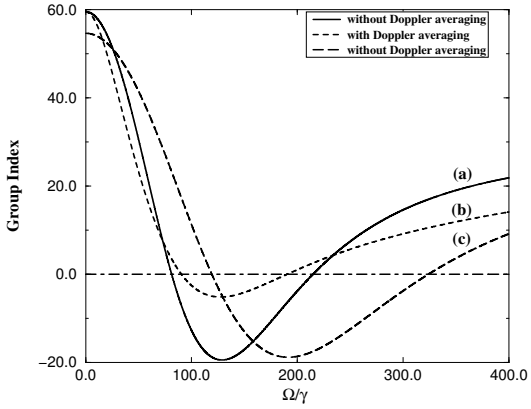

Figure 2.6: *Group index variation with the Rabi frequency of LL coupling field. The curves (a) and (b) are for propagation in Rubidium vapor with density* $\mathcal{N}= 2 \times 10^{12}$ *atoms/cc. Other parameters are chosen as* $G= 200\gamma$, $\Delta_1 = \Delta_2 = \Delta_3 = 0$, $\Gamma_{12} = \Gamma_{13} = \Gamma_{23} = 0$, $\gamma = 3 \times \pi \times 10^6$ *rad/sec. For curve (b) the Doppler width parameter* δ *is chosen as* 1.33×10^9 *rad/sec. Curve (c) shows variation of group index* n_g *with the Rabi frequency of LL coupling field in* ^{208}*Pb vapor with density* $\mathcal{N}= 2 \times 10^{14}$ *atoms/cc,* $G= 297\gamma$, $\Delta_1 = \Delta_2 = \Delta_3 = 0$, $\Gamma_{12} = \Gamma_{13} = \Gamma_{23} = 0$, $\gamma = 4.75 \times 10^7$ *rad/sec.*

For our numerical simulation, we can also set $k_1 \approx k_2$. For a Doppler broadened system, one needs to average n_g over the Maxwell-Boltzmann distribution for the atomic velocities, defined by

$$\mathrm{P}(k_1 v)d(k_1 v) = \frac{1}{\sqrt{2\pi \mathrm{D}^2}} e^{-(k_1 v)^2/2\mathrm{D}^2} d(k_1 v), \;\; \mathrm{D} = \sqrt{K_B T \omega_1^2 / M c^2}. \tag{2.22}$$

Therefore, the velocity distribution function for δ_1 is given by

$$\mathrm{P}(\delta_1) = \frac{1}{\sqrt{2\pi \mathrm{D}^2}} e^{-(\delta_1 - \Delta_1)^2/2\mathrm{D}^2} \tag{2.23}$$

where D is the width of Gaussian distribution which is dependent on the temperature, T, and atomic mass, M, for the relevant atomic transition. The group index, n_g, averaged over the Doppler distribution, is obtained from

$$\langle n_g \rangle = \int_{-\infty}^{\infty} n_g(\delta_1) P(\delta_1) d\delta_1 \tag{2.24}$$

In Fig. (2.6) we show the results for the group index with and without Doppler averaging. It is known from the work of Kash *et al.* [54] that Doppler broadening was insignificant in the behavior of the pulse propagation through a Λ-system in the presence of a control laser. However, the situation changes with the application of the LL coupling field at $|2\rangle \leftrightarrow |3\rangle$ transition (with a wavelength $\sim 1.3\mu m$) particularly in the region where the group index is negative. In Fig. (2.6), we also show the results for propagation in a much heavier ^{208}Pb

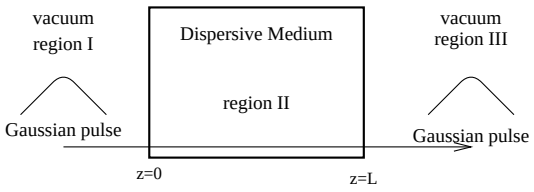

Figure 2.7: *Gaussian pulse propagation through a transparent anomalous dispersion medium of length L.*

vapor . This was the system used earlier by Kasapi *et al.* [47] to demonstrate subluminal propagation. The application of the LL coupling field can lead to the superluminal propagation. The results obtained in this case are not sensitive to Doppler broadening because the Doppler width parameter δ ($\cong 25\gamma$) is much smaller than the Rabi frequency G ($= 297\gamma$) of the pump.

2.5 Kinematics of Superluminal Light

We are using stationary phase method in order to understand the counter-intuitive phenomena of superluminal propagation. A smooth Gaussian pulse can propagate with superluminal velocity through a medium which has a gain-assisted linear anomalous dispersion. The medium extends from $z = 0$ to $z = L$ and is in vacuum as illustrated in Fig (2.7). The electric field of the propagating Gaussian pulse can be written as

$$\begin{aligned} \mathcal{E}_{out}(z,t) &= \int d\omega \mathcal{E}_{in}(\omega) e^{-i(\omega t - k(\omega)z)}; \quad k(\omega) = \frac{n(\omega)\omega}{c} \\ &= \int d\omega \mathcal{E}_{in}(\omega) e^{-i\phi(\omega)} \end{aligned} \tag{2.25}$$

where

$$\mathcal{E}_{in}(\omega) = \frac{\mathcal{E}_0}{\sqrt{\pi\Gamma^2}} \exp\left[-(\omega-\omega_0)^2/\Gamma^2\right], \tag{2.26}$$

and the spectral width Γ will decide how many Fourier components are involved in forming a Gaussian pulse. In a dispersive medium, the speed of each Fourier component of the pulse is determined by the refractive index at that frequency. All Fourier components appear in the medium as soon as the leading edge of the pulse touches the entrance point of the medium. It is not necessary for the peak of the pulse to appear at the entrance point of the medium because it does not carry new information which is not already present at its weak forward leading edge. From Eq. (2.25), one can find out the position z and time t at which all Fourier components are in same phase and interfere constructively to form

the peak of the pulse. All the points exhibit destructive interference to form weaker part of the pulse except the point satisfying the interference conditions. For a linear dispersive medium, the phase $\phi(\omega)$ of Eq. (2.25) can be expand by Taylor expansion

$$\phi(\omega) = \phi(\omega_0) + (\omega - \omega_0)\frac{d\phi}{d\omega}\bigg|_{\omega=\omega_0}. \tag{2.27}$$

The phase $\phi(\omega)$ becomes independent of ω when $d\phi/d\omega|_{\omega=\omega_0} = 0$. This is the condition of stationary phase method [122]. Let us define the *rephasing length* l of the medium

$$l = c\,\frac{d\phi}{d\omega}\bigg|_{\omega=\omega_0} = c\frac{d\left[\omega t - k(\omega)z\right]}{d\omega} = c\left(t - \frac{z}{v_g}\right) = 0. \tag{2.28}$$

where v_g is the group velocity of Gaussian pulse.

The superluminal phenomena can be well understood by examining the *rephasing length* l of the medium. The peak of the pulse arrives at the entry point of the medium at time $t = 0$. From Eq. (2.28), one can find

$$l_I = ct - z \qquad (z < 0) \tag{2.29}$$

$$l_{II} = ct - n_g z \qquad (0 < z < L) \tag{2.30}$$

$$l_{III} = ct + (1 - n_g)L - z \qquad (z > L) \tag{2.31}$$

Let us consider the situation $n_g < 0$ which corresponds to the negative group delay meaning that the peak of pulse arrives at the output end before it touches the entrance interface of the medium. At a time $t < 0$ before the peak of the pulse arrives at the entry point of the medium, the *rephasing length* l_{II} inside the medium becomes zero at a position $z_0 = ct/n_g$. Since group index n_g and t both are negative, the range of rephasing position is $0 < z_0 < L$. At the position $z_0 = ct/n_g$ the relative phase difference between different Fourier components vanishes and a peak of the pulse is reproduced due to constructive interference and localized near the exit point of the medium such that $0 > t > n_g L/c$. The exit pulse is formed long before the peak of the pulse enters the medium. As the incident pulse moves toward the entrance point of the medium at a later time t' such that $0 > t' > t$, the position of the rephasing point inside the medium $z_0' = ct/n_g$ decreases *i.e.*, $z_0' < z_0$ and hence the peak moves with negative velocity $-v_g$ inside the medium. At the time $t = 0$ the peak of incident pulse touches the entrance interface of the medium, at the same time reverse propagating pulse inside the medium also reaches the entry point and destructively interfere with the input pulse at the entrance point of the medium thereby suppressing the

input pulse propagation. In region III, the rephasing position can be obtained by putting Eq. (2.31) equal to zero. This gives rephasing position $z_0^{''} = L + ct - n_g L$. From rephasing condition, we have $0 > t > n_g L/c$, and hence rephasing position in the region III : $z_0^{''} > L$ (note that both $t, n_g < 0$). At a later time t' such that $0 > t' > t$, the rephasing position $z_0^{'''}$ in region III, the peak moves forward direction because $z_0^{'''} > z_0^{''}$.

An interesting situation arises when the group index $n_g = 0$ corresponds to infinite group velocity ($v_g = \infty$). In this case, we have zero transit time means that the peak of the pulse emerging from the medium occurs at same time as the peak of the pulse entering the medium. The *rephasing length* l_{II} becomes independent of position z *i.e.,* the relative phase difference between different Fourier components will remain same throughout the length of the medium. In region III, the leading edge of the pulse is formed at $z > L$ due to the phase difference between different components of the pulse are reproduced again. Therefore, the peak of the pulse simultaneously appear at the entrance and exit point of the medium for $n_g = 0$ case. Hence, superluminal propagation is a manifestation of the pulse rephasing phenomena that is already contained inside the medium.

2.6 Summary

In summary we have demonstrated how the Λ system can produce a variety of new results, as regard to light pulse propagation, if we apply an additional LL coupling field. In particular we have demonstrated how the application of the LL coupling can produce regions of anomalous dispersion with gain and how this results in superluminal propagation of a weak pulse of light. The advantageous feature of our model configuration is that subluminal as well as superluminal propagation can be achieved by changing the intensity of the LL coupling field, in the same configuration. We have shown that distortion free pulse propagation is possible only when the intensity of the LL coupling field is chosen suitably. The narrowing or broadening of the output pulse can be explained from the study of group velocity dispersion which is very much sensitive to the intensity of the LL coupling field. We have also shown that Doppler broadening is significant in the behavior of the superluminal pulse propagation through a Λ-system driven by the control and LL coupling field.

CHAPTER 3

Storage and Retrieval of Light Pulses

Storage of light can be achieved by electromagnetically induced transparency wherein an external control field switches the medium from opaque to transparent near an atomic resonance, thereby allowing the weak probe pulse to propagate without distortion in shape. Coherent interaction of control and probe pulses in a three level Λ-system creates atomic coherence between the ground states which can serve as storage element of the information of the probe pulse. A weak probe pulse moves with substantially reduced velocity due to the formation of dark state polariton, which is a combination of atomic coherence and the probe pulse, introduced by Fleishhauer and Lukin [88]. The relative weightage of the dark state polariton depends on the temporal shape of the control pulse. After the whole probe pulse has entered the medium, the control field is switched off, mapping the information of the probe pulse on to the atomic coherence. At that instant the dark state polariton has a purely atomic character and, therefore, the storage of probe pulse is possible inside the medium in the form of atomic coherence. Switching on the control pulse, the polariton starts acquiring the field character that eventually dominates. The storage and retrieval of weak pulses thus become possible. In this chapter, we discuss the possibility of storage and retrieval of the light pulse that are not necessarily weak in Λ configuration atomic systems. The spatio-temporal evolution of both control pulse and probe pulse becomes important when they are of comparable strengths. We use the adiabatic theory of Grobe *et al.* [147] to understand our numerical simulations on the storage and retrieval of light pulses at moderate powers. We also demonstrate that a robust way of storage and re-

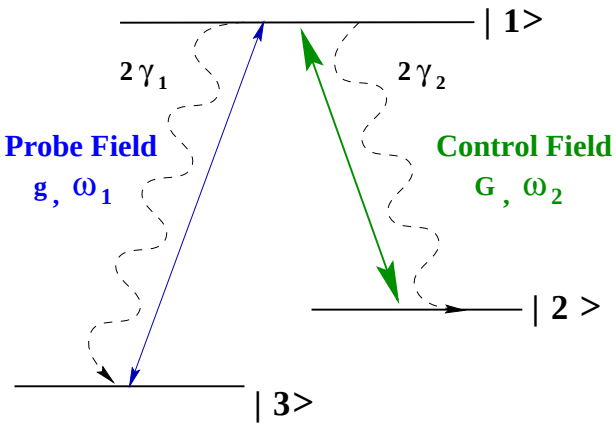

Figure 3.1: *Three-level Λ-type medium resonantly coupled to a control field with Rabi frequency $2G$ and probe field $2g$.*

trieval of information on frequency of the weak modulation signal is possible by applying suitable control pulse.

3.1 Dynamics of Pulse Propagation

The physical system under consideration is an isotropic homogeneous medium where relevant atomic transitions are taking in the Λ-configuration as shown in Fig. (3.1). Consider the propagation of a pulse (called probe) defined by the electric field

$$\vec{E}_p(z,t) = \vec{\mathcal{E}}_p(z,t)\, e^{-i(\omega_1 t - k_1 z)} \;+\; c.c. \tag{3.1}$$

Here $\vec{\mathcal{E}}_p$ is the slowly varying envelop of the probe field. We define a pump pulse by

$$\vec{E}_c(z,t) = \vec{\mathcal{E}}_c(z,t)\, e^{-i(\omega_2 t - k_2 z)} \;+\; c.c., \tag{3.2}$$

will act as a control on the propagation of the probe pulse. The probe pulse is tuned close to the transition $|1\rangle \longleftrightarrow |3\rangle$. The control field is tuned to the transition $|1\rangle \longleftrightarrow |2\rangle$. We further assume that the states $|2\rangle$ and $|3\rangle$ are metastable states. We work with the density matrix equations for the medium, taking into account the radiative decay of the excited state. For the case, when the fields are in resonance with their respective transitions, the semiclassical density matrix equations of motion under the rotating wave approximation

can be written as

$$\begin{aligned}
\dot{\rho}_{11} &= -2(\gamma_1+\gamma_2)\rho_{11} + iG\rho_{21} + ig\rho_{31} - iG^*\rho_{12} - ig^*\rho_{13}\ , \\
\dot{\rho}_{22} &= 2\gamma_2\rho_{11} + iG^*\rho_{12} - iG\rho_{21}\ , \\
\dot{\rho}_{12} &= -[\gamma_1+\gamma_2]\rho_{12} + iG\rho_{22} + ig\rho_{32} - iG\rho_{11}, \\
\dot{\rho}_{13} &= -[\gamma_1+\gamma_2]\rho_{13} + iG\rho_{23} + ig\rho_{33} - ig\rho_{11}, \\
\dot{\rho}_{23} &= iG^*\rho_{13} - ig\rho_{21}\ .
\end{aligned} \tag{3.3}$$

These Bloch equations are to be supplemented by the population conservation law

$$\rho_{11} + \rho_{22} + \rho_{33} = 1. \tag{3.4}$$

In original frame of reference, the density matrix elements are given by $\rho_{13}e^{-i\omega_1 t}$, $\rho_{12}e^{-i\omega_2 t}$, $\rho_{23}e^{-i(\omega_1-\omega_2)t}$, ρ_{11}, and ρ_{22}. The state $|1\rangle$ decay at rates $2\gamma_1$ $(2\gamma_2)$ to the state $|3\rangle$ $(|2\rangle)$, respectively. The Rabi frequency of the probe and control field $2g$ and $2G$ are related to the slowly varying amplitudes of $\mathcal{E}_p$ and $\mathcal{E}_c$ according to the relation

$$2g = \frac{2\vec{d}_{13}\cdot\vec{\mathcal{E}}_{\rm p}}{\hbar} \tag{3.5}$$

$$2G = \frac{2\vec{d}_{12}\cdot\vec{\mathcal{E}}_{\rm c}}{\hbar}, \tag{3.6}$$

where $\vec{d}_{ij}$ is the dipole matrix element corresponding to the atomic transitions. The atomic medium consists of a large number of atoms. The induced atomic polarization at frequency ω_1 will be obtained from off-diagonal matrix element ρ_{13}:

$$\vec{\mathcal{P}}_0 = \mathcal{N}\vec{d}_{31}\rho_{13} \tag{3.7}$$

where $\mathcal{N}$ is the density of the medium. It should be borne in mind that g and G are dependent on both space and time coordinates. Therefore, the polarization $\vec{\mathcal{P}}_0$ is also a slowly varying function of both space and time coordinates. We are using the Maxwell equations to obtain the spatiotemporal evolutions of both probe and control pulses through the medium. The Maxwell equations for the slowly varying amplitudes of $\vec{\mathcal{E}}_p$ and $\vec{\mathcal{E}}_c$ are given by

$$\begin{aligned}
\left(\frac{\partial}{\partial z} + \frac{1}{c}\frac{\partial}{\partial t}\right)\vec{\mathcal{E}}_p &= 2i\pi\mathcal{N}k_1\vec{d}_{31}\rho_{13} \\
\left(\frac{\partial}{\partial z} + \frac{1}{c}\frac{\partial}{\partial t}\right)\vec{\mathcal{E}}_c &= 2i\pi\mathcal{N}k_2\vec{d}_{21}\rho_{12}\ .
\end{aligned} \tag{3.8}$$

The above Maxwell equations can be expressed in terms of slowly varying Rabi frequencies as fellows:

$$\begin{aligned}\left(\frac{\partial}{\partial z}+\frac{1}{c}\frac{\partial}{\partial t}\right)g &= i\eta_p\rho_{13}; \quad \eta_p=\frac{2\pi\mathcal{N}k_1|d_{13}|^2}{\hbar}\\ \left(\frac{\partial}{\partial z}+\frac{1}{c}\frac{\partial}{\partial t}\right)G &= i\eta_c\rho_{12}; \quad \eta_c=\frac{2\pi\mathcal{N}k_2|d_{12}|^2}{\hbar}\,. \end{aligned} \tag{3.9}$$

For simplicity we will assume same coupling constant ($\eta_p \approx \eta_c = \eta$) for the two transitions *i.e.,* $\lambda_{12} \simeq \lambda_{13} \simeq \lambda$ and it has a form in Gaussian units,

$$\eta = 3\lambda^2\mathcal{N}\gamma/4\pi\,. \tag{3.10}$$

where we consider the same decay rates of different channel of excited state *i.e.,*$\gamma_1 = \gamma_2 = \gamma$. The solution of Eqs. (3.3) and (3.9) gives the complete spatiotemporal evolution of the atom-field system.

3.2 Numerical Simulations

Generally, the analytical solutions of the Maxwell-Bloch equation is very difficult except under very certain special approximation [148, 149]. Therefore, the study of pulse propagation inside the medium is only possible by the numerical simulation. In Appendix, we present a basic algorithm for solving the coupled Maxwell-Bloch equations numerically.

3.2.1 Pulse Propagation: Effect of Nonlinearities

We solve the propagation problem numerically for a homogeneously broadened gas of cold atoms in the travelling window frame of reference: $\tau = t - z/c$, $\zeta = z$. We consider initial probe pulses of two different shapes given by

$$g(0,\tau) = \begin{cases} g^0 e^{-\left(\frac{\tau-\tau_0}{\sigma}\right)^2} & \text{Gaussian pulse} \\ g^0[\mathrm{sech}(\frac{\tau-\tau_0}{\sigma}) + f \times \mathrm{sech}(\frac{\tau-\tau_1}{\sigma})] & \text{Sech pulse.} \end{cases}$$

Here, g^0 is the real constant characterizing the peak amplitude of the Rabi frequency before the pulse enter the homogeneous medium, σ is the temporal width of the input pulse and τ_i $(i = 0, 1)$ gives the location of peaks. All the atoms are initially in the state $|3\rangle$ and thus $\rho_{33}(\zeta, 0) = 1$, with all other density matrix elements equal to zero.

In order to appreciate the effect of nonlinearities due to the moderate power of the probe pulse, we first consider the control field as a continuous wave (cw) $G(0, \gamma\tau) \equiv \text{constant}$ $[(G/\gamma)^2 = 10]$. We work under the condition of electromagnetically induced transparency, i.e., $\omega_1 - \omega_2 = \omega_{13} - \omega_{12}$. Figs. 3.2(a), 3.2(b) [3.2(c), 3.2(d)] display the propagation of a Gaussian pulse (Sech combination pulse) inside the medium. From Figs. 3.2(a) and 3.2(c), we see that the weaker probe pulse would propagate without any significant absorption and broadening inside the medium. Figs. 3.2(b) and 3.2(d) show that the intense probe pulse suffers absorption and broadening. This is one of our key results. The shape of the pulse remains almost identical to the input pulse. This behavior of the intense probe pulse can be explained using the form of steady state probe absorption spectra. In Fig. 3.3, we show the behavior of the probe absorption as a function of the probe detuning when the control field is at resonance. It is clear from the Fig. (3.3) that, increase of the probe field intensity results in the increased absorption of the probe for a given frequency in the neighborhood of the frequency satisfying two photon resonance condition. Note that the width of the transparency window depends on the intensities of the control and probe fields. For a fixed intensity of the control field, the width of the transparency window becomes smaller when the probe field intensity is increased. Note that the condition for distortionless pulse propagation is that the spectral width of the probe pulse should be contained within the transparency window of the medium. If the pulse becomes too short, or its spectrum too broad relative to the transparency window of the medium, absorption and also the higher order dispersion need to be taken into account. The dispersion of the medium also causes the distortion of the probe pulse.

3.2.2 Storage and Retrieval of Electromagnetic Fields at Moderate Powers

Fleischhauer and Lukin [88] showed that it is possible to store and retrieve weak pulses of the electromagnetic radiation by using atomic coherences. They demonstrated how a control pulse and a probe pulse creates atomic coherence and that by slowly switching off the control pulse, the probe pulse disappears and gets stored in the form of atomic coherence. Switching on the control field can retrieve the stored probe pulse. The smooth switch off and on of the control field is made possible by gradually varying the intensity of the control field with respect to time. Therefore, the switching off and on of the control

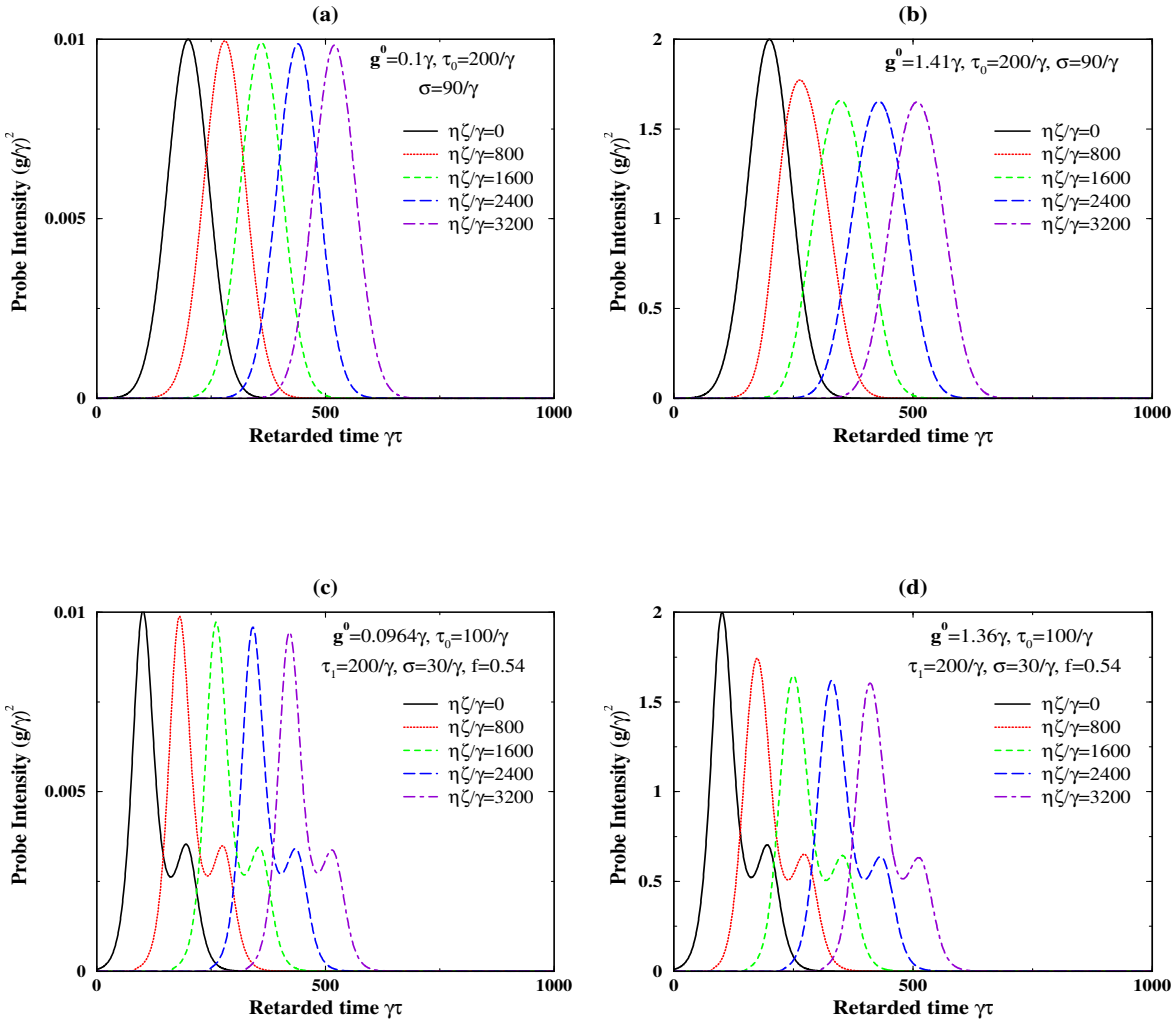

Figure 3.2: *The probe field intensity in the medium is plotted against retarded time at different propagation distances within the medium. Fig (a) and (c) show the probe pulse propagation with non-diminishing amplitude, for small intensities. Fig (b) and (d) depict the broadening and loss of intensity in case of an intense probe pulse. In all the cases, the control field is taken as a cw with* $G = 3.16\gamma$.

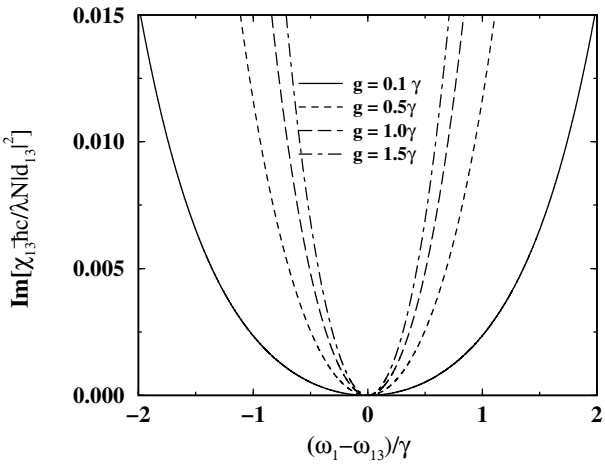

Figure 3.3: *Imaginary part of susceptibility* $[\chi_{13}\hbar c/N\lambda|d_{13}|^2]$ *as a function of probe frequency* ω_1 *in the presence of control field as a cw with* $\mathrm{G} = 3.16\gamma$. *The width of the transparency window decreases with increase in the intensity of the probe field.*

field can be modelled by a super-Gaussian shape given by

$$G(0,\tau) \;=\; G^0[1 \;-\; e^{-\left(\frac{\tau-\tau_2}{\sigma'}\right)^{\alpha}}], \tag{3.11}$$

where the parameter α determines how the pulse is switched on. For $\alpha = 4\ (100)$ we will have adiabatic (nonadiabatic) switching. Fig. (3.4) shows the adiabatic switching of the control field . Switching off of the control field can give rise to the absorption of the probe pulse when the entire probe pulse is inside the medium. The group velocity of the probe pulse is reduced to zero and its propagation is stopped by switching off the control field. The stored probe pulse can be retrieved by switching on the control field. The time difference between switching off and on is dependent on the life time of the atomic coherence between the state $|2\rangle$ and $|3\rangle$. As seen from Figs. (3.5(a)) and (3.5(c)), for weaker probe pulse, the shape of the retrieved pulse is same as the original one because the width of the probe pulse spectrum is very much less than width of the EIT window. Therefore, almost perfect storage and retrieval of light is possible by adiabatic switching of the control field as pointed out by Fleischhauer *et al.* [88]. When the probe field intensity is large, we observe from Figs. (3.5b) and (3.5d) ,that the retrieved probe pulse suffers absorption as well as broadening because of narrowing of the width of EIT window. Remarkably, the probe pulse can be retrieved even for a probe that is not necessarily weak. The switching off of the control field gives rise to a probe pulse that is stored inside the medium in form of atomic coherence ρ_{32}. Fig. (3.6) shows the behavior of the atomic coherence ρ_{32} as a

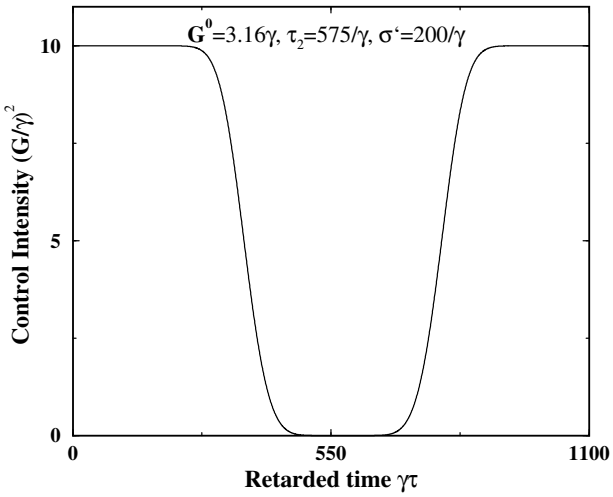

Figure 3.4: *The intensity of the control field as a function of retarded time at the entry surface of the medium at $\zeta = 0$. Switching mode of the super Gaussian control field is adiabatic.*

function of retarded time at different distances. The atomic coherence retains value that it attains before switching off. The atomic coherence starts generating the replica of the probe pulse at the moment the control field is switched on. Therefore, the atomic coherence is responsible for storage and retrieval of the probe pulse. In the presence of control field, the temporal shape of the atomic coherence ρ_{32} is same as the shape of the input probe pulse. A comparison of the Figs. (3.5(a)) and (3.6(a)) shows very close connection between the probe pulse at different points in the medium and atomic coherence. For example, for $\eta\zeta/\gamma = 3200$ and $\gamma\tau \ll 550$, the negligible amount of coherence leads to very little pulse power. Similar observations apply to the storage and retrieval of pulses at higher powers. On comparison of the Figs. 3.6a (3.6c) with 3.6b (3.6d) we find that the generated atomic coherence ρ_{32} is much more significant for larger values of the probe intensity. It is clear from Fig. (3.5), that the retrieval of intense probe pulse is possible at $\eta\zeta/\gamma = 3200$ which corresponds to the actual physical length of the medium $L = 2.13$ cm. Here, we have used the parameters for ^{87}Rb with spontaneous decay rate of the excited state $|1\rangle$ $2\gamma = 3\pi \times 10^6$ rad/sec, the wavelength for the ground state $|3\rangle$ to excited state $|1\rangle$ transition $\lambda = 795$ nm, density $\mathcal{N} = 10^{12}$ atom/cc.

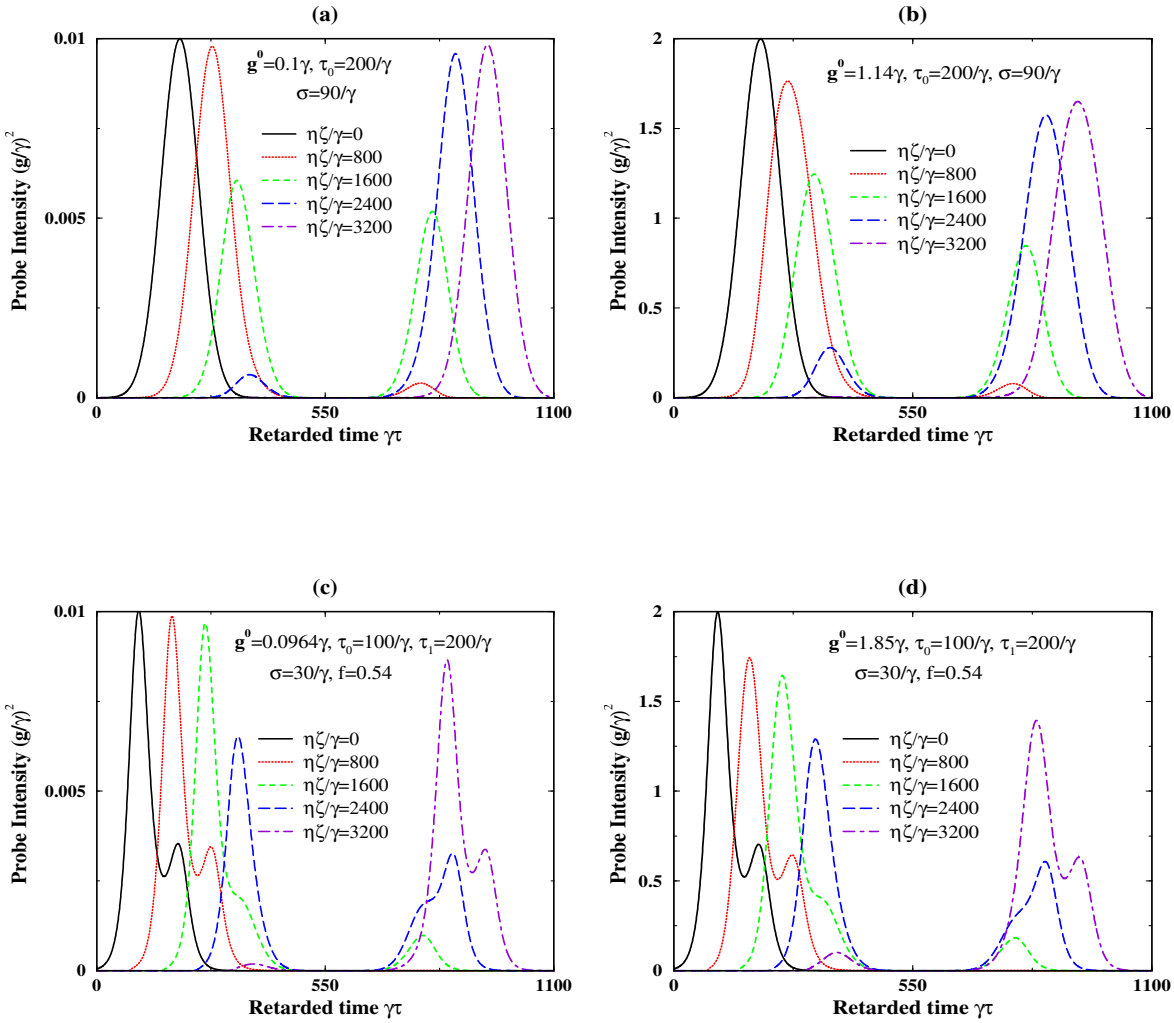

Figure 3.5: *The frames (b) and (d) show the time evolution of the weaker probe pulse at different propagation distances; and the frames (c) and (e) depict the time profile of the intense probe pulse at different propagation distances.*

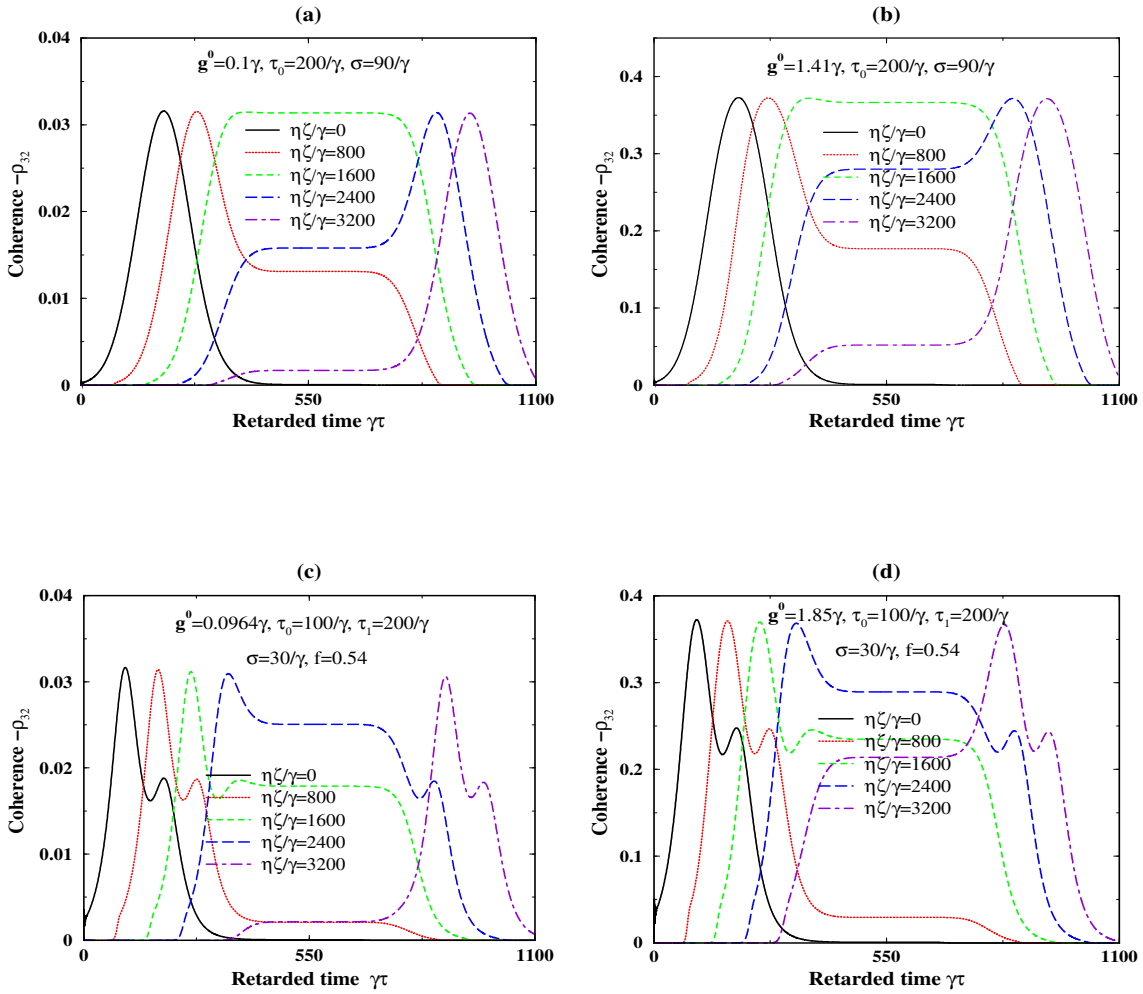

Figure 3.6: *Fig. (a)-(d) shows the temporal profile of atomic coherence $-\rho_{32}$ against retarded time at different propagation distances.*

3.2.3 Storage and Retrieval of Information on Modulating Signal

In communication engineering, the faithful reproduction of the frequency of the signal is a tremendous task. Generally, the signal can be sent as amplitude or frequency modulated carrier wave, where the amplitude or frequency of the carrier wave is modulated according to the frequency of the modulating signal. The modulation is necessary for long distance communication because of presence of environmental thermal noise which prevents the propagation of signal in free space. Therefore, the study of modulated wave in the context of storage and retrieval of information on frequency of the modulating signal becomes important in its own right. For this issue, we consider the propagation of the amplitude modulated Gaussian pulse acting as a initial probe pulse and define as

$$\mathcal{E}_p(0,\tau) = \mathcal{E}_p\left(1 + \frac{k_a\mathcal{E}_m}{\mathcal{E}_p}\cos\omega_m t\right) e^{-\left(\frac{\tau-\tau_0}{\sigma}\right)^2} \tag{3.12}$$

where $\mathcal{E}_m$ and ω_m are respectively the amplitude and frequency of the modulating signal $\mathcal{E}_m \cos\omega_m t$. In practice, ω_m is small compared to the carrier frequency ω_1 of the probe pulse. The modulating circuit determines the proportionality constant k_a. Hence the complete expression for the probe pulse in terms of the Rabi frequency is given by

$$g(0,\tau) = g^0(1 + m_a\cos\omega_m t)e^{-\left(\frac{\tau-\tau_0}{\sigma}\right)^2} \tag{3.13}$$

Here $m_a = k_a\mathcal{E}_m/\mathcal{E}_p$, is termed as the modulation index or the depth of modulation. It is defined as the ratio of the maximum deviation of the modulated probe pulse amplitude from the unmodulated value [150]. The storage and retrieval of the modulated Gaussian pulse is possible by dynamical switching off and on the control pulse, shaped as super-Gaussian, shown in the inset of Fig. (3.7). Here the intensity of the probe pulse is much weaker than the intensity of the control pulse. Therefore, almost there is no effect on the population of levels with which the pulse interacts. As seen from Fig. (3.7), the faithful reproduction of modulating frequency of the probe pulse is also possible even for the case of amplitude modulated probe pulse. This implies that a robust way of storage and retrieval of information on frequency of modulating signal is possible via a suitably driven control pulse.

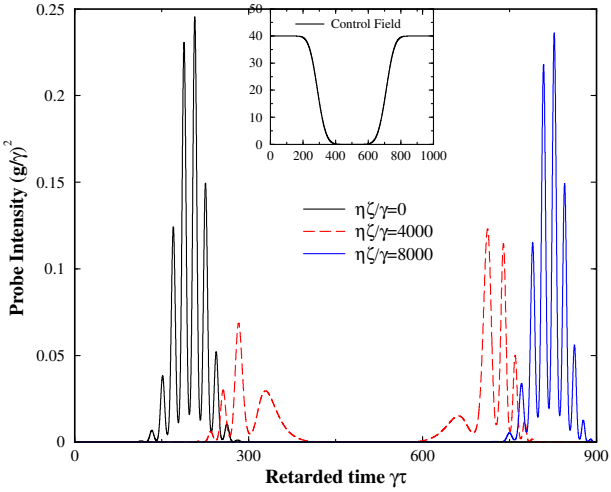

Figure 3.7: *The above frame show the time evolution of the weaker amplitude modulated probe pulse at different propagation distances; The used parameter for probe pulse: modulation index* $g^0 = 0.5\gamma$, $m_a = 0.5$, $\omega_m = \gamma/3$, *and* $\sigma = 50/\gamma$.

3.2.4 Dynamical Evolution of the Control Field

The dynamical evolution of the control field becomes important when the intensities of the control and probe fields are comparable. Fig. (3.8) depicts time evolution of the control field at different propagation distances within the medium. It is evident from this figure that a dip and a bump develops in the amplitude of the control field as it propagates through the medium. The shape of the bump and dip in the control field depends on the initial shape of the probe pulse at the entry of the medium. The changes in the control field are quite significant. Even for the cw control field, the output control field is a combination of both cw and a pulse.

3.2.5 Nonadiabatic Results

Matsko et al.[83] have shown that for any switching time of the control field, an almost perfect storage and retrieval of weak probe pulse is possible. We have found that their results can be extended to probe with moderate powers. We show the results in Fig. (3.9) for an intense probe pulse and nonadiabatic switching of the control field. For both adiabatic and nonadiabatic switching, the retrieved intense probe pulse is the same as the original one. However, there is overall broadening and loss in intensity of the retrieved probe pulse. We

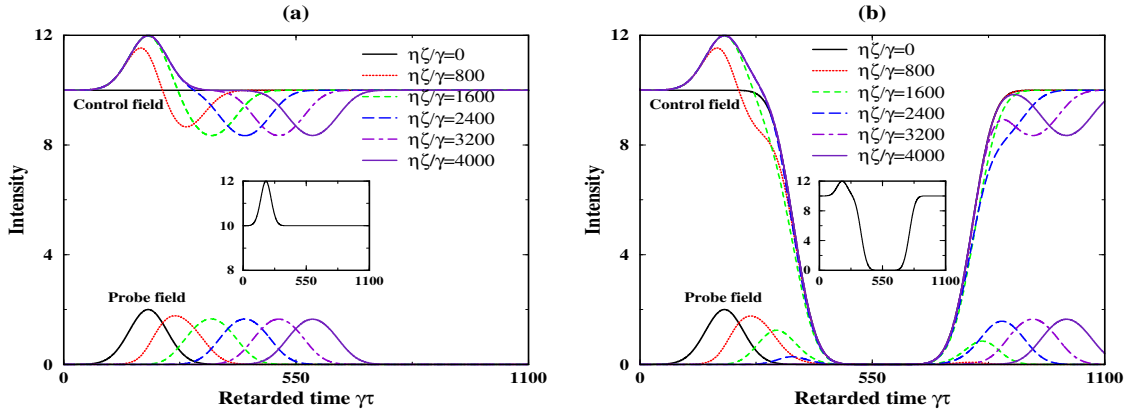

Figure 3.8: *(a) and (b) shows temporal profiles of the control $(G/\gamma)^2$ and probe field $(g/\gamma)^2$ at different propagation distances within the medium. Temporal shape of $(V/\gamma)^2$ as shown in the inset does not depend on ζ. In Fig. (a) the input control field is a cw. In Fig (b) the input control field is a Super-Gaussian shape with parameters $\tau_2 = 575/\gamma, \sigma\prime = 200/\gamma$. The common parameters of the above two graphs are chosen as: $G^0 = 3.16\gamma, g^0 = 1.414\gamma, \tau_0 = 200/\gamma, \sigma = 90/\gamma$. The results of simulations using Maxwell-Bloch equations are indistinguishable from the results based on adiabaton theory.*

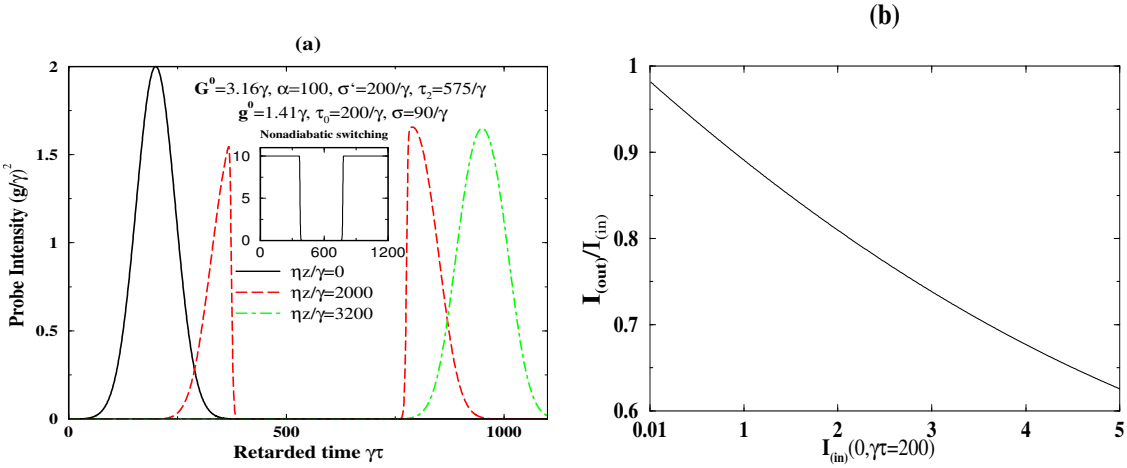

Figure 3.9: *(a) shows storage and retrieval of intense probe pulse even for nonadiabatic switching of the control field. Nonadiabatic switching is shown in the inset. (b)drop in intensity ratio of the probe retrieved to the input pulse as a function of input probe intensity for the case of non adiabatic switching of the control field ; the I_{out} is measured at $\eta\zeta/\gamma = 3200$ and $\gamma\tau = 1000$.*

show in Fig. (3.9b) the drop in the intensity of the output pulse as the intensity of the input pulse increases.

3.3 Adiabaton Theory and Its Relation to Light Storage

In a remarkable paper Grobe *et al.* [147] discovered what they called as adiabatons. These are the pulse pairs which are generated in a Λ-system under adiabatic conditions. We show the deep connection of the problem of storage and retrieval of pulses to the theory of adiabatons. The control field is switched on before the probe field. This is to keep the system in the dark state, which is an essential condition for the adiabaton formation. Under conditions of negligible damping, Grobe *et al.* [147] find that the response of the medium can be very well approximated by the solutions

$$\begin{aligned} \rho_{13} &\approx \frac{i}{V}\frac{\partial}{\partial\tau}\left(\frac{g}{V}\right) \\ \rho_{12} &\approx \frac{i}{V}\frac{\partial}{\partial\tau}\left(\frac{G}{V}\right) \\ \rho_{32} &\approx -\frac{gG}{V^2}\,, \end{aligned} \tag{3.14}$$

where $V^2 = (G^2 + g^2)$. The approximate solutions (3.14) holds provided the following adiabacity condition is satisfied by the two fields:

$$G\frac{\partial g}{\partial\tau} - g\frac{\partial G}{\partial\tau} \ll V^3. \tag{3.15}$$

By inserting solution (3.14) into the Maxwell equation (3.9), we obtain a pair of coupled nonlinear wave equations

$$\begin{aligned} \frac{\partial g}{\partial\zeta} &= -\frac{\eta}{V}\frac{\partial}{\partial\tau}\left(\frac{g}{V}\right) \\ \frac{\partial G}{\partial\zeta} &= -\frac{\eta}{V}\frac{\partial}{\partial\tau}\left(\frac{G}{V}\right). \end{aligned} \tag{3.16}$$

These two, one dimensional PDE are nonlinearly coupled through the variable V. With the help of equation (3.16), one can easily show that V does not depend on the space variable i.e. ζ, during the propagation, V satisfies the relation

$$V\left(\frac{\eta\zeta}{\gamma}, \gamma\tau\right) = V\left(0, \gamma\tau\right) \tag{3.17}$$

Thus the conservation law would imply that any change in probe field is compensated by a corresponding change in the control field for V to remain independent of the spatial coordinates. The input fields determine the temporal shape of V. Analytical solutions of equation (3.16) can be obtained by changing the variable τ to $z(\gamma\tau) \equiv \frac{1}{\gamma^2}\int_{-\infty}^{\gamma\tau} V^2(0,\gamma\tau)d(\gamma\tau)$:

$$\begin{aligned} g\left(\frac{\eta\zeta}{\gamma},\gamma\tau\right) &= V(0,\gamma\tau)F_g\left[z(\gamma\tau)-\frac{\eta\zeta}{\gamma}\right] \\ G\left(\frac{\eta\zeta}{\gamma},\gamma\tau\right) &= V(0,\gamma\tau)F_G\left[z(\gamma\tau)-\frac{\eta\zeta}{\gamma}\right], \end{aligned} \tag{3.18}$$

where $F_g[x] = g[0,z^{-1}(x)]/V[0,z^{-1}(x)]$ and $z^{-1}(x)$ denotes the inverse function of z. We have chosen the initial fields strong enough to ensure the formation of an adiabaton pair. The input fields g and G are chosen such that V is constant after a certain time T. Therefore, for $\tau \geq T$, the integral $z(\gamma\tau)$ can be analytically performed. For a cw control field and a Gaussian probe pulse, we find the explicit results for the probe and control fields

$$\begin{aligned} g\left(\frac{\eta\zeta}{\gamma},\gamma\tau\right) &= \frac{\sqrt{[g^{0^2}e^{-\frac{2(\gamma\tau-\gamma\tau_0)^2}{\sigma^2}}+G^{0^2}]}}{\sqrt{[g^{0^2}e^{-\frac{2(\gamma\tau-\gamma\tau_0-\frac{\eta\zeta}{\gamma G^0})^2}{\sigma^2}}+G^{0^2}]}}g^0 e^{-\frac{(\gamma\tau-\gamma\tau_0)^2}{\sigma^2}} \\ G\left(\frac{\eta\zeta}{\gamma},\gamma\tau\right) &= \frac{\sqrt{[g^{0^2}e^{-\frac{2(\gamma\tau-\gamma\tau_0)^2}{\sigma^2}}+G^{0^2}]}}{\sqrt{[g^{0^2}e^{-\frac{2(\gamma\tau-\gamma\tau_0-\frac{\eta\zeta}{\gamma G^0})^2}{\sigma^2}}+G^{0^2}]}}G^0 \;;\; t \geq T \end{aligned} \tag{3.19}$$

For the case when the control field is taken as a super Gaussian pulse and the probe field as a Gaussian pulse, it is not possible to evaluate the function z analytically. The solutions of equation (3.14) for both these cases, are superimposed on the numerical results obtained from density matrix equations in Fig. (3.8). It is remarkable that, the solutions of equations (3.16) obtained under the adiabatic approximation, matches extremely well with the numerical solutions of the complete set of density matrix equations. As shown in Fig. (3.6), the adiabatic approximation for the atomic coherence ρ_{32} of the equation (3.14) is also indistinguishable from the result obtained from density matrix equations. It should be noted that the adiabatic approximation starts breaking down when the control field is switched off, although the created atomic coherence survives. It is evident from the temporal profiles of the control and probe field at different propagation distances that a dip and a bump develops in the control field intensity as it propagates through the medium. Fig. (3.8) unambiguously confirms that the adiabaton pair (consisting of the dip in the

pump and broadened probe) travels loss-free distances which exceed the weak probe absorption length (here typical value of $\eta\zeta/\gamma = 2400$) by several orders of magnitude with an unaltered shape. In principle, V could have both space and time dependence. Within the adiabatic approximation, V does not depend on space coordinate as shown in the inset of Fig. (3.8). From this Fig., it is very much clear that the temporal shape of V depends on the input shape of the control and probe field and it propagates inside the medium with unaltered shape. To keep V constant in space domain, any change in temporal shape of the control field is compensated by change in temporal shape of probe field. When V^2 and control field are zero, then the probe field is also zero which suggests that probe field gets stored inside the medium. The retrieved probe pulse which is a replica of the input probe pulse is a part of adiabaton pair. The numerical results on the storage and retrieval of light obtained from density matrix formalism matches extremely well with those obtained from adiabatic approximation. Clearly adiabaton pair propagation is quite important for understanding the storage and retrieval of light.

3.4 Summary

In summary, we have investigated the possibility of storage and retrieval of moderately intense probe pulses in a system with relevant atomic transition in Λ configuration. We numerically integrate the full set of the density matrix equations and the Maxwell equations for both control and probe fields. The numerical results show that the storage and retrieval of probe pulses with moderate powers is possible. The dynamical evolution of the control field is important. It may be worth noting that a cw control field becomes pulsed due to its coupling to the probe pulse via the atomic polarization. We find that even though the storage and retrieval at larger powers is possible, the probe field gets absorbed and broadened, however they are not very significant. This behavior is explained in terms of the narrowing of the EIT window as the power of the probe increases. We show how the adiabaton theory of Grobe *et al.*[147] enables us to understand the storage and retrieval of pulses. We further show that the storage and retrieval of information on frequency of modulating signal such as amplitude modulated probe pulse is also possible in the same system via a suitably driven control pulse.

CHAPTER 4

Subluminal and Superluminal Propagation of Intense Pulses at Room Temperature Solid

In the previous two chapters we have demonstrated that light pulses can be propagated "superluminally" or, "subluminally" or to bring them to a complete halt (storage of light) inside atomic gases. However, most of the experiments on slow, fast or storage of light have been carried out in atomic gases with modest density of the order of 10^{12} atoms/cm^3 maintained at cryogenic or room temperature. It would be interesting to produce super and subluminal light pulses in solids, where the density of the relevant atoms is million times larger than in gases. Turukhin *et al.* first demonstrated the propagation of slow light with a velocity of 45 m/sec in solid state material, Y_2SiO_5 doped with Pr, maintained at a cryogenic temperature of 5K [56]. Also quite recently, Bigelow *et al.* demonstrated a new method for controlling the speed of light pulses propagating through a solid state material [57]. This experiment differs considerably from all earlier experiments which were based on conventional electromagnetically induced transparency [26]. They recognize that a two level system driven by a strong field and a probe gives rise to a hole in the probe response function with a width of the order of $1/T_1$, where T_1 is the longitudinal relaxation time [151]. These very narrow spectral hole in the homogeneously broadened probe absorption spectrum caused by coherent population oscillation leads to the ultra-slow group velocity. These authors also discovered that they need not use separate pump and probe fields. A field with peak power of the order of saturation intensity could be slowed down considerably to about 57.5 m/s. Further they extended their work to a material like alexandrite,

where they reported superluminal pulse propagation. In this chapter we develop models for the propagation of intense pulse in nonlinear solid state media which can have either saturated absorption or reverse saturated absorption. We show that the experiments of Bigelow *et al.* on subluminal propagation in ruby [Phys. Rev. Lett. **90**, 113903 (2003)], and superluminal propagation in alexandrite [Science **301**, 200 (2003)] are well explained by modeling them as three level and four level systems respectively, coupled to Maxwell equations. We present results well beyond the traditional pump-probe approach.

4.1 Saturated Absorption

In order to understand the basic idea of the saturated absorption, we consider there-level atomic system as shown in Fig. (4.1(a)) where single intense pump field interact between the ground state $^4A_2$ and the excited state $^4F_2$. Therefore incident field promotes an atoms from ground state $^4A_2$ to excited state $^4F_2$. The excited state $^4F_2$ can rapidly decay to the state $2\bar{A}$ and $\bar{E}$ by a non-radiative transition. The intensity of the pump field is such that the rate of transition of the atoms from ground state $^4A_2$ to excited state $2\bar{A}$ and $\bar{E}$ becomes larger than the relaxation rate of the excited state $2\bar{A}$ and $\bar{E}$. This leads to a pronounced decrease of the population in the ground state. Therefore, the net result is that the system can not absorb as large a fraction of the incident field as it can under low intensity conditions. This process is called saturated absorption. For saturated absorption case, the absorption cross-section of the excited state $2\bar{A}$ and $\bar{E}$ are smaller than that of the ground state $^4A_2$. Therefore, the transmission of the system is increased due to smaller absorption cross-section of the excited state. In this chapter we treat the homogeneous case, while the saturation of inhomogeneous line profile is discussed in next chapter. The material like ruby where the transverse relaxation time $T_2 \ll T_1$ can exhibit the saturated absorption.

4.2 Model Description and Dynamical Equations

Ruby was the first synthetic material used by Maimen to built a laser in 1960 [152]. It consists a crystalline aluminium oxide (Al_2O_3, also known as corundum), in which a small fraction of aluminium ion's Al^{3+} have been replaced by chromium ion's Cr^{3+}. Chromium

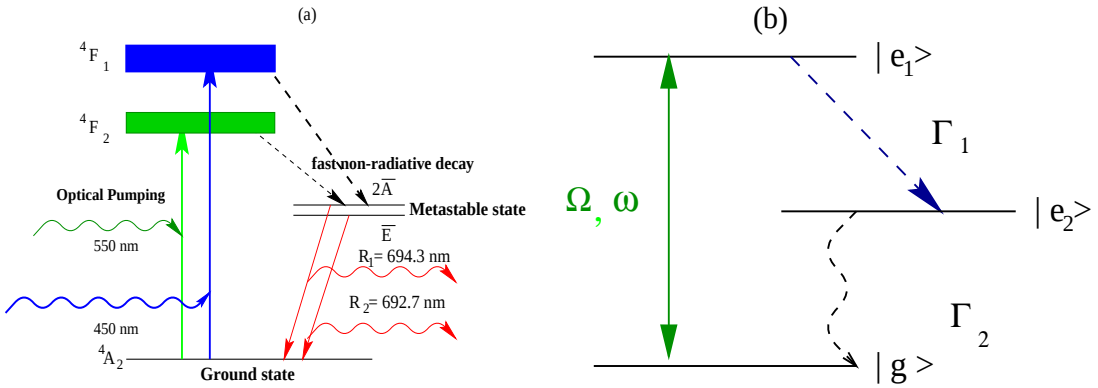

Figure 4.1: *(a) Energy levels of chromium ions in ruby. (b) Three level model for Ruby Crystal*

ion's is transition metal with electronic configuration

$$1s^2\ 2s^2\ 2p^6\ 3s^2\ 3p^6\ 3d^3 = [Ar]3d^3.$$

The unpaired d-electrons from a high-spin ground state referred to as ^{4}F. The first excited state of the free ion is a ^{2}G state and it is 2eV higher than the ground state ^{4}F. The ground state ^{4}F and first excited state ^{2}G have high orbital degeneracy. When these Cr^{3+} ions is placed in a crystalline aluminium oxide, the levels ^{4}F and ^{2}G are split under the action of crystalline electric fields according to the symmetry of the field as $^4A_2$+$^4F_1$+$^4F_2$ and E+other terms, respectively. The $^4A_2$ level is singly degenerate. The E level is doubly degenerate $(2\bar{A}, \bar{E})$. The energy level diagram for the chromium ion in ruby is shown in the Fig. (4.1(a)). These Cr^{3+} are active in absorbing any green (blue) light to pump population from the ground state to the broad $^4F_2$ ($^4F_1$) absorption band. The absorption band $^4F_2$ is homogeneously broadened and has width of $\sim$ 100 nm which corresponds to a dephasing time T_2 of a few fs. The population in $^4F_2$ absorption band decays very rapidly to the levels $2\bar{A}$ and $\bar{E}$ where it is trapped due to the long life time of these levels before it decays back to the ground state. The relaxation time of the metastable states $2\bar{A}$ and $\bar{E}$ is of the order of few ms. Ruby has no fluorescence at the absorbing wavelength since the metastable state decays to the ground state by radiating red fluorescent light which is completely different wavelength compared to the wavelength of absorbing light. In light of energy level diagram of chromium ion's in ruby, it is a three level system [153]. To study the propagation of intense pulses in ruby, we represent the ground state $^4A_2$ as $|g\rangle$, the $^4F_2$ absorption band as $|e_1\rangle$ and the levels $2\bar{A}$ and $\bar{E}$ as $|e_2\rangle$ as shown in Fig. (4.1(b)). The

propagation of an intense pulse is defined by the electric field

$$\vec{E}(z,t) = \vec{\mathcal{E}}(z,t)\, e^{-i(\omega t - kz)} \; + \; c.c., \tag{4.1}$$

where $\vec{\mathcal{E}}$ is the slowly varying envelope of the intense field. The carrier frequency of intense field, ω, is in resonance with the frequency of the $|g\rangle \longleftrightarrow |e_1\rangle$ transition. The total Hamiltonian of the atom interacting with the intense field under RWA is

$$\mathcal{H} = \hbar\omega_{1g}|e_1\rangle\langle e_1| + \hbar\omega_{2g}|e_2\rangle\langle e_2| - \hbar\Omega e^{-i\omega t}|e_1\rangle\langle g| - \hbar\Omega^* e^{i\omega t}|g\rangle\langle e_1|, \tag{4.2}$$

where the Rabi frequency Ω is defined by $\Omega(z,t) = 2\vec{d}_{1g} \cdot \vec{\mathcal{E}}(z,t)/\hbar$, and $\vec{d}_{1g}$ is the dipole matrix element. Some of the atomic coherences become irrelevant on experimental time scale due to the very rapid decay of the level $|e_1\rangle$ to $|e_2\rangle$. Therefore, the density matrix equations for the model in Fig. (4.1) are

$$\dot{\rho}_{gg} = 2\Gamma_2\rho_{22} + i\frac{\Omega}{2}(\rho_{1g} - \rho_{g1}) \tag{4.3}$$

$$\dot{\rho}_{22} = 2\Gamma_1\rho_{11} - 2\Gamma_2\rho_{22} \tag{4.4}$$

$$\dot{\rho}_{1g} = -\Gamma_1\rho_{1g} + i\frac{\Omega}{2}(\rho_{gg} - \rho_{11}) \tag{4.5}$$

$$\rho_{gg} \; + \; \rho_{11} \; + \; \rho_{22} = 1, \tag{4.6}$$

where $\rho_{ij} = \langle e_i|\rho|e_j\rangle$; $i,j = 1,2$. Note that the density matrix elements in the original frame are given by $\rho_{1g}e^{-i\omega t}$, ρ_{gg}, ρ_{22} and ρ_{11}. Under the approximation, $\Gamma_1 \gg \Gamma_2, \Omega$, $\dot{\rho}_{1g} \sim 0$, Eq. (4.5) simplifies to

$$\rho_{1g} \cong \frac{i\Omega(\rho_{gg} - \rho_{11})}{2\Gamma_1}. \tag{4.7}$$

Therefore, we derive the approximate equation for the evolution of the ground state population as,

$$\begin{aligned} \dot{\rho}_{gg} &= 2\Gamma_2\rho_{22} + i\frac{\Omega}{2}(\rho_{1g} - \rho_{g1}) \\ &= 2\Gamma_2\rho_{22} - \frac{\Omega^2(\rho_{gg} - \rho_{11})}{2\Gamma_1} \\ &= 2\Gamma_2(1 - \rho_{gg}) - \frac{\Omega^2}{2\Gamma_1}\rho_{gg} \end{aligned} \tag{4.8}$$

Note that we can easily prove that $\rho_{11} \approx 0$ if $\Gamma_1 \gg \Gamma_2, \Omega$. Under the same conditions and the slowly varying envelop approximation, the evolution equation for the Rabi frequency of the field is written by

$$\frac{\partial\tilde{\Omega}}{\partial z} = -\frac{\alpha_0}{2}\tilde{\Omega}\rho_{gg}, \quad \tilde{\Omega} = \Omega/\Omega_{sat}, \tag{4.9}$$

where $\alpha_0 = 4\mathcal{N}\pi\omega|d_{_{1g}}|^2/c\hbar\Gamma_1$ and $\Omega_{sat} = 2\sqrt{\Gamma_1\Gamma_2}$. Therefore, we have derived coupled Maxwell-Bloch equations for pulse propagation in the three level model in ruby

$$\frac{\dot{\rho}_{gg}}{2\Gamma_2} = (1-\rho_{_{gg}}) - \tilde{\Omega}^2\rho_{_{gg}} \tag{4.10}$$

$$\frac{\partial\tilde{\Omega}}{\partial z} = -\frac{\alpha_0}{2}\tilde{\Omega}\rho_{gg}. \tag{4.11}$$

In Eqs. (4.10) and (4.11) we have used the pulse coordinates i.e., $t - z/c, z$. The time derivative in Eq. (4.10) is with respect to $(t - z/c)$. The time t can be expressed in units of $1/2\Gamma_2$.

4.3 Numerical Results on Ultra-slow Pulse Propagation

To delineate various aspects of the pulse propagation, we solve the system of coupled equations (4.10) and (4.11) numerically for a homogeneous broadened ruby crystal. For numerical computation, we consider two different types of input pulses, viz, a Gaussian pulse with a temporal width $\gtrsim 1/\Gamma_2$

$$\tilde{\Omega}_{in} = \tilde{\Omega}^0\, e^{[-t^2/2\sigma^2]} \tag{4.12}$$

and amplitude modulated pulse

$$\tilde{\Omega}^2_{in}(t) = I = I_0\left(1 + m\cos[\Delta t]\right). \tag{4.13}$$

Here $\tilde{\Omega}^0 = \sqrt{I_0}$ is a real constant characterizing the peak amplitude of the Rabi frequency before the pulse enters the homogeneous ruby medium. The equations (4.10) - (4.13) are used for numerical computations. We do not make any approximation on the strength of the pulses so that we can model experimental observations on strong pulses. We calculate the evolution of pulse for arbitrary values of $\tilde{\Omega}^0$ or I_0. Some typical results for the Gaussian pulses are shown in the Fig. (4.2). We get group velocities in the range of 50 m/s for $\Omega/\Omega_{sat} \backsim 1$ and the transmission is rather small. Group velocity of the intense pulse can be calculated from the relative delay between the peak positions of the reference pulse and output pulse, though the group velocity concept may not be very relevant as the pulse is not weak. It is well known that the group velocity concept is introduced for a linear dispersive medium, however, in the present case the medium is nonlinear, dispersive and the refractive index of the medium is modified by the propagating intense light pulse itself. Next, we consider the input pulse as a modulated pulse given by Eq. (4.13). The ampli-

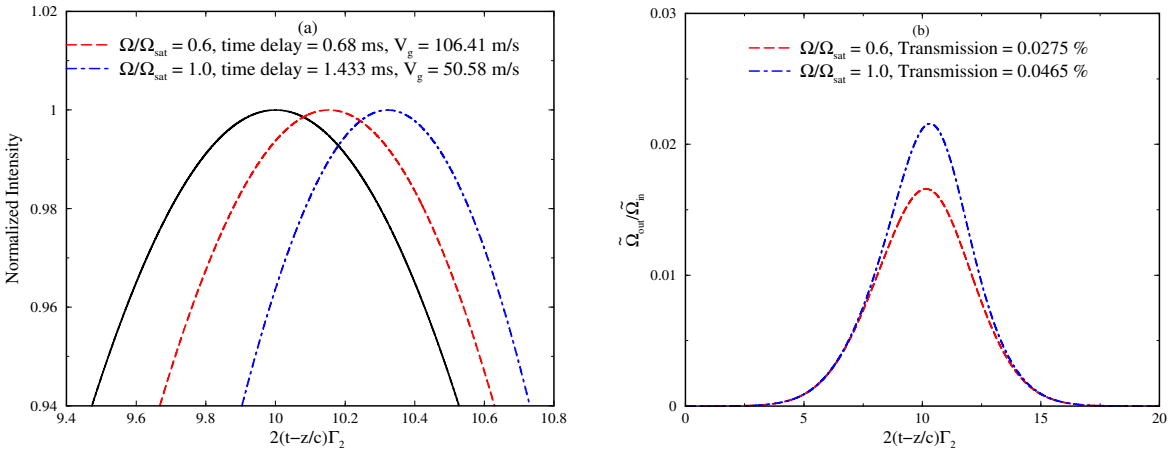

Figure 4.2: *(a) The solid curve shows light pulse propagating at speed c through 7.25 cm in vacuum. The long dashed and dot-dashed curves show light pulses propagating through a medium of length 7.25 cm at different input amplitudes. The temporal width σ of the Gaussian pulse is 20 ms and $1/2\Gamma_2 = 4.45$ ms. The part (b) gives the amplitudes, of the output pulse normalized to the input amplitudes. The transmission increases with increasing the input field intensity.*

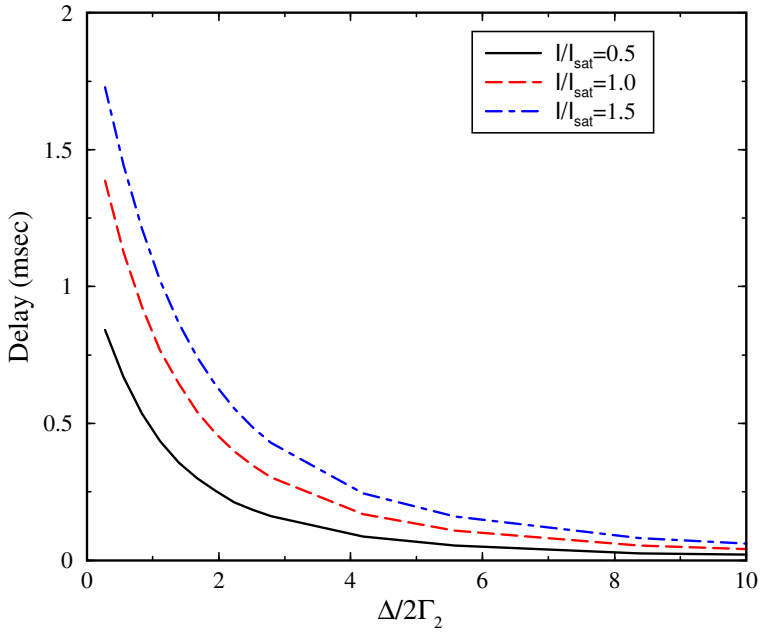

Figure 4.3: *Time delay of the light pulse as a function of modulation frequency for three different input powers for modulation index, $m = 0.06$. Note that $\Delta/2\Gamma_2 \sim 1$ corresponds to a modulation frequency ~ 35 Hz.*

tude modulated pulse contains a strong pump of intensity I_0 and two side bands acting as probes of intensity mI_0 when modulation index $m = 0.06$ is very small. The strong pump that creates a hole in the probe absorption spectrum becomes prominent when the beating frequency Δ between pump and probe is less than or approximately equal to $2\Gamma_2$. This narrow hole causes an amplitude modulated pulse to experience a large group delay. We show this time delay as a function of modulation frequency for three different pump powers in Fig. (4.3). As seen from Fig. (4.3), at large modulation frequency the amplitude modulated pulse moves with speed c/n, where n is refractive index of the medium. Bigelow *et al.* have used pulses with incident power I_{in} of 0.25 Watts [57] and they have measured group delay 1.26 ms corresponds to the group velocity 57.5 m/s. Let us evaluate the Rabi frequency corresponding to the power level 0.25 Watts. The incident beam I_{in} of power 0.25 Watts was focused with 40 cm focal length lens to a beam waist (w_0) 84μm near the entrance face of a 7.25 cm long ruby rod. Therefore, the peak power at the entrance face of the ruby rod is given by

$$\begin{aligned} I_{in}^0 &= \frac{I_{in}}{\pi r^2}; \qquad r = \frac{w_0}{\sqrt{2}} \\ &= 2.25 \text{ kWatt/cm}^2. \end{aligned} \tag{4.14}$$

The value of saturated intensity I_{sat} of ruby at 514.5 nm is 1.5 kWatt/cm^2 [153]. Therefore, the Rabi frequency corresponds to the power level 0.25 Watts is as fellows:

$$\tilde{\Omega}^0 = \sqrt{\frac{I_{in}^0}{I_{sat}}} \approx 1.15. \tag{4.15}$$

As shown in Fig (4.2(a)), we get group velocity of the order of 50 m/s corresponds to the Rabi frequency $\tilde{\Omega}^0 \sim 1$ which is qualitative agreement with the experimental result of Bigelow *et al.* [57]. Note that the measurement conditions in Refs.[153] and [57] are not same.

4.4 Comparison between Two and There Level Model for Ruby

To study the group velocity and transmission for the intense pulse propagation through a conventional two level model described by the traditional Bloch equations. Therefore, the

Bloch equations for this conventional system are given by

$$\dot{\rho}_{_{1g}} = -\frac{1}{T_2}\rho_{_{1g}} + i\frac{\Omega}{2}(\rho_{_{gg}} - \rho_{_{11}}), \tag{4.16}$$

$$\dot{\rho}_{_{gg}} = \frac{1}{T_1}\rho_{_{11}} + i\frac{\Omega}{2}(\rho_{_{1g}} - \rho_{_{g1}}). \tag{4.17}$$

At the limit of longitudinal relaxation time, T_1 very much greater than transverse relaxation time T_2, $\dot{\rho}_{_{1g}} \sim 0$, Eqs. (4.16) and (4.17) are simplified to

$$\rho_{_{1g}} \cong \frac{i\Omega T_2(\rho_{_{gg}} - \rho_{_{11}})}{2} \tag{4.18}$$

$$\dot{\rho}_{_{gg}} = \frac{1}{T_{_1}}(1 - \rho_{_{gg}}) - \frac{|\Omega|^2 T_2}{2}(2\rho_{_{gg}} - 1). \tag{4.19}$$

Therefore, the coupled Maxwell-Bloch equations are

$$\dot{\rho}_{_{gg}} T_{_1} = (1 - \rho_{_{gg}}) - \frac{|\tilde{\Omega}|^2}{2}(2\rho_{_{gg}} - 1) \tag{4.20}$$

$$\frac{\partial\tilde{\Omega}}{\partial z} = -\frac{\alpha_0}{2}\tilde{\Omega}(2\rho_{_{gg}} - 1), \tag{4.21}$$

where $\tilde{\Omega} = \Omega\sqrt{T_1 T_2}$ and dot denotes $\partial/\partial(t - z/c)$. In Fig.(4.4), we also show for comparison the results of the group velocities and the transmission for the propagation of an intense pulse through a two level system described by the traditional Bloch equations. As seen from Fig. (4.4), there are substantial differences in the propagation of pulses in two level and three level media. Note that the time T_1 is equal to $1/2\Gamma_2$. We believe that, in light of the energy level diagram of ruby, it is more appropriate to model it as a three level system. The two level model misses the interesting physics since, in the effective two level model there would be field induced transition from $|e_2\rangle$ to $|g\rangle$ whereas, in the three level scheme this does not occur. The steady state population of the ground state $|g\rangle$ for two level and three level model obtained from Eqs. (4.20) and (4.10) are respectively given by

$$\rho_{gg}\big|_{two} = \frac{1 + \frac{\Omega^2}{2\Omega_{sat}^2}}{1 + \frac{\Omega^2}{\Omega_{sat}^2}} \tag{4.22}$$

$$\rho_{gg}\big|_{three} = \frac{1}{1 + \frac{\Omega^2}{\Omega_{sat}^2}};\ \ \Omega_{sat} = 2\sqrt{\Gamma_1\Gamma_2} \tag{4.23}$$

At $\Omega = \Omega_{sat}$, the saturated value of population in the ground state $|g\rangle$ are $3/4$ and $1/2$ for two and three level systems, respectively. As a result, two and three level systems saturate in distinct ways which leads an important difference between two model configuration.

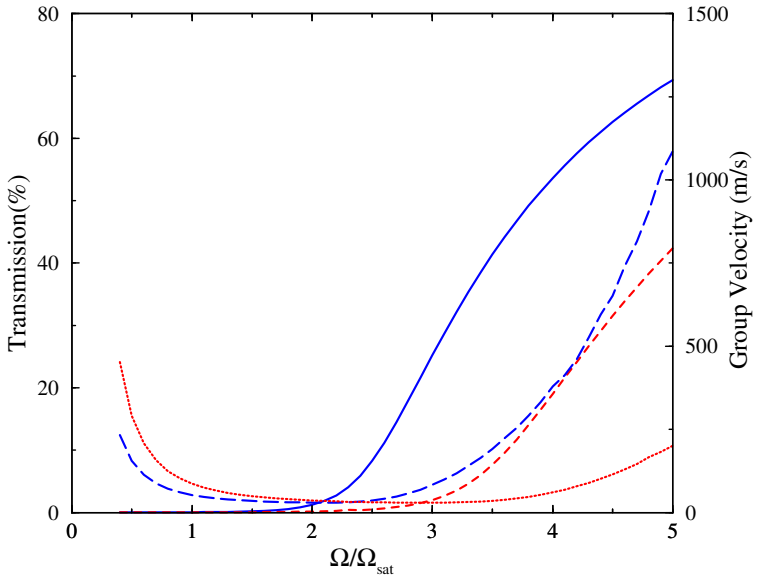

Figure 4.4: *Variation of transmissions and group velocities as a function of the input amplitude of the light pulse. The solid (dashed) curve gives the intensity transmission of the pulse for the three (two) level model of the medium. The corresponding group velocities are given by the dotted curve (two level model) and the long dashed curve (three level model). The light pulse is propagating through the medium of length 7.25 cm.*

While our results in Figs. (4.2) - (4.3) are in broad agreement with the experimental data, we do not make a precise comparison due to the sensitive dependence on pump powers, focusing of the pump and the possible uncertainty in the known value of the saturation power for experimental conditions.

4.5 Reverse Saturated Absorption

We explicate the basic understanding of reverse saturation absorption, considering a four level system interacting with single intense pump field, as shown in Fig. (4.5(a)), as seen in alexandrite crystal. The process of absorption in a four level system is as follows. Absorption of incident field promotes an atoms to the first excited state $^4T_2$. From the excited state $^4T_2$ can rapidly make a transition to the state ^2E by a non-radiative transition. A higher-lying state $|e_3\rangle$ that may be radiatively coupled to the state ^2E, and for which the energy difference is in near resonance with the incident field. Therefore, before the atoms are completely relaxes to the ground state, it may experience absorption that promotes it to the higher-lying state $|e_3\rangle$. This process is named as excited state absorption. When the

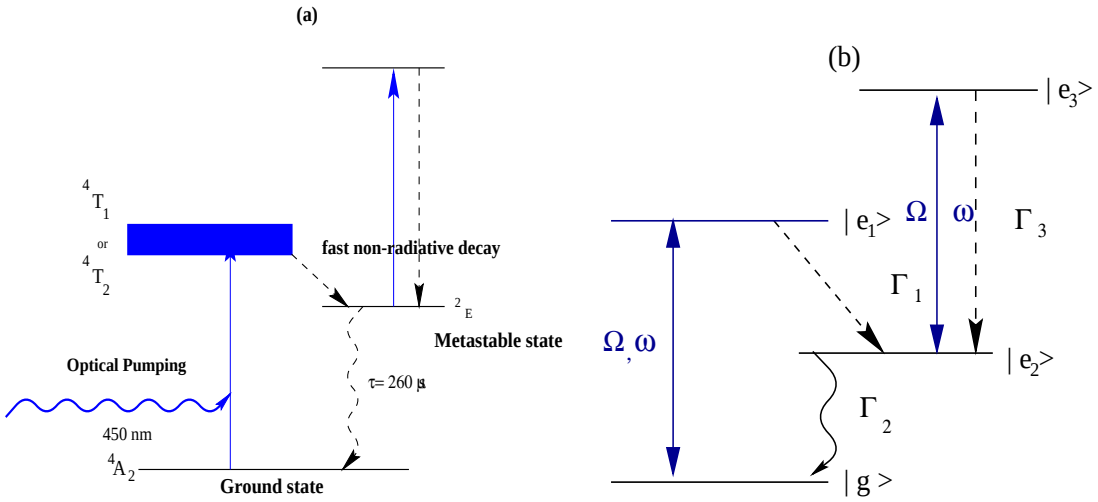

Figure 4.5: *(a) The energy level diagram of chromium ion's in $BeAl_2O_4$ crystal. (b)Four level model for Alexandrite crystal*

absorption cross-section of the excited state is larger than that of the ground state, then the system will exhibit reverse saturated absorption phenomena and display less transmissive when excited. Therefore, an anti hole is produced (instead of a hole) in the probe absorption spectrum. The system becomes less transmissive due to the presence of anti hole in the probe absorption spectrum at the frequency of pump field. The width of the anti hole is the order of inverse of the relaxation time T_1 of the excited state. A spectral hole leads to slow light, whereas an anti hole leads to superluminal light associated with small transmission.

4.6 Superluminal Pulse Propagation in Alexandrite

Alexandrite (Cr^{3+}:$BeAl_2O_4$) is chromium-doped chrysoberyl, in which the chromium ion's (Cr^{3+}) are embedded in the $BeAl_2O_4$ crystal at the amount 0.01%-0.04%. Fig. (4.5 (a)) shows energy levels of chromium ion's in alexandrite. These chromium ion's absorbing the excitation of wavelengths in the approximate range 450-510 nm to pump population from ground state $^4A_2$ to the absorption bands $^4T_2$ or $^4T_1$. The population in this absorption band decays very rapidly to the ^2E level, where it is trapped because of long life time of this level (260 μs). At the excitation wavelength, the absorption cross-section of the ^2E state exceeds that of the ground state. Thus, alexandrite exhibits inverse of the

normal saturation *i.e.,* reverse saturation absorption [154]. Reverse saturation absorption produces a narrow antihole in the susceptibility for the probe in presence of a pump field. Bigelow *et al.* experimentally demonstrate how the anti-hole can result in the superluminal propagation through alexandrite [138]. In order to model the experiment, we model alexandrite as a four level system to account for reverse absorption as shown in Fig. (4.5(b)), where the ground state $^4A_2$ is designated as $|g\rangle$, the absorption bands $^4T_2$ and $^4T_1$ as $|e_1\rangle$ and the level ^2E as $|e_2\rangle$. The intense pulse is defined by the electric field, $\vec{E}(z,t) = \vec{\mathcal{E}}(z,t)\, e^{-i(\omega t - kz)} + c.c.$, which is couples $|e_1\rangle \longleftrightarrow |g\rangle$, can also drive $|e_3\rangle \longleftrightarrow |e_2\rangle$. The Hamiltonian of the system under the action of these field in the RWA approximation can be written as

$$\mathcal{H} = \hbar\omega_{_{1g}}|e_{_1}\rangle\langle e_{_1}| + \hbar\omega_{_{2g}}|e_{_2}\rangle\langle e_{_2}| + \hbar\omega_{_{3g}}|e_{_3}\rangle\langle e_{_3}| - \hbar\Omega e^{-i\omega t}|e_{_1}\rangle\langle g| - \hbar\Omega e^{-i\omega t}|e_{_3}\rangle\langle e_{_2}| + h.c. \quad (4.24)$$

The density matrix equations are now given by

$$\begin{aligned}
\dot{\rho}_{_{gg}} &= 2\Gamma_2\rho_{_{22}} + i\Omega(\rho_{_{1g}} - \rho_{_{g1}})/2 && (4.25a)\\
\dot{\rho}_{_{22}} &= 2\Gamma_1\rho_{_{11}} - 2\Gamma_2\rho_{_{22}} + 2\Gamma_3\rho_{_{33}} + i\Omega(\rho_{_{32}} - \rho_{_{23}})/2 && (4.25b)\\
\dot{\rho}_{_{33}} &= -2\Gamma_3\rho_{_{33}} + i\Omega(\rho_{_{23}} - \rho_{_{32}})/2 && (4.25c)\\
\dot{\rho}_{_{32}} &= -\Gamma_3\rho_{_{32}} + i\Omega(\rho_{_{22}} - \rho_{_{33}})/2 && (4.25d)\\
\dot{\rho}_{_{1g}} &= -\Gamma_1\rho_{_{1g}} + i\Omega(\rho_{_{gg}} - \rho_{_{11}})/2 && (4.25e)\\
\rho_{_{gg}} &+ \rho_{_{11}} + \rho_{_{22}} + \rho_{_{33}} = 1. && (4.25f)
\end{aligned}$$

Here we consider the intense pulse is in resonance with $|e_1\rangle \longleftrightarrow |g\rangle$ and $|e_3\rangle \longleftrightarrow |e_2\rangle$, respectively. The Rabi frequency Ω is defined by $\Omega(z,t) = 2\vec{d}_{_{1g}} \cdot \vec{\mathcal{E}}(z,t)/\hbar$, where $\vec{d}_{_{1g}}$ is the dipole moment matrix element and $\vec{\mathcal{E}}(z,t)$ is the slowly varying envelope of the pulse. In the original frame of reference, the matrix elements are given by $\rho_{_{1g}}e^{-i\omega t}$, and $\rho_{_{32}}e^{-i\omega t}$, whereas the other elements remain unchanged. Under the approximation, $\Gamma_1, \Gamma_3 \gg \Gamma_2, \Omega$; $\dot{\rho}_{32}$ and $\dot{\rho}_{_{1g}} \sim 0$, therefore Eqs. (4.25(d)) and (4.25(e)) can be expressed in the following form:

$$\begin{aligned}
\rho_{_{1g}} &\cong \frac{i\Omega(\rho_{_{gg}} - \rho_{_{11}})}{\Gamma_1} = \frac{i\Omega\rho_{_{gg}}}{\Gamma_1} && (4.26a)\\
\rho_{_{32}} &\cong \frac{i\Omega(\rho_{_{22}} - \rho_{_{33}})}{\Gamma_3} = \frac{i\Omega(1 - \rho_{_{gg}})}{\Gamma_3} && (4.26b)
\end{aligned}$$

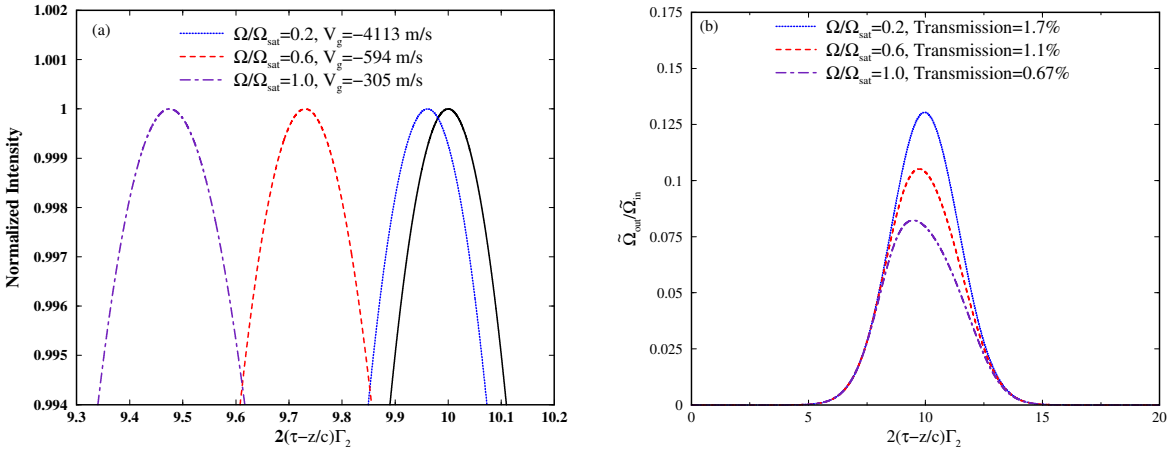

Figure 4.6: *The solid curve of (a) shows light pulse propagating at speed c through a distance of 4 cm in vacuum. The dotted, long dashed and dot-dashed curves depict light pulse propagating through a medium of length 4 cm at different input amplitudes. The pulse width σ is 500 μs, whereas $1/2\Gamma_2$=250μs. Fig (b) shows the amplitude of the output pulse normalized with input amplitude. The transmission is decreased with increase in the input field intensity .*

where ρ_{11} & $\rho_{33} \sim 0$, that can be easily prove under the same approximation. Thus we obtain the approximate equation for the evolution of ground state population as

$$\frac{\dot{\rho}_{gg}}{2\Gamma_2} = (1-\rho_{gg}) - |\tilde{\Omega}^2|\rho_{gg}. \tag{4.27}$$

The evolution equation for the slowly varying Rabi frequency of the intense field under the same conditions is

$$\frac{\partial\tilde{\Omega}}{\partial z} = -\frac{\alpha_0}{2}\tilde{\Omega}\rho_{gg} - \frac{\tilde{\alpha_0}}{2}\tilde{\Omega}(1-\rho_{gg}), \;\; \tilde{\Omega} = \frac{\Omega}{\Omega_{sat}}, \tag{4.28}$$

where α_0 and $\tilde{\alpha}_0$ gives the saturation and reverse saturation, respectively. Shand *et al.* have shown that, for excitation wavelength of 457 nm, the excited-state $|e_2\rangle$ absorption cross-section σ_2 $(4.05 \times 10^{-20}$ cm$^2)$ exceeds that of the ground state $|g\rangle$ absorption cross-section σ_1 $(0.9 \times 10^{-20}$ cm$^2)$ [155]. Thus the absorption rate for excitation at these wavelength displays the reverse saturation absorption in that the total absorption coefficient increases rather than decreases with input intensity. Following these experimental data, we estimate $(\tilde{\alpha}_0/\alpha_0) \approx 4$. The coupled differential Eqs. (4.27) and (4.28) are numerically integrated for studying the input Gaussian pulse given by Eq. (4.12) through the resonant systems. We show a number of our numerical results in Fig. (4.6). This Figure also shows that the group velocity and net transmission depends on the peak intensity of the Gaussian

pulses. It is clear from Fig. (4.6b) that an increase in the input pulse intensity results in increased absorption of the pulse at the resonant condition. It should be borne in mind that in the range of the intensities of Fig. (4.6), no perturbation theory can be used and one has to study the full nonlinear behavior. We also notice that the shape of input pulses get distorted. The nonlinearity of the medium becomes more pronounced as the intensity of the input pulse increases leading to severe distortion of the input pulses.

4.7 Summary

In summary, we have shown how to model the propagation of intense pulse in solid state media with very strong relaxation effects. The media can exhibit either saturated absorption or reverse absorption. We solve numerically the system of Maxwell-Bloch equations without any approximation on the strength of the input pulses. We calculate the group velocity of the intense pulses from the relative delay or advancement between reference pulse and the output pulse. Our modelling goes well beyond the traditional pump-probe approach. We specifically present results on the propagation of pulses in ruby and alexandrite. Our model would also be applicable to other systems, such as Er^{+3} doped fluoroindogallate glasses [156], where reverse absorption could be dominant.

CHAPTER 5

Saturated Absorption for Production of Slow Light in Doppler-Broadened Two Level Systems

In the previous chapters, we have discussed the propagation of light pulse through a homogeneously broadened atomic medium. In this chapter, we demonstrate that light pulse can be slowed down considerably in an inhomogeneously broadened medium. This is somewhat counterintuitive as one would think that inhomogeneous line shape would make the dispersion, or more precisely, the derivative of susceptibility, rather negligible. We, however, suggest the use of the method of saturation absorption spectroscopy[19, 20, 21, 22, 23] to produce a hole of the order of the homogeneous width in the Doppler broadened line. The application of a counter propagating saturated beam can result in considerable reduction in absorption, and adequate normal dispersion to produce slow light.

5.1 Basic Equation for Driven Two Level System

We have considered the standard geometry of a Doppler broadened system as shown in Fig. (5.1) where the atom interacts with counterpropagating probe and control field. Here a probe pulse propagates in the direction $\hat{z}$ in a medium of two level atoms. For simplicity, we consider the incident probe pulse of the form

$$\vec{E}(t) \equiv \vec{\mathcal{E}} e^{i(kz-\omega t)} + c.c., \;\; k = \frac{\omega}{c} \tag{5.1}$$

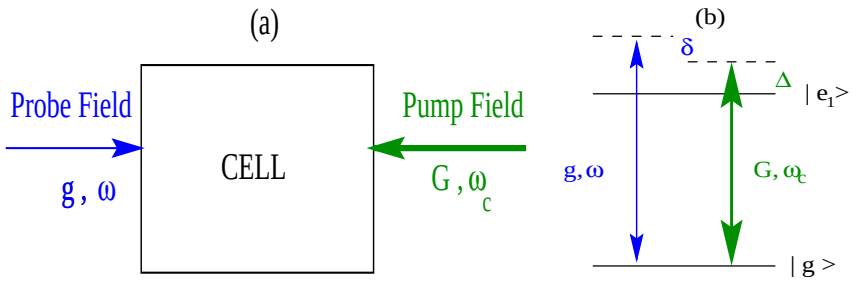

Figure 5.1: *(a) A block diagram where the pump (ω_c) and probe (ω) field are counter propagating inside the medium. (b) Schematic representation of a two level atomic system with ground state $|g\rangle$ and excited state $|e_1\rangle$.*

A counter propagating cw pump field, $\vec{E}_c(t)$, is used for producing saturation

$$\vec{E}_c(t) \equiv \vec{\mathcal{E}}_c e^{i(kz-\omega_c t)} + c.c. \tag{5.2}$$

What is the relevant for further consideration is that the effective linear susceptibility $\chi(\omega)$ of the two level system which is interacting with the field $\vec{\mathcal{E}} e^{i(kz-\omega t)}$ and $\vec{E}_c(t)$. The Hamiltonian of the system under the action of theses field in dipole moment approximation is given by

$$\begin{aligned} \mathcal{H} &= \mathcal{H}_0 + \mathcal{H}_I \\ &= \hbar\omega_{1g}|1\rangle\langle 1| - \hbar\left[Ge^{-i\omega_c t}|1\rangle\langle g| + ge^{-i\omega t}|1\rangle\langle g| + \text{h.}c.\right], \end{aligned} \tag{5.3}$$

where $2G$ and $2g$ are the Rabi frequency of the pump and probe field, respectively. By making a unitary transformation from the density matrix ρ to σ via

$$\sigma_{11} = \rho_{11}, \quad \sigma_{1g} = \rho_{1g}e^{i\omega_c t}, \quad \sigma_{gg} = \rho_{gg}, \tag{5.4}$$

we have the corresponding density matrix equations

$$\dot{\sigma}_{11} = -\dot{\sigma}_{gg} = -\frac{1}{T_1}\sigma_{11} + i(G + ge^{-i\delta t})\sigma_{g1} - i(G^* + g^* e^{i\delta t})\sigma_{1g}, \tag{5.5}$$

$$\dot{\sigma}_{1g} = \dot{\sigma}^*_{g1} = -(\frac{1}{T_2} - i\Delta)\sigma_{1g} + i(G + ge^{-i\delta t})(\sigma_{gg} - \sigma_{11}), \tag{5.6}$$

where T_1 and T_2 are called "longitudinal" and "transverse" relaxation times and the detunings Δ and δ are defined by

$$\Delta = \omega_c - \omega_{1g}, \quad \delta = \omega - \omega_c \tag{5.7}$$

Equations (5.5) and (5.6) cannot be solved exactly. The strategy will be to find a solution that is exact for saturating control field and is correct to first order for the amplitude of g, the weak probe field. Hence, we require that the steady-state solution of the density matrix can be written in the form

$$\sigma_{_{ij}} = \sigma_{ij}^{(0)} + \sigma_{ij}^{(+)} g e^{-i\delta t} + \sigma_{ij}^{(-)} g^* e^{i\delta t}. \tag{5.8}$$

where $\sigma_{ij}^{(0)}$ denote the solution for the case in which the control field is only present in the system and the other terms are assumed to be small in the sense that $|\sigma_{ij}^{(+)}|$, $|\sigma_{ij}^{(-)}| \ll \sigma_{ij}^{(0)}$. We now substitute the above expression in the density matrix equations and equate the coefficients of $ge^{-i\delta t}$, $g^* e^{i\delta t}$ and the constant terms. Thus we obtain a set of twelve coupled simultaneous equations. The solutions of simultaneous equations for steady state density matrix elements are given all relevant coefficients as fellows:

$$\sigma_{11}^{(0)} = \frac{2|G|^2 T_1 T_2}{1 + \Delta^2 T_2^2 + 4|G|^2}, \tag{5.9a}$$

$$\sigma_{1g}^{(0)} = \frac{iG}{(1/T_2 - i\Delta)} \frac{\left(1 + \Delta^2 T_2^2\right)}{(1 + \Delta^2 T_2^2 + 4|G|^2 T_1 T_2)} \tag{5.9b}$$

$$\sigma_{1g}^{(+)} = -\frac{\left(1 + \Delta^2 T_2^2\right)}{(\Delta + \delta + i/T_2)(1 + \Delta^2 T_2^2 + 4|G|^2 T_1 T_2)} \times \left[1 - \frac{2|G|^2 (\Delta - i/T_2)^{-1} (\delta + 2i/T_2)(\delta - \Delta + i/T_2)}{(\delta + i/T_1)(\delta - \Delta + i/T_2)(\delta + \Delta + i/T_2) - 4|G|^2(\delta + i/T_2)}\right] \tag{5.9c}$$

$$\sigma_{1g}^{(-)} = -\frac{2|G|^2 \left(1 + \Delta^2 T_2^2\right)}{(\Delta + i/T_2)(1 + \Delta^2 T_2^2 + 4|G|^2 T_1 T_2)(\Delta - \delta + i/T_2)} \times \frac{(\delta - \Delta - i/T_2)(-\delta + 2i/T_2)}{(\delta - i/T_1)(\delta - \Delta - i/T_2)(\delta + \Delta - i/T_2) - 4|G|^2(\delta - i/T_2)} \tag{5.9d}$$

$$\sigma_{11}^{(+)} = \frac{i\sigma_{g1}^{(0)} + iG\sigma_{g1}^{(+)} - iG^*\sigma_{g1}^{(+)}}{1/T_1 - i\delta}$$

$$\sigma_{11}^{(-)} = \frac{-i\sigma_{g1}^{(0)} - iG\sigma_{g1}^{(+)} + iG^*\sigma_{g1}^{(+)}}{1/T_1 + i\delta} \tag{5.9e}$$

and $\sigma_{g1}^{(0)} = \sigma_{1g}^{(0)*}$, $\sigma_{g1}^{(\pm)} = \sigma_{1g}^{(\mp)*}$. Now, the steady state value of atomic coherence $\sigma_{1g}^{(+)}$ will yield the susceptibility at frequency ω as given below:

$$\chi = -\frac{N|d|^2}{\hbar} \frac{1 + \Delta^2 {T_2}^2}{(1 + \Delta^2 {T_2}^2 + 4|G|^2 T_1 T_2)(\Delta + \delta + i/T_2)} \times \left[1 - \frac{2|G|^2 (\Delta - i/T_2)^{-1} (\delta + 2i/T_2)(\delta - \Delta + i/T_2)}{(\delta + i/T_1)(\delta + \Delta + i/T_2)(\delta - \Delta + i/T_2) - 4|G|^2(\delta + i/T_2)}\right], \tag{5.10}$$

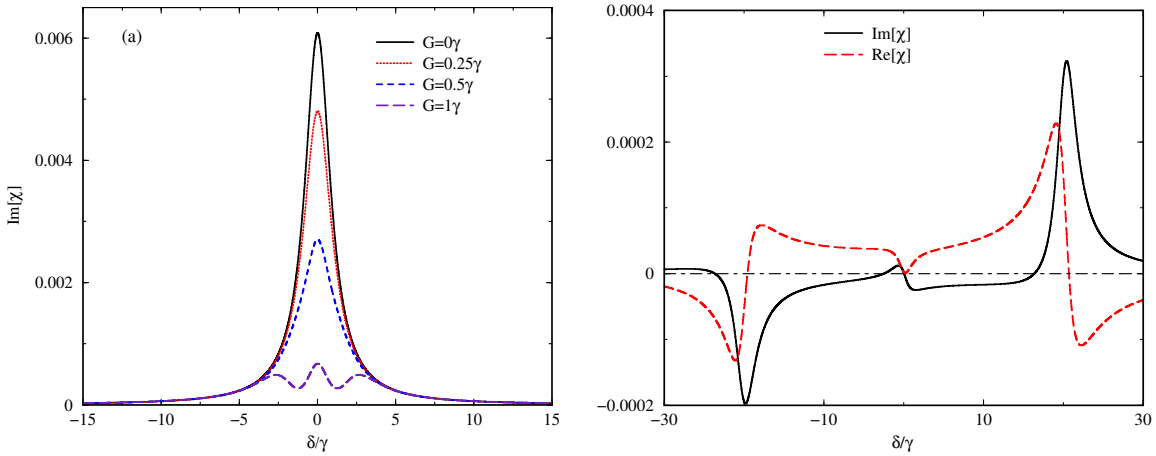

Figure 5.2: *(a) The absorptive response of the probe is shown as a function of the probe detunning δ/γ for a pump field at resonance condition $\Delta = 0\gamma$. (b)Probe absorption and dispersion spectra for a driven two level atom as function of probe detuning δ/γ with pump detunning $\Delta = -2.5\gamma$, $G = 10\gamma$,. The common parameters of the above two graphs for ^{87}Rb vapor are chosen as density N$= 2 \times 10^{11}$ atoms/cc, T_1=$T_2/2 = 1/2\gamma$, and $\gamma = 3\pi \times 10^6$ rad/sec.*

This susceptibility expression was first derived by Mollow in a driven two level system [157]. The Fig. (5.2(a)) shows the imaginary part of χ as a function of the probe detunning δ/γ, where the pump field is tuned directly to the atomic resonance condition $\Delta = 0$. It is clear from the Fig. (5.2(a)) that the probe absorption spectrum begins to saturate as the pump field intensity is increased from zero to well above saturation. At $G = 1\gamma$, the probe absorption spectrum split up into three-peaked spectrum and the positions of the three peaks are at ω, $\omega - 2G$ and $\omega + 2G$ respectively. The probe absorption spectrum become asymmetric when $\Delta < 0$ as shown in the Fig. (5.2(b)). The probe field absorption acquires negative values at frequency $\omega - 2G$, representing stimulated emission even though population inversion does not occur as shown in the Fig. (5.2(b)). This was first dealt by Mollow in 1972 [157] and observed [158] a few years later. It is also clear from the Fig. (5.2(b)), a dispersive characteristics appears around $\omega \approx \omega_c$ in the absorption spectra which corresponds to stimulated Rayleigh scattering. The dispersion like behavior in the absorption spectrum was explained by Agarwal [159] in great detail. The gain associated with dispersive type feature has been utilized for optical parametric oscillation [160]. The understanding of such physical phenomena was provided by Cohen-Tannoudji and Reynaud by introducing a dressed state picture of the atom-field system [161].

5.2 Saturation Absorption Spectroscopy and Lamb Dip

Saturation absorption spectroscopy [19, 20, 21, 22, 23] was perhaps the first spectroscopically interesting nonlinear optical phenomena, discovered just after the operation of the first gas laser by Javan in 1961 [162]. This spectroscopy is based on the velocity-selective saturation of the Doppler broadened atomic medium and is often called Lamb-dip spectroscopy. The broadening of the spectral line is a result of the thermal motion of the atoms in the atomic gas.

We first consider the Doppler effect qualitatively. If a laser, having frequency (ω) is incident on the cell containing the thermal atoms. The frequency of the laser as seen by the moving atom with a velocity v along the z-direction is given by

$$\omega(v) = \omega\left(1 \pm \frac{v}{c}\right). \tag{5.11}$$

where the lower (upper) sign corresponds to a co-propagating (counter-propagating) atom and field. The probability that an atom has a velocity between v and $v + dv$ is given by the Maxwell distribution

$$\mathrm{P}(kv)d(kv) = \frac{1}{\sqrt{2\pi\mathrm{D}^2}} e^{-(kv)^2/2\mathrm{D}^2} d(kv), \tag{5.12}$$

where D is the Doppler width defined by

$$D = \sqrt{K_B T\omega^2/Mc^2}. \tag{5.13}$$

and it is therefore dependent on the temperature of atomic gas. If the incident powerful laser (pump) has a smaller bandwidth than the Doppler width of the absorbing atoms, saturation occurs only for a subset of atoms within the Doppler spread. In laser spectroscopy, Doppler broadening is often called as an inhomogeneous broadening. The narrow band laser at frequency ω travelling in the z-direction is absorbed only by the particular subset of atoms with z component of the velocity such that their rest resonance frequency ω_{1g} matches with Doppler shifted frequency ω:

$$\frac{v}{c} = \frac{\omega - \omega_{1g}}{\omega} \tag{5.14}$$

This particular velocity component is absent in the Doppler velocity distribution and hence it produces a hole in the lower level population distribution. A probe laser (weak field)

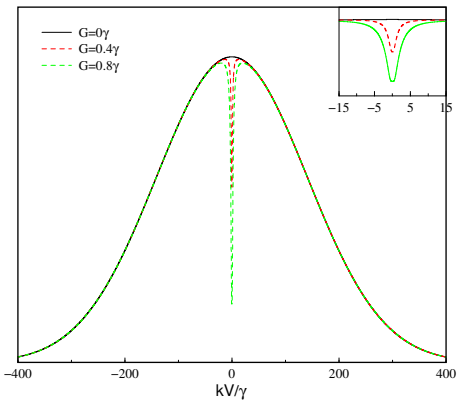

Figure 5.3: *"Lamb dip" or a hole in the probe absorption spectrum caused by the counterpropagating pump field at resonance condition. The inset shows the close up of the "Lamb dip" near kv/γ=0*

tuned to the same frequency finds the gas transparent because of the population depletion of the lower level. The gas become transparent if the probe laser is travelling in the same direction, but if its direction is reversed it probes atoms which have velocity, $-v$, and the gas no longer appears transparent. The velocity dependent susceptibility can give rise the dip in the probe spectrum when the doppler shifted probe $(\omega - kv)$ and pump field $(\omega_c + kv)$ are taken into account of the Eq. (5.10). A dip of width of the order of $1/T_1$ is created when the strong pump and weak probe laser are at the resonance with the system as shown in the Fig. (5.3). The dip in the probe absorption spectrum corresponds to a hole in the lower level population distribution. It is clear from the Fig. (5.3) that the dip never go to zero no matter how strong the pump laser is and attains the minimum value when the medium saturates. At that instant the population distribution between lower and upper level become equal. The dip in the probe absorption spectrum accompanied with a rapid variation of refractive index is able to produced slow light in Doppler-broadened system.

5.3 Susceptibilities $\chi(\omega)$ of the Doppler Broadened Medium

In the present case, we consider that the probe and the control field are co-propagating $(\omega - kv)$ and counter-propagating $(\omega_c + k_c v)$ with the atom, respectively. Therefore, the Doppler shift of the detunings of the Eq. (5.7) can be written as

$$\Delta(v) = \Delta + kv, \quad \delta(v) = \delta - 2kv \tag{5.15}$$

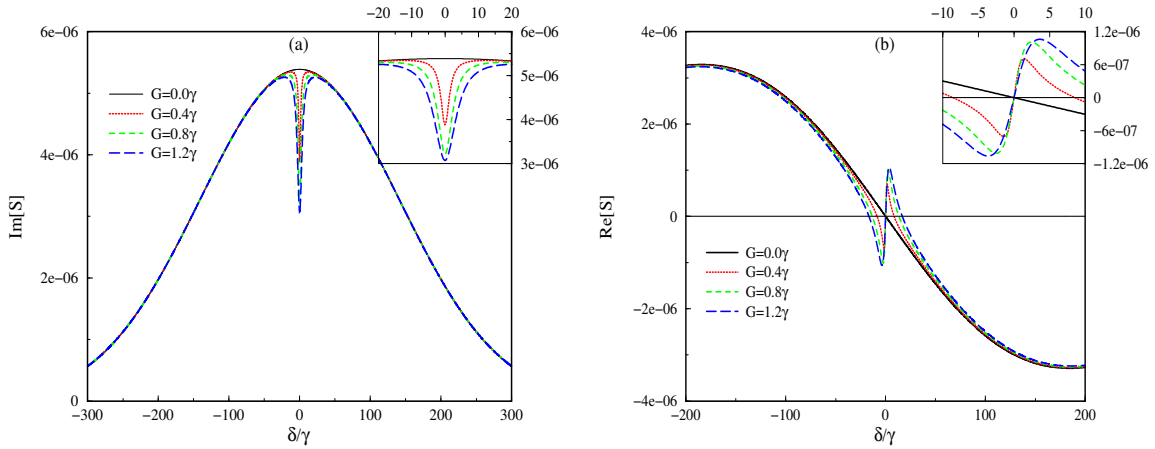

Figure 5.4: *The imaginary (a) and real parts (b) of susceptibility $S(\omega)$ at the probe frequency ω in the presence of pump field G. Here we considered the pump field is in resonance. The insets shows a zoom part of the same near $\delta/\gamma = 0$. The common parameters of the above four curve for ^{87}Rb vapor are chosen as: Doppler width parameter D= 1.33×10^9 rad/sec, density N= 2×10^{11} atoms/cc, $\gamma = 3\pi \times 10^6$ rad/sec.*

where we assume $k = k_c$ for simplicity of our numerical calculation. Next we need to take into account the atomic thermal motion which is assume to obey the Maxwellian distribution

$$\mathrm{P}(kv)d(kv) = \frac{1}{\sqrt{2\pi \mathrm{D}^2}} e^{-(kv)^2/2\mathrm{D}^2} d(kv), \tag{5.16}$$

with D is the Doppler width defined by

$$D = \sqrt{K_B T \omega^2 / Mc^2}. \tag{5.17}$$

For a Doppler broadened system, one needs to averages the susceptibility χ over the Doppler distribution which is given by

$$\langle \chi \rangle = \int_{-\infty}^{\infty} \chi(kv) P(kv) d(kv) \tag{5.18}$$

We denote the average of $\chi(\omega)$ by $\mathcal{S}(\omega)$. We show in Fig. (5.4), the behavior of imaginary and real parts of the susceptibility, $S(\omega)$, assuming that the counter propagating pump is in resonance with atomic transition i.e, $\omega_c = \omega_{1g}$. The imaginary part of $S(\omega)$ shows the typical Lamb dip [163] which becomes deeper with the increase in the intensity of the saturating beam. We show the behavior in the region of Lamb dip. The width of the Lamb dip is the order of 2γ. The real part of $S(\omega)$ exhibits normal dispersion, which in fact, is very pronounced. It is this sharp dispersion which can produce slow light. In our numerical simulation we have chosen typical parameters corresponds to the D_1 absorption

line of ^{87}Rb: $T_1 = T_2/2 = 1/2\gamma$, $\gamma = 3\pi \times 10^6$ rad/sec, D$= 1.33 \times 10^9$ rad/sec (at room temperature), N$= 2 \times 10^{11}$ atom/cc and $\lambda = 795$ nm.

5.4 Pulse Propagation and Verification

Consider the incident pulse of the form

$$\vec{E}(t) \equiv \vec{\mathcal{E}}(1 + \mathrm{m}\cos\nu t)e^{-i(\omega t - kz)} + c.c., \;\; k = \frac{\omega}{c} \tag{5.19}$$

where m and ν are the modulation index and frequency respectively. For small modulations, we can use the approximation

$$S(\omega \pm \nu) = S(\omega) \pm \nu\frac{\partial S}{\partial \omega} \tag{5.20}$$

Therefore, the probe field at the output face $z = l$ of the medium, can be expressed as

$$\begin{aligned}
\vec{E}(l,t) &= \vec{\mathcal{E}}\,(1 + m\cos[\nu t])\, e^{-i(\omega t - \frac{\omega l n(\omega)}{c})} + c.c., \;\; k = \frac{\omega n(\omega)}{c} \text{ and } n(\omega) = 1 + 2\pi S(\omega) \\
&= \vec{\mathcal{E}} e^{-i(\omega t - \frac{\omega l n(\omega)}{c})} + \frac{m\vec{\mathcal{E}}}{2} e^{-i(\omega-\nu)t} e^{i\frac{(\omega-\nu)l}{c} n(\omega-\nu)} + \frac{m\vec{\mathcal{E}}}{2} e^{-i(\omega+\nu)t} e^{i\frac{(\omega+\nu)l}{c} n(\omega+\nu)} + c.c., \\
&= \left[1 + \frac{m}{2}\left(e^{i\nu\left\{t + \frac{l}{c}(1 + 2\pi S + 2\pi\omega\frac{\partial S}{\partial\omega})\right\}} + e^{-i\nu\left\{t + \frac{l}{c}(1 + 2\pi S + 2\pi\omega\frac{\partial S}{\partial\omega})\right\}}\right)\right] \times \\
&\quad \vec{\mathcal{E}} e^{-i\omega(t - \frac{l}{c} + \frac{2\pi i\omega l S}{c})} + c.c., \\
&\approx \left[1 + \frac{m}{2}\left(e^{i\nu\left\{t + \frac{2\pi\omega l}{c}\frac{\partial S}{\partial\omega}\right\}} + e^{-i\nu\left\{t + \frac{2\pi\omega l}{c}\frac{\partial S}{\partial\omega}\right\}}\right)\right] \vec{\mathcal{E}} e^{-i\omega(t - \frac{l}{c} + \frac{2\pi i\omega l S}{c})} + c.c., \\
&= \vec{\mathcal{E}}(1 + m\cos[\nu(t+\theta)]) e^{-i(\omega t - kl) + i\frac{\omega}{c} 2\pi l S(\omega)} + c.c.,
\end{aligned} \tag{5.21}$$

where the delay time, θ, is defined by

$$\theta = 2\pi l \frac{\omega}{c}\frac{\partial Re[S]}{\partial\omega}. \tag{5.22}$$

Note that θ will be positive if $\partial Re[S]/\partial\omega > 0$, i.e, if the medium exhibits normal dispersion. Note further the relation of the parameter θ to the group velocity and the group index :

$$v_g = \frac{c}{n_g} = \frac{c}{\left(1 + 2\pi Re[S(\omega)] + 2\pi\omega\frac{\partial Re[S]}{\partial\omega}\right)}, \tag{5.23}$$

where real part of $S(\omega)$ is zero at resonance condition and has very small value of order of 10^{-7} in the neighborhood of resonance. Therefore, one can drop the term $2\pi Re[S(\omega)]$ from the group index expression and it reduces to $(1 + 2\pi\omega\partial Re[S]/\partial\omega)$. The imaginary

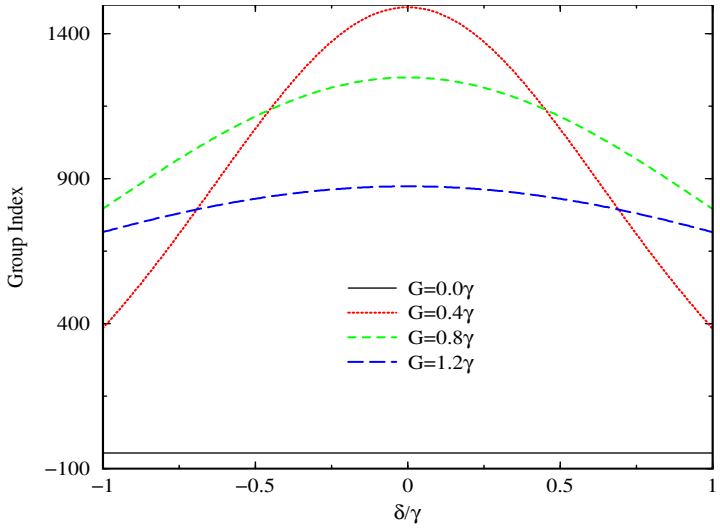

Figure 5.5: *The variation of group index with the detuning of the probe field. The parameters are chosen as :* N=2×10^{11} *atoms/cc,* D=1.33×10^{9} *rad/sec,* $\gamma = 3\pi \times 10^{6}$ *rad/sec and* $\Delta = 0$.

part of $S(\omega)$ will give the overall attenuation of the probe pulse inside the medium. We will present numerical results for the group index by evaluating Eq. (5.23) at different intensities of the counter propagating beam. The calculated group index, n_g, as a function of the detuning of the probe from the atomic transition is shown in Fig. (5.5). Clearly the group index is larger for values of the intensity of the saturating pump $G = 0.4\gamma$. One can calculate n_g as a function of G, for $\delta = 0$, and the result is shown in the Fig. (5.6).

To confirm these results, we also studied the propagation of a Gaussian pulse with an envelope given by

$$\begin{aligned} \mathcal{E}(t - L/c) &= \frac{\mathcal{E}_0}{2\pi} \exp\left[-(t - L/c)^2/\tau^2\right] \\ \mathcal{E}(\omega) &= \frac{\mathcal{E}_0}{\sqrt{\pi\Gamma^2}} \exp\left[-(\omega - \omega_0)^2/\Gamma^2\right], \end{aligned} \tag{5.24}$$

where $\Gamma\tau$ is equal to 2. We use $\Gamma = 120$ KHz for our numerical simulation. The electric field of input pulse is given by

$$\begin{aligned} \vec{E}_{in}(z,t) &\equiv \hat{\epsilon} \int_{-\infty}^{\infty} d\omega \mathcal{E}(\omega) e^{-i(\omega t - kz)} \\ &\equiv \hat{\epsilon} e^{-\frac{\Gamma^2}{4}(t - z/c)^2} e^{-i\omega_0(t - z/c)} \end{aligned} \tag{5.25}$$

Here, we consider the atomic system is dilute, for this reason the back reflections are very

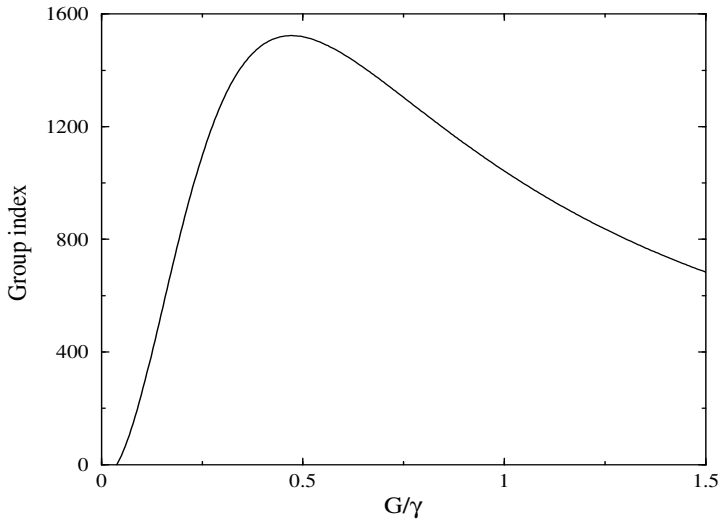

Figure 5.6: *Group index variation with the Rabi frequency of the saturating field. The parameters are chosen as : N=2* $\times 10^{11}$ *atoms/cc, D=1.33* $\times 10^{9}$ *rad/sec,* $\gamma = 3\pi \times 10^{6}$ *rad/sec,* $\Delta = 0$*, and* $\delta = 0$*.*

negligibly small. Therefore, the electric field of the output pulse can be written as

$$\vec{E}_{out}(L,t) \equiv \hat{\epsilon} \int_{-\infty}^{\infty} d\omega \mathcal{E}(\omega) e^{\left[-i\omega(t-L/c)+\frac{2i\pi\omega S(\omega)}{c}\right]} \tag{5.26}$$

Using Eqs.(5.18) and (5.24) we evaluate numerically the output pulse and show the result in Fig. (5.7). The pulse delay of $0.05\ \mu sec$ due to the medium is seen in the Fig. (5.7). The group velocity of the pulse, calculated from the relative delay between the reference pulse and the output pulse, is in good agreement, with the value of group index $[(c/v_g) = 1500]$. We get 2.1% transmission of Gaussian pulse. The transmitted intensity is almost same as in any saturation absorption experiment [164]. This value of transmission can be understood by evaluating Im$[4\pi l\omega S(\omega)/c]$(cf. Eq. (5.21)) which is found to be 3.84. This implies a transmission $e^{-3.84} \sim 2.1\%$. The condition for distortionless pulse propagation is that the spectral width of the Gaussian pulse to be well contained within the region of Lamb dip of the medium. If the pulse spectrum becomes too broad relative to width of the Lamb dip then simple expression like (5.23) does not hold. One can, however still calculate numerically the output pulse.

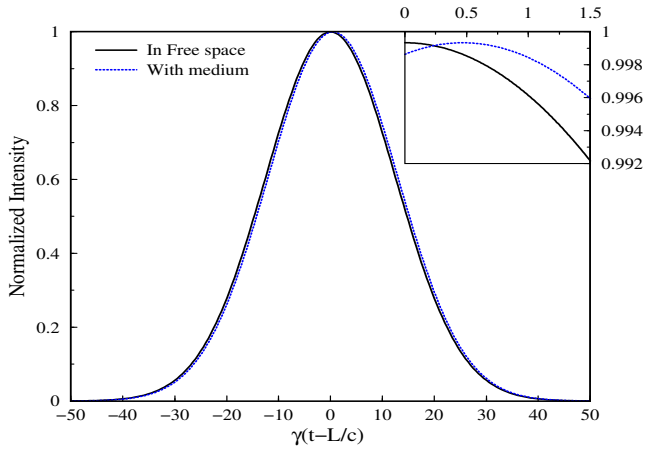

Figure 5.7: *The Solid curve shows light pulse propagating at speed c through 1 cm of vacuum. The dotted curve shows same light pulse propagation through a medium of length 1 cm with time delay .05μsec in the presence of saturating pump with Rabi frequency $G = 0.4\gamma$. The common parameters of the above graph for ^{87}Rb vapor are chosen as $N = 2 \times 10^{11}$ atoms/cc, D= 1.33×10^9 rad/sec, $\gamma = 3\pi \times 10^6$ rad/sec, $\Delta = 0$ and $\delta = 0$. The transmission intensity is 2.1%. The inset shows the close up of the Gaussian pulse with a spectral width 120 KHz.*

5.5 Summary

In summary, we have studied how Lamb dip and saturated absorption spectroscopy can be used to produce slow light with group indices of the order of 10^3 in a Doppler broadened medium, which otherwise has very flat dispersion. We also studied the propagation of Gaussian pulse to verify the results that are obtained from susceptibility calculation. We illustrate our results using the case of the rubidium atomic vapors. We believe that a very similar result or even more remarkable results on slowing of light can be obtained for inhomogenously broadened solid state systems, where the densities are large.

CHAPTER 6

Stoppage of Light in Hot Atomic Gases

In the previous chapter we have demonstrated that subluminal propagation of light in Doppler-broadened medium can be achieved by using the phenomenon of saturation absorption. Slowing down the group velocity of light pulse to zero in a Doppler-broadened medium is especially intriguing. Kocharovskaya *et al.* demonstrated how the light can be stopped in a coherently driven Doppler-broadened medium via electromagnetically induced transparency [71]. This can be achieved by using the property of spatial dispersion of the refractive index of the medium. It is well known from both theory and experiments how control fields can produce spatially varying refractive index profiles [70]. Kocharovskaya *et al.* argued that the motion of atoms leads naturally to a refractive index or a susceptibility that is dependent on both the propagation vector and the frequency. Explicit calculation for a Λ-system shows that the stoppage of light occurs when the control fields are suitable detunned from the atomic transition and when the central frequency of the probe pulse satisfies two photon resonance condition. This stoppage light mechanism is quite different from that in [69], as it does not require switching off and on of the control field. All these have a remarkable bearing on the pulse propagation. In this chapter we demonstrate how the application of a lower level coupling field in Doppler-broadened EIT medium makes it easy to change the group velocity from negative value to positive value and hence helps in stopping light inside the medium.

6.1 Group Velocity and Spatial Dispersive Hot Atomic Medium

The evolution of the slowly varying electric field amplitude along the z-direction is described by Maxwell's equations

$$\frac{\partial \mathcal{E}_0}{\partial z} + \frac{1}{c}\frac{\partial \mathcal{E}_0}{\partial t} = 2\pi i k \mathcal{P}_0. \tag{6.1}$$

where the electric field $\vec{E}(z,t)$ and the polarization $\vec{P}(z,t)$ are given by

$$\vec{E}(z,t) = \hat{e}\vec{\mathcal{E}}_0(z,t)e^{-i(\omega_0 t - k_0 z)} + \text{c.}c. \tag{6.2}$$

$$\vec{\mathcal{P}}(z,t) = \hat{e}\vec{\mathcal{P}}_0(z,t)e^{-i(\omega_0 t - k_0 z)} + c.c. \tag{6.3}$$

and we have assumed the central frequency, ω_0, is very close to the atomic transition frequency ($\omega_0 = \omega_{13}$). For a linear response medium, the polarization $\mathcal{P}(z,t)$ is related to the electric field by

$$\mathcal{P}(z,t) = \int_{-\infty}^{\infty} \chi(\omega,k)E(\omega,k)e^{-i(\omega t - kz)}dkd\omega. \tag{6.4}$$

The electric field $E(k,\omega)$ and susceptibility $\chi(\omega,k)$ are related with $E(z,t)$ and $\chi(t-t',z-z')$ by Fourier transformation as given below:

$$E(z,t) = \int_{-\infty}^{\infty} E(k,\omega)e^{-i(\omega t - kz)}dkd\omega \tag{6.5}$$

$$\chi(z-z',t-t') = \int_{-\infty}^{\infty} \chi(k,\omega)e^{-i[\omega(t-t') - k(z-z')]}dkd\omega. \tag{6.6}$$

As is well known, a spatially dispersive medium [165] is characterized by a susceptibility $\chi(k,\omega)$ that is dependent on the propagation vector, $\vec{k}$, and frequency, ω. Further, the allowed wavevectors are given by the dispersion relation

$$k^2 = \frac{\omega^2}{c^2}\left[1 + 4\pi\chi(k,\omega)\right]. \tag{6.7}$$

The above dispersion relation can lead to many real solutions for k, for a fixed ω, and thus one has the possibility of additional waves in a spatially dispersive medium. For a dilute atomic gas, where $|\chi| \ll 1$, optical refractive index can be expressed as $n = 1 + 2\pi\chi(k,\omega)$. In this case we would basically have a single wave. It is convenient to decompose $\chi(\omega,k)$ in a Taylor series as

$$\chi(\omega,k) = \chi(\omega_0,k_0) + (\omega-\omega_0)\left[\frac{\partial\chi}{\partial\omega}\right]_{\omega_0} + (k-k_0)\left[\frac{\partial\chi}{\partial k}\right]_{k_0} + \cdots \tag{6.8}$$

and we obtain expression for induced polarization (keeping terms only upto first order),

$$\mathcal{P}(z,t) = \left[\chi(\omega_0,k_0)\mathcal{E}_0(z,t) + i\frac{\partial\chi(\omega_0,k_0)}{\partial\omega}\frac{\partial\mathcal{E}_0}{\partial t} - i\frac{\partial\chi(\omega_0,k_0)}{\partial k}\frac{\partial\mathcal{E}_0}{\partial z}\right]e^{-i(\omega_0 t - k_0 z)}. \tag{6.9}$$

Substituting the polarization (6.9) into the wave equation (6.1), we can obtain the wave equation in a simplified form

$$\frac{\partial\mathcal{E}_0}{\partial z} + \frac{1}{c}\frac{\partial\mathcal{E}_0}{\partial t} = 2\pi i k_0\left[\chi(\omega_0,k_0)\mathcal{E}_0(z,t) + i\frac{\partial\chi(\omega_0,k_0)}{\partial\omega}\frac{\partial\mathcal{E}_0}{\partial t} - i\frac{\partial\chi(\omega_0,k_0)}{\partial k}\frac{\partial\mathcal{E}_0}{\partial z}\right]. \tag{6.10}$$

Subsequent rearrangement of the Eq. (6.10) gives

$$\frac{\partial\mathcal{E}_0}{\partial z} + \frac{1}{V_g}\frac{\partial\mathcal{E}_0}{\partial t} = 0, \tag{6.11}$$

where the group velocity of the light pulse is expressed as:

$$V_g \equiv \mathrm{Re}\frac{d\omega}{dk} = \mathrm{Re}\left[\frac{c\,(1 - 2\pi k_0\partial\chi/\partial k)}{1 + 2\pi\chi + 2\pi\omega_0\partial\chi/\partial\omega}\right]. \tag{6.12}$$

This formula assumes weak spatial as well as temporal dispersion and negligible absorption. In a hot atomic gases, the Doppler-broadening has to be taken into the calculation of susceptibility $\chi(k,\omega)$ expression. Therefore, susceptibility $\chi(k,\omega)$ is to be replaced by the average values $\chi(\omega - kv)$ over the Maxwell distribution of velocities. Then the expression for the group velocity becomes

$$V_g = \mathrm{Re}\left[\frac{c\left(1 + 2\pi k\langle v\frac{\partial\chi}{\partial\omega}\rangle\right)}{1 + 2\pi\langle\chi\rangle + 2\pi\omega\langle\frac{\partial\chi}{\partial\omega}\rangle}\right]. \tag{6.13}$$

Note that

$$\langle v\frac{\partial\chi}{\partial\omega}\rangle \neq \langle v\rangle\langle\frac{\partial\chi}{\partial\omega}\rangle \neq 0, \tag{6.14}$$

and hence the stoppage of light takes place if the numerator in Eq. (6.13) vanishes. In the following section, we derive the expression of the susceptibility $\chi(\omega)$ for a closed Λ-system by solving the density matrix equation in the steady state limit.

6.2 Model Configuration and Its Basic Equations

We consider the scheme as shown in Fig. (6.1). We apply a control field $E_c(z,t)$ of frequency ω_2 on the optical transition $|1\rangle \leftrightarrow |2\rangle$. The transition $|2\rangle \leftrightarrow |3\rangle$ is generally an electric dipole forbidden transition. The states $|2\rangle$ and $|3\rangle$ are metastable states. We apply an additional

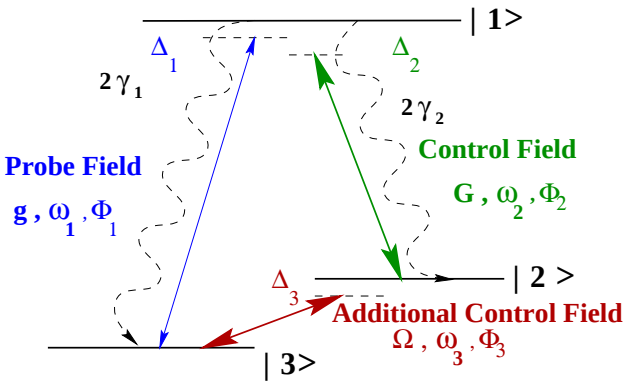

Figure 6.1: *Schematic diagram of three level Λ-system; the probe pulse is applied on the transition $|1\rangle \leftrightarrow |3\rangle$; other fields are cw.*

control field of frequency ω_3 on the transition $|2\rangle \leftrightarrow |3\rangle$. The probe pulse $E_p(z,t)$ acts on the transition $|1\rangle \leftrightarrow |3\rangle$. Here $E_i(z,t) = \mathcal{E}_i(z,t)e^{i(\omega_i t - k_i z)} + c.c.$, with $\mathcal{E}_i(z,t)$ being the slowly varying amplitude of the field envelope and k_i, the propagation vector; $i = c, p$ refers to the control field and probe field, respectively. The state $|1\rangle$ decays to the states $|3\rangle$ and $|2\rangle$ at the rates $2\gamma_1$ and $2\gamma_2$. Let $2g = 2\vec{d}_{13}.\vec{E}_p/\hbar$, $2G = 2\vec{d}_{12}.\vec{E}_c/\hbar$ and 2Ω be the Rabi frequencies of the probe field, control field $\vec{E}_c$ and the LL coupling field, respectively. The susceptibility $\chi(\omega_1)$ of medium can be obtained by solving the density matrix equations for the Λ-system as shown in Fig. (6.1). The calculation of the density matrix element ρ_{13} is done upto first order in the applied optical field on the transition $|1\rangle \leftrightarrow |3\rangle$ but to all orders in the control field and the LL coupling field. It is not necessary to calculate upto first order in probe; exact calculation is also possible. However one studies concepts like group velocity in a linear medium and therefore we treat probe to first order so that the medium is linear as far as probe is concerned. In order to proceed further we make the following transformation on the off-diagonal matrix elements of the density matrix

$$\rho_{12} = \sigma_{12}e^{-i(\omega_2 t+\phi_2)}, \quad \rho_{13} = \sigma_{13}e^{-i(\omega_2+\omega_3)t-i(\phi_2+\phi_3)}, \quad \rho_{23} = \sigma_{23}e^{-i(\omega_3 t+\phi_3)}, \tag{6.15}$$

However it should be born in mind that the full density matrix in Schrödinger picture is to be obtained by using Eq. (6.15). We can write the equations for the density matrix elements

as

$$\begin{aligned}
\dot{\sigma}_{11} &= iG\sigma_{21} + ige^{-i(\Delta_4 t+\delta\phi)}\sigma_{31} - iG^*\sigma_{12} - ig^*e^{i(\Delta_4 t+\delta\phi)}\sigma_{13} - 2(\gamma_1+\gamma_2)\sigma_{11}, \\
\dot{\sigma}_{22} &= iG^*\sigma_{12} + i\Omega\sigma_{32} - iG\sigma_{21} - i\Omega^*\sigma_{23} + 2\gamma_2\sigma_{11}\ , \\
\dot{\sigma}_{12} &= -[\gamma_1+\gamma_2+\Gamma_{12} - i\Delta_2]\sigma_{12} + iG\sigma_{22} + ige^{-i(\Delta_4 t+\delta\phi)}\sigma_{32} - iG\sigma_{11} - i\Omega^*\sigma_{13} \\
\dot{\sigma}_{13} &= -[\gamma_1+\gamma_2+\Gamma_{13} - i(\Delta_2+\Delta_3)]\sigma_{13} + iG\sigma_{23} + ige^{-i(\Delta_4 t+\delta\phi)}\sigma_{33} \\
&\quad -ige^{-i(\Delta_4 t+\delta\phi)}\sigma_{11} - i\Omega\sigma_{12}, \\
\dot{\sigma}_{23} &= -(\Gamma_{23} - i\Delta_3)\sigma_{23} + iG^*\sigma_{13} + i\Omega\sigma_{33} - ige^{-i(\Delta_4 t+\delta\phi)}\sigma_{21} - i\Omega\sigma_{22},
\end{aligned} \tag{6.16}$$

with $\sigma_{ji} = \sigma^*_{ij}$ and $\sigma_{11} + \sigma_{22} + \sigma_{33} = 1$. Here Γ's give collisional dephasing terms; Δ_i's are the detunings

$$\Delta_1 = \omega_1 - \omega_{13},\ \ \Delta_2 = \omega_2 - \omega_{12},\ \ \Delta_3 = \omega_3 - \omega_{23},\ \ \Delta_4 = \omega_1 - \omega_2 - \omega_3, \tag{6.17}$$

and the relative phase difference of the probe field to the sum of the pump and additional control field is

$$\delta\phi = \phi_1 - \phi_2 - \phi_3. \tag{6.18}$$

The susceptibility χ can be obtained by considering the steady state solution of (6.16) to first order in the probe field on the transition $|1\rangle \leftrightarrow |3\rangle$. For this purpose we assume $\gamma_1 = \gamma_2 = \gamma$ and write the solution as

$$\sigma = \sigma^0 \ + \ \frac{g}{\gamma}\, e^{-i(\Delta_4 t+\delta\phi)}\ \sigma^+ \ + \ \frac{g^*}{\gamma}\, e^{i(\Delta_4 t+\delta\phi)}\ \sigma^- + ... \tag{6.19}$$

On combining Eqs.(6.16) and (6.19), we note that to first order $\rho_{13}(t) \equiv (g/\gamma)e^{-i(\omega_1 t+\phi_1)}$ σ^+_{13}. Thus 13-element of σ^+ will give the susceptibility at the frequency ω_1 which now can be expressed in the form

$$\chi(\omega_1) = \frac{\mathcal{N}|\vec{d}_{13}|^2}{\hbar\gamma}\sigma^+_{13}, \tag{6.20}$$

where $\mathcal{N}$ is the density of the atoms. The phase dependence of different fields does not appear in the susceptibility. Note that the zeroth order contribution in Eqs.(6.19) can result in phase dependent components. However for the range of parameters used in this paper, the zeroth order term is so small that it can be ignored.

To obtain the probe response in a Doppler-broadened medium, σ^+_{13} should be averaged over the Maxwell-Boltzmann velocity distribution of the moving atoms. For a single atom,

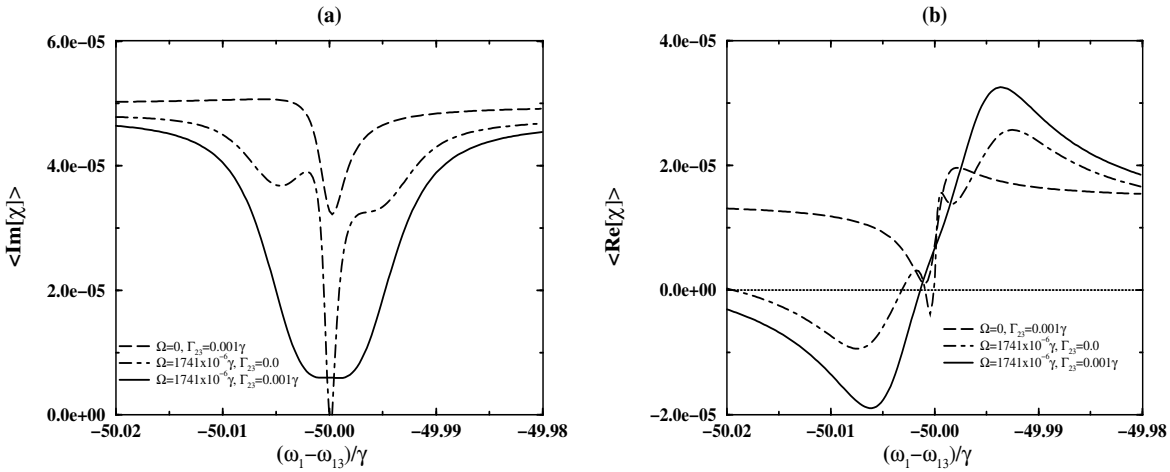

Figure 6.2: *(a) and (b) The imaginary and real parts of susceptibility $\langle[\chi]\rangle$at the probe frequency ω_1 in the presence of control field G and LL coupling field Ω. Detuning Δ_2 of the control field is chosen as -50γ. The common parameters of the above two graphs for ^{87}Rb vapor are chosen as: Doppler width parameter D= 1.33×10^9 rad/sec, density $\mathcal{N} = 10^{12}$ atoms/cc, $G = 0.3\gamma$, $\Delta_3 = 0$, $\Gamma_{12} = \Gamma_{13} = 0$, $\gamma = 3\pi \times 10^6$ rad/sec.*

moving with a velocity v along the z axis, the probe frequency $\omega_1(v)$ and frequencies $\omega_2(v)$, $\omega_3(v)$ of the two control fields as seen by the atom are given by

$$\omega_1(v) = \omega_1 - k_1 v, \;\; \omega_2(v) = \omega_2 - k_2 v, \;\; \omega_3(v) = \omega_3 - k_3 v. \tag{6.21}$$

Thus susceptibilities for moving atoms are obtained by using the substitution (6.21) in the solution of Eqs. (6.16). Note that the velocity dependence of ω_3 is insignificant and can be dropped. For simplicity we can also set $k_1 \approx k_2$. These susceptibilities are to be averaged over the Maxwell-Boltzmann distribution for the atomic velocities, defined by

$$\mathrm{P}(k_1 v) d(k_1 v) = \frac{1}{\sqrt{2\pi \mathrm{D}^2}} e^{-(k_1 v)^2/2\mathrm{D}^2} d(k_1 v), \;\; \mathrm{D} = \sqrt{K_B T \omega_1^2 / M c^2}. \tag{6.22}$$

6.3 Numerical Results on Stoppage of Light

In this section we present numerical results to demonstrate how the stoppage of light is made possible by the application of LL coupling field. Note that the parameters space is rather large and the result will depend on the proper choice of G, Ω, control field detuning Δ_2 and of course the probe field detuning Δ_1. We have carried out the numerical results for a large range of parameters and we present a number of numerical results in Figs. (6.2), (6.3) and (6.4). We have used the parameters for ^{87}Rb with Doppler width parameters

D= 1.33×10^9 rad/sec, $\gamma = 3\pi \times 10^6$ rad/sec, $\lambda = 7950\mathring{A}$, and density $\mathcal{N} = 10^{12}$ atom/cm^3. In Fig. (6.2(a)) and Fig. (6.2(b)) we show the behavior of the susceptibility as a function of the detuning of the probe when the control field ω_2 is detuned, $\Delta_2 = -50\gamma$. It is clear from the Fig.(6.2(a)) that increase of the microwave field intensity results in decrease of the probe absorption in presence of collisional dephasing. At two-photon resonance condition *i.e.,* $\Delta_1 = \Delta_2 = -50\gamma$, the absorption of the probe is very small. Therefore the transparency window is obtained at two-photon resonance condition, *i.e.,* $\omega_1 - \omega_2 = \omega_{13} - \omega_{12}$. Note that the transparency dip that appears in the absorption spectrum has finite bandwidth and its width depends on intensities of control fields. To avoid severe absorption of the probe pulse, one has to choose a narrow-band probe pulse, so that it remains well contained within the bandwidth of the transparency window. However, the transparency dip is a accompanied by a steep variation of $\langle \mathrm{Re}[\chi] \rangle$ with probe detuning. We find that if two control fields are *suitably detuned* then the light can be stopped. We show in the Fig. (6.3(a)) how the group velocity $\langle V_g \rangle$ (defined in Eq. (6.13)), changes from negative values to large positive values as the intensity of the LL coupling field is increased. This change allows to stop the light pulse inside the atomic medium. It is clearly seen from Fig. (6.3(a)), the group velocity $\langle V_g \rangle$ become zero at the value of $\Omega = 1741 \times 10^{-6}\gamma$ when the control field G is out of one-photon resonance but satisfies the two photon resonance condition ($\Delta_1 = \Delta_2 = -50\gamma$). Note that for $^{87}\mathrm{Rb}$, a Rabi frequency of $10^{-6}\gamma$ implies a magnetic field of the order of .993μG. The slope of $\langle \mathrm{Re}[\chi] \rangle$ with respect to central frequency of the probe pulse depends on the intensity of the two control fields and density of atoms. The group velocity becomes zero [Fig. 6.3(b)] as the numerator in Eq. (6.13) changes sign when the LL coupling field is increased. Fig. (6.3(c)) gives the group velocity in the absence of spatial dispersion. A comparison of the Figs. 6.3(a) and 6.3(c) shows the important role played by spatial dispersion. Further we notice from the Fig. 6.3(d) that at resonance condition ($\Delta_1 = \Delta_2 = 0$) light cannot be stopped. In order to understand how the application of the microwave field leads to the stoppage of light, we show in the Fig. (6.4) the behavior of the Doppler average of $\langle \partial\chi/\partial\omega_1 \rangle$ and $\langle 1 - 2\pi k_1 \frac{\partial\chi}{\partial k_1} \rangle$ as a function of ω_1. The latter quantity crosses zero which results in the stoppage of light. Figs. (6.3) and (6.4) show how the application of the microwave field changes all the physical quantities. At a more fundamental level the microwave field and pump field together produce new dressed states of the system. Such dressed states determine the response of the system to the applied probe field. However all

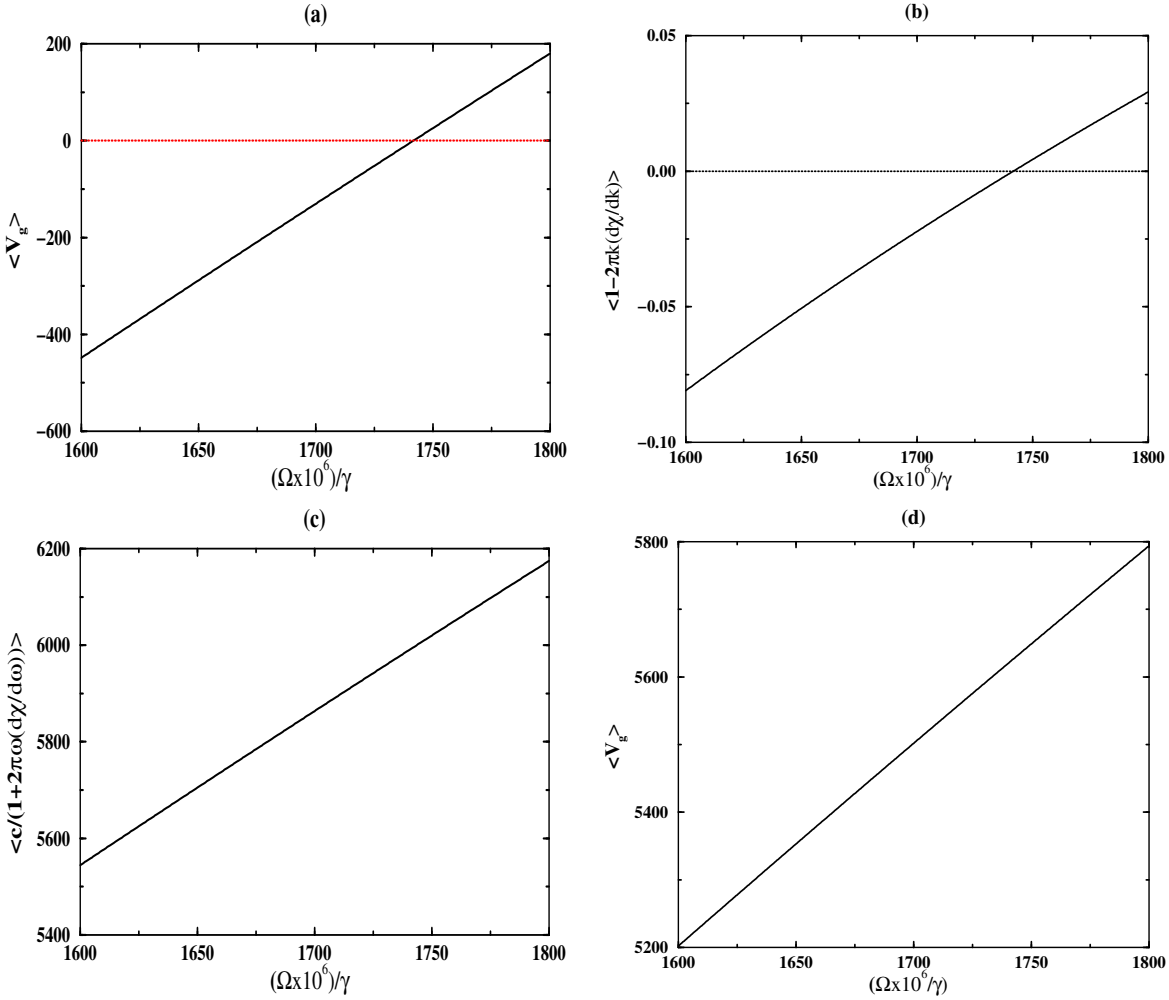

Figure 6.3: *(a) shows variation of group velocity, in cm per sec, (Eq. (6.13)) with the strength Ω of the LL coupling field. The group velocity becomes zero because the numerator in Eq. (6.13) becomes zero as shown in the Fig. 6.3(b). Figs. 6.3(c), 6.3(d) gives the behavior of the group velocity if the spatial dispersion of the susceptibility were ignored. The common parameters of the above three graphs for ^{87}Rb vapor are chosen as: Doppler width parameter D= 1.33×10^9 rad/sec, density $\mathcal{N} = 10^{12}$ atoms/cc, $G = 0.3\gamma$, $\Delta_3 = 0$, $\Gamma_{12} = \Gamma_{13} = 0$, $\Gamma_{23} = 0.001\gamma$, $\gamma = 3\pi \times 10^6$ rad/sec, $\Delta_1 = \Delta_2 = -50\gamma$. For comparison we also show in the Fig. 6.3(d) the result for $\Delta_1 = \Delta_2 = 0$.*

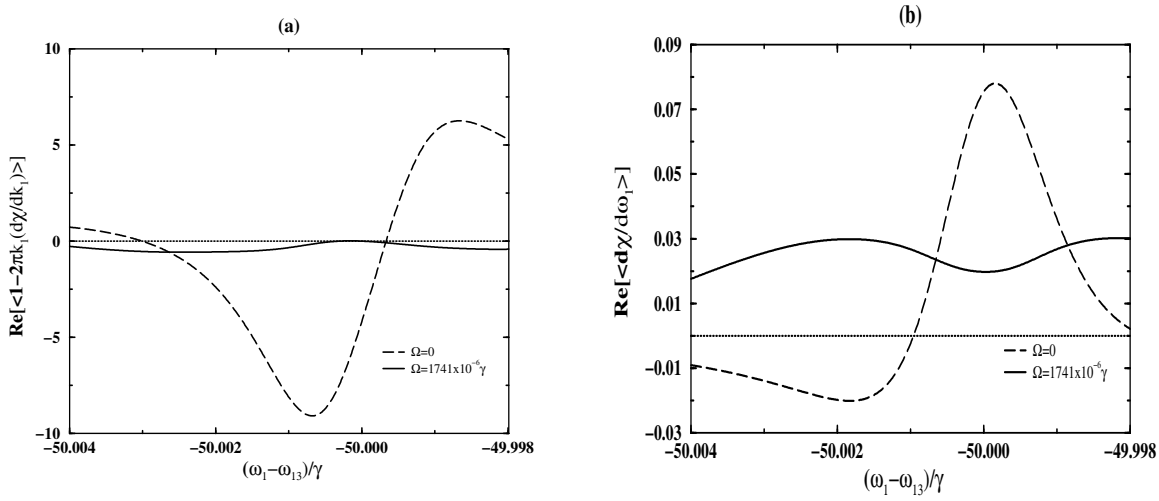

Figure 6.4: *(a) shows the variation of the numerator in Eq. (**??**) with the probe detuning taking Doppler effect into account. Fig. 6.4(b) gives the slope of the susceptibility. The common parameters of the above two graphs for ^{87}Rb vapor are chosen as: Doppler width parameter $D = 1.33 \times 10^9$ rad/sec, density $\mathcal{N} = 10^{12}$ atoms/cc, $G = 0.3\gamma$, $\Delta_3 = 0$, $\Delta_2 = -50\gamma$ $\Gamma_{12} = \Gamma_{13} = 0$, $\Gamma_{23} = 0.001\gamma$, $\gamma = 3\pi \times 10^6$ rad/sec.*

these can be understood easily only for a homogeneously broadened system. Rostovtsev *et al.* have demonstrated that the control fields provide the stoppage of light via dragging effect due to population distribution between the lower levels of different velocity groups [166].

6.4 Summary

In summary, we have demonstrated how the application of an LL coupling field in the Λ system helps one to change the group velocity of the pulse inside the medium from a negative to a positive value, and thereby helps in stopping light. Thus for a suitable detuning of the pump and probe fields, one can stop light by just changing the intensity of the LL coupling field.

Conclusions and Future Outlook

In conclusion, this thesis reports coherent control of subluminal and superluminal propagation of electromagnetic fields in different atomic media. Manipulation of atomic coherence by external coherent control fields leads to changes in the group velocity of the light pulses from subluminal to superluminal range. Our new findings are presented with extensive numerical results which are further substantiated by physical explanations. In the following, we present a brief summary of important conclusions of each chapter and discuss the future outlook of the problems.

In chapter 2, it was shown how one can realize sub- as well as superluminal propagation of light pulses by controlling only the intensity of the additional LL coupling field in Λ-type atomic configuration. The additional LL coupling field is like a knob which changes the dispersive property of the medium from normal to anomalous with a very low absorption or gain. Superluminal velocity of Gaussian pulse was discussed. It was shown that distortionless pulse propagation is possible only when the intensity of the LL coupling field is chosen suitably. Furthermore it was shown that the thermal motion of atoms becomes important in the behavior of the superluminal light pulse propagation through medium driven by the control and LL coupling field.

In chapter 3, we have demonstrated that, the possibility of storage and retrieval of moderately intense probe pulse in an EIT based storage medium via adiabatic as well as nonadiabatic switching of the control field. We found that the retrieved probe pulse remains a replica of the original one, although there is overall broadening and loss of the intensity. These phenomena can be explained in terms of the dependence of the absorption on the intensity of the probe. The dynamical evolution of the control field becomes

important when the intensities of the control and probe fields are comparable. The storage and retrieval of the intense probe pulse can be well understood from the theory of adiabaton. We further showed that the storage and retrieval of information in the form of a modulation is also possible.

In chapter 4, we set out to explain the experimental results of Bigelow *et al.* on the sub and superluminal propagation of optical pulses in nonlinear solid state materials at room temperature [57, 138]. We modeled subluminal propagation in ruby and superluminal propagation in alexandrite as three and four level systems, respectively, coupled to Maxwell equations. The systems under consideration posses very strong transverse and longitudinal relaxation effects. We presented numerical results on the propagation of Gaussian and modulated pulses and showed qualitative agreement with the experimental findings of Bigelow *et al.* [57, 138]. We also pointed out that the input pulses get distorted in shape because the presence of nonlinearity of medium. Our modeling goes well beyond the traditional pump-probe approach and is applicable to other systems with very strong relaxation effects.

In chapter 5, we examined whether it is possible to slow down the light pulses in a Doppler-broadened atomic medium even though such a medium exhibits very flat dispersion. This was made possible by applying a saturating counter propagating beam that produces a hole in the inhomogeneous line shape. A hole, that is, a narrow spectral region of decreased absorption, leads to slow light. In rubidium atomic vapor, we calculated group indices of the order of 10^3. However, similar or even more remarkable results on slowing of light can be obtained for inhomogeneously broadened solid-state system, where the atomic densities are large.

In chapter 6, we presented a new way of freezing the light pulses in a inhomogeneously-broadened atomic medium via electromagnetically induced transparency. We have shown how the application of LL coupling field in a closed Λ-system helps us to change the group velocity of the pulse inside the medium from a negative to positive value and thereby, helps in stopping light. Stoppage of light is made possible by using the dependence of the refractive index on the wave number which is the origin of spatial dispersion of the medium. In this case, the dynamical switching off and on of the control field is not necessary for the stoppage of light.

Recently, Stenner and his coworkers [144] have shown experimentally that the time to

detect information propagation through a gain assisted anomalous dispersive medium is slightly longer than the time required to detect the information travelling the same distance in vacuum, even though superluminal group velocity exceeds the speed of light c. Further, it would be interesting if one can study the information velocity of the intense light pulses through a nonlinear solid-state material like ruby or alexandrite, wherein the light pulse propagates with subluminal or superluminal velocity, respectively.

One can extend the spectral hole burning phenomenon in a Doppler-broadened atomic medium that can be ensemble of atoms with relevant energy levels in Λ-configuration wherein a weak probe pulse together with counter-propagating saturating field couples one arm of the Λ-system and a strong coupling field couples to other arm. One can study the possibility of obtaining ultra-slow light of the weak probe pulse in the presence of both coupling and saturating fields in Doppler-broadened atomic system.

Appendix

Numerical Integration Procedure for Light Pulse Propagation

The Interaction of optical fields with a three level Λ-system are described by the Maxwell-Bloch equations, which are solved consistently. This equations are solved analytically in a few specialized case. In general, the solutions of the Maxwell-Bloch equations can be obtained numerically. The coupled Maxwell-Bloch equation has the following form in the travelling window reference frame with local time $\tau = t - z/c$ and space $\zeta = z$:

$$\begin{aligned}
\frac{\partial \rho_{11}}{\partial \tau} &= -2(\gamma_1+\gamma_2)\rho_{11} + iG\rho_{21} + ig\rho_{31} - iG^*\rho_{12} - ig^*\rho_{13}\ , \\
\frac{\partial \rho_{22}}{\partial \tau} &= 2\gamma_2\rho_{11} + iG^*\rho_{12} - iG\rho_{21}\ , \\
\frac{\partial \rho_{12}}{\partial \tau} &= -[\gamma_1+\gamma_2]\rho_{12} + iG\rho_{22} + ig\rho_{32} - iG\rho_{11}, \\
\frac{\partial \rho_{13}}{\partial \tau} &= -[\gamma_1+\gamma_2]\rho_{13} + iG\rho_{23} + ig\rho_{33} - ig\rho_{11}, \\
\frac{\partial \rho_{23}}{\partial \tau} &= iG^*\rho_{13} - ig\rho_{21}\ .
\end{aligned} \tag{A.1}$$

$$\begin{aligned}
\frac{\partial g}{\partial \zeta} &= i\eta\rho_{13} \\
\frac{\partial G}{\partial \zeta} &= i\eta\rho_{12}
\end{aligned} \tag{A.2}$$

For studying the spatiotemporal evolution of the optical pulses through the resonant systems, the above partial differential equations need to be integrated. The numerical scheme deals with the field-matter as coupled ordinary differential equations instead of solving the partial differential equations. This is made possible since the incoming fields at the entry plane $\zeta = 0$ are known. In this case the Bloch equations are coupled ordinary differ-

ential equations for the variables $\rho_{ij}(\tau, \zeta = 0)$. Given the initial values at $\tau \leq 0$, the values of ρ_{ij} can be determined for all τ in the plane $\zeta = 0$.

The obtained value of matter can be substituted in the field equations (A.2), which gives the field slope along the marching direction ζ. This allows to determine the field at all values of τ at some small depth, $\delta\zeta$, in the system. Having found the field values on the plane at $\zeta = \delta\zeta$, ρ_{ij} is determined everywhere on this plane. In this way the whole (τ, ζ) space may be determined.

The (τ, ζ) plane is covered with a rectangular mesh grid, the step sizes $\delta\zeta$ along the ζ and $\delta\tau$ along the τ being independently chosen. The space step $\delta\zeta$ and time step $\delta\tau$ is totally dependent upon envelope shape of the propagating pulse. Our numerical simulation deals with long Gaussian pulses, sampling point along τ and ζ direction are 4×10^6 and 2×10^6, respectively. The integration of the Maxwell-Bloch equations are performed by predictor corrector method. We prefer the parallization of the sequential code because of the large number of sampling points which requires large execution time. The sequential code can be easily parallelized if each iteration is independent of the other, that is no variables that are written in some iteration will be read and/or written in another iteration. But in our code each iteration is dependent on the previous iteration. Thus for our flow dependence case, the parallelization of the code is difficult and we do the parallelization manually by using OPEN MP directives on RS6000 in IBM machine.

The numerical code has been tested systematically by insuring the reproduction of numerical results of problems such as storage and retrieval of light [83], shape-preserving adiabatic pulse propagation [147] and dynamics of solitons in a coherently driven media [167].

References

[1] Lord Rayleigh, Nature(London) **XXIV**, 382 (1881).

[2] L. Brillouin, *Wave propagation and group velocity* (Academic, New York, 1960).

[3] J.D. Jackson, *Classical Electrodynamics*, (Wiley, New York, 1962).

[4] M.O. Scully and M.S. Zubairy, *Quantum Optics*, (Cambridge University Press, Cambridge, 1997), pg.168.

[5] L. Allen and J.H. Eberly, *Optical resonance and two-level atoms* (Wiley, New York, 1975).

[6] H.A. Kramers, Nature(London) **117**, 775 (1926); R.deL. Kronig, J. Opt. Soc. Am. **12**, 547 (1926).

[7] C. Cohen-Tannoudji, B. Diu and F. Laloë, *Quantum Mechanics*, Vol.2 (John Wiley & Sons, 1977), pg.1307.

[8] A. Einstein, Phys. Z. **18**, 121(1917).

[9] R.Loudon, *The qunatum theory of light*, (Oxford, 1973).

[10] P. Meystre and M. Sergent III, *Elements of Quantum Optics*, Springer-Verlag, Berlin (1989).

[11] I.I. Rabi, Phys. Rev. A **51**, 652 (1937).

[12] C. Cohen-Tannoudji, *Atom in Strong Resonant Fields*, In Balian *et. al.*, editor, *Proceeding of Les Houches* XXVI, page 3, Amsterdam, North Holland (1977).

[13] Y.R. Shen, *The Principles of Nonlinear Optics*(John Wiley & Sons, New York, 1984).

[14] G.S. Agarwal, *Quantum Statistical Theories of Spontaneous Emission and their relation to other approaches*, Springer-Verlag, Berlin (1974).

[15] U. Fano, Phys. Rev. **124**, 1866 (1961).

[16] S.P. Tewari and G.S. Agarwal, Phys. Rev. Lett. **56**, 1811 (1986).

[17] S. Harris, J.E. Field, and A. Imamoglu, Phys. Rev. Lett. **64**, 1107 (1990).

[18] K.J. Boller, A. Imamoglu, and S.E. Harris, Phys. Rev. Lett. **66**, 2539 (1991).

[19] T.W. Hansch, M.D. Levenson, and A.L. Schawlow, Phys. Rev. Lett. **26**, 946 (1971).

[20] S. Haroche and F. Hartmann, Phys. Rev. A **6**, 1280 (1972).

[21] B. Couillaud and A. Ducasse, Phys. Rev. Lett. **35**, 1276 (1975).

[22] M. Sargent III, Phys. Rep. C **43**, 223 (1978).

[23] P.G. Pappas, M.M. Burns, D. D. Hinshelwood, M.S. Feld and D.E. Murnick, Phys. Rev. A **21**, 1955 (1980).

[24] S.H. Autler and C.H. Townes, Phys. Rev. **100**, 707 (1955).

[25] Y. Li and M. Xiao, Phys. Rev. A **51**, 4959 (1995).

[26] S. E. Harris, Physics Today, **50**(7), 36 (1997).

[27] E. Arimondo, in *Progress in Optics* **XXXV** Ed. E. Wolf (North Holland, Amsterdam, 1996), p. 257.

[28] J. P. Marangos, J. Mod. Opt., **45**, 471 (1998).

[29] M.O. Scully, Phys. Rep. **219**, 191 (1992).

[30] M.O. Scully, Phys. Rev. Lett. **67**, 1855 (1990).

[31] M.O. Scully and S.-Y. Zhu, Opt. Commun. **87**, 134 (1992).

[32] U. Rathe, M. Fleishhauer, M. Zhu, S.-Y. Zhu, T.W. Hansch, and M.O. Scully, Phys. Rev. A **47**, 4994 (1993).

[33] A.D. Wilson-Gordon and H. Friedmann, Opt. Commun. **94**, 238 (1992).

[34] M. Fleischhauer, C.H. Keitel, M.O. Scully, C. Su, B.T. Ulrich and S.-Y. Zhu, Phys. Rev. A **46**, 1468 (1992).

[35] M. Fleischhauer, C.H. Keitel, M.O. Scully, and C. Su, Opt. Commun. **87**, 109 (1992).

[36] T.W. Mossberg, *Private communication*.

[37] S.L. McCall and E.L. Hahn, Phys. Rev. Lett. **18**, 908 (1967); S.L. McCall and E.L. Hahn, Phys. Rev. **183**, 457 (1967).

[38] G.L. Lamb, Jr., Rev. Mod. Phys. **43**, 99 (1971).

[39] H.A. Haus, Rev. Mod. Phys. **51**, 331 (1971).

[40] A.I. Maimistov, A.M. Bhasrov, S.O. Elyutin, and M.Y. Sklyarov, Phys. Rep. **191**, 1 (1990).

[41] I.M. Asher and M.O. Scully, Opt. Commun. **3**, 395 (1971).

[42] H.M. Gibbs and R.E. Slusher Phys. Rev. Lett. **24**, 638 (1970).

[43] R.E. Slusher and H.M. Gibbs Phys. Rev. A **5**, 1634 (1972).

[44] R.S. Bennink, R.W. Boyd, C.R. Stroud,Jr., and V. Wong, Phys. Rev. A **63**, 033804 (2001).

[45] S.E. Harris, J.E. Field, and A. Kasapi, Phys. Rev. A **46**, R29 (1992).

[46] M. Xiao, Y-Q. Li, S-Z. Jin, and J. Gea-Banacloche, Phys. Rev. Lett. **74**, 666 (1995).

[47] A. Kasapi, M. Jain, G.Y. Yin, and S.E. Harris, Phys. Rev. Lett. **74**, 2447 (1995).

[48] O. Schmidt, R. Wynands, Z. Hussein, and D. Meschede, Phys. Rev. A **53**, R27 (1995).

[49] M.G. Payne and L. Deng, Phys. Rev. A **64**, 031802 (2001).

[50] E. Paspalakis and P.L. Knight, Phys. Rev. A **66**, 015802 (2002).

[51] J.Q. Liang, M. Katsuragawa, F.L. Kien, K. Hakuta, Phys. Rev. A **65**, 031801 (2002).

[52] L. V. Hau, S. E. Harris, Z. Dutton, and C. H. Behroozi, Nature (London) **397**, 594 (1999).

[53] G. Morigi and G.S. Agarwal, Phys. Rev. A **62**, 013801 (2000).

[54] M.M. Kash, V.A. Sautenkov, A.S. Zibrov, L. Hollberg, G.R. Welch, M.D. Lukin, Y. Rostovtsev, E.S. Fry, and M.O. Scully, Phys. Rev. Lett. **82**, 5229 (1999).

[55] D. Budker, D.F. Kimball, S.M. Rochester, and V.V. Yashchuk, Phys. Rev. Lett. **83**, 1767 (1999).

[56] A.V. Turukhin, V.S. Sudarshanam, M.S. Shahriar, J.A. Musser, B.S. Ham and P.R. Hemmer, Phys. Rev. Lett. **88**, 023602 (2002).

[57] M.S. Bigelow, N.N. Lepeshkin, and R.W. Boyd, Phys. Rev. Lett. **90**, 113903 (2003).

[58] U. Leonhardt and P. Piwnicki, Phys. Rev. A **60**, 4301 (1999).

[59] U. Leonhardt and P. Piwnicki, Phys. Rev. Lett. **84**, 822 (2000).

[60] U. Leonhardt, Phys. Rev. A **65**, 043818 (2002).

[61] R.J. Cook, H. Fearn, and P.W. Milonni, Am J. Phys. **63**, 705 (1995).

[62] Y. Aharonov and D. Bohm, Phys. Rev. **115**, 485 (1959); M. Peshkin and A. Tonomura, The Aharonov-Bohm Effect (Springer-Verlag, Berlin,1989).

[63] M.V. Berry, R.G. Chambers, M.D. Large, C. Upstill, and J.C. Walmsley, Eur. J. Phys. **1**, 154 (1980); P. Roux, J. de Rosny, M. Tanter, and M. Fink, Phys. Rev. Lett. **79**, 3170 (1997); H. Davidowitz and V. Steinberg, Europhys. Lett. **38**, 297 (1997).

[64] H. Wei, R. Han, and X. Wei, Phys. Rev. Lett. **75**, 2071 (1995).

[65] S.E. Harris and L.V. Hau, Phys. Rev. Lett. **82**, 4611 (1999).

[66] J. Fiurásek, U. Leonhardt, and R. Parentani, Phys. Rev. A **65**, 011802 (2002).

[67] M.D. Lukin and A. Imamoglu, Phys. Rev. Lett. **84**, 1419 (2000).

[68] M.D. Lukin, S.F. Yelin, and M. FLeischhauer, Phys. Rev. Lett. **84**, 4232 (2000).

[69] M. Fleischhauer and M.D. Lukin, Phys. Rev. Lett. **84**, 5094 (2000).

[70] R. Kapoor and G.S. Agarwal, Phys. Rev. A **61**, 053818 (2000); R.R. Moseley, S. Shepherd, D.J. Fulton, B.D. Sinclair, and M.H. Dunn, Phys. Rev. Lett. **74**, 670 (1995); R.R. Moseley, S. Shepherd, D.J. Fulton, B.D. Sinclair, and M.H. Dunn, Phys. Rev. A **53**, 408 (1996); H.Y. Ling, Y.Q. Li, and M. Xiao, Phys. Rev. A **57**, 1338 (1998).

[71] O. Kocharovskaya, Y. Rostovtsev, and M.O. Scully, Phys. Rev. Lett. **86**, 628 (2001).

[72] T.W. Mossberg, Opt. Lett. **7**, 77 (1982).

[73] N.W. Carlson, L.J. Rothberg, A.G. Yodh, W.R. Babbitt, and T.W. Mossberg, Opt. Lett. **8**, 483 (1983).

[74] P.R. Hemmer, K.Z. Cheng, J. Kierstead, M.S. Shariar, and M.K. Kim, Opt. Lett. **19**, 296 (1994); B.S. Ham, M.S. Shariar, M.K. Kim, and P.R. Hemmer, Opt. Lett. **22**, 1849 (1997).

[75] K.P. Leung, T.W. Mossberg, and S.R. Hartmann, Opt. Commun. **43**, 145 (1982).

[76] P. Hu, S. Geschwind, and T.M. Jedju, Phys. Rev. Lett. **37**, 1357 (1976).

[77] H. Schmidt and A. Imamolu, Opt. Lett. **21**, 1936 (1996); 23, 1007 (1998); A. Imamolu, H. Schmidt, G. Woods, and M. Deutsch, Phys. Rev. Lett. **79**, 1467 (1997); M. Lukin and A. Imamolu, Phys. Rev. Lett. **84**, 1419 (2000).

[78] A.S. Zibrov, M.D. Lukin, and M.O. Scully, Phys. Rev. Lett. **83**, 4049 (1999).

[79] M.D. Lukin, S.F. Yelin, and M. Fleischhauer, Phys. Rev. Lett. **84**, 4232 (2000).

[80] A.E. Kozhekin, K. Mlmer, and E. Polzik, Phys. Rev. A **62**, 033809 (2000).

[81] I.E. Mazets and B.G. Matisov, JETP Lett. **64**, 515 (1996).

[82] M. Fleischhauer and M.D. Lukin, Phys. Rev. A **65**, 022314 (2002).

[83] A.B. Matsko, Y.V. Rostovtsev, O. Kocharovskaya, A.S. Zibrov, and M.O. Scully, Phys. Rev. A **64**, 043809 (2001).

[84] G. Juzelinuas and H.J. Carmichael, Phys. Rev. A **65**, 021601 (2002).

[85] A. Raczynski and J. Zaremba, Opt. Commun. **209**, 149 (2002); A. Raczynski, J. Zaremba, and S. Zielinska-Kaniasty, Opt. Commun. **209**, 149 (2002); A. Raczynski, J. Zaremba, and S. Zielinska-Kaniasty, Phys. Rev. A **69**, 043801 (2004).

[86] C. Mewes and M. Fleischhauer, Phys. Rev. A **66**, 033820 (2002).

[87] G. Juzeliunas, M. Masalas, M. Fleischhauer, Phys. Rev. A **67**, 023809 (2003).

[88] D.F. Phillips, A. Fleischhauer, A. Mair, R.L. Walsworth, and M.D. Lukin, Phys. Rev. Lett. **86**, 783 (2001).

[89] C. Liu, Z. Dutton, C.H. Behroozi, and L.V. Hau, Nature (London) **409**, 490 (2001).

[90] H. Gao, M. Rosenberry, and H. Batelaan, Phys. Rev. A **67**, 053807 (2003).

[91] M. Bajcsy, A.S. Zibrov, and M.D. Lukin, Nature (London), **426**, 638 (2003).

[92] A.S. Zibrov, A.B. Matsko, O. Kocharovskaya, Y.V. Rostovtsev, G.R. Welch, and M.O. Scully, Phys. Rev. Lett. **88**, 103601 (2002).

[93] A. Mair, J. Hager, D.F. Phillips, R.L. Walsworth, and M.D. Lukin, Phys. Rev. A **65**, 031802 (2002).

[94] M. Kozuma, D. Akamatsu, L. Deng, E.W. Hagley, and M.G. Payne, Phys. Rev. A **66**, 031801 (2002).

[95] M.G. Payne, L. Deng, C. Schmitt, and S. Anderson, Phys. Rev. A **66**, 043802 (2002).

[96] M.D. Lukin and A. Imamoglu, Nature(London) **413**, 273 (2001).

[97] L.M. Duan, M.D. Lukin, J.I. Cirac, and P. Zoller, Nature(London) **414**, 413 (2001).

[98] M. Fleischhauer and S. Gong, Phys. Rev. Lett. **88**, 070404 (2002).

[99] M.D. Lukin, Rev. Mod. Phys. **75**, 457 (2003).

[100] A.B. Mastko, O. Kocharovskaya, Y. Rostovtsev, A.S. Zibrov, and M.O. Scully, Adv. At., Mol., Opt. Phys. **46**, 191 (2001).

[101] R.W. Boyd and G.J. Gauthier, in *Progress in Optics* Ed. E. Wolf (Elsevier Amsterdam, 2002), Vol. 43, pg. 500.

[102] A. Sommerfeld, Phys. Z. **8**, 841 (1907).

[103] Y. Aharonov, A. Komar, and L. Susskind, Phys. Rev. **182**, 1400 (1969).

[104] N.G. Basov, R.V. Ambartsumyan, V.S. Zuev, P.G. Kryukov, and V.S. Letkhov, Sov. Phys. JETP **23**, 16 (1966).

[105] A. Icsevgi and W.E. Lamb, Phys. Rev. **185**, 517 (1969).

[106] E. Picholle, C. Montes, C. Leycuras, O. Legrand, and J. Botineau, Phys. Rev. Lett. **66**, 1454 (1991).

[107] D.L. Fisher and T. Tajima, Phys. Rev. Lett. **71**, 4338 (1993).

[108] C.G.B. Garrett and D.E. McCaummber, Phys. Rev. A **1**, 305 (1970).

[109] S. Chu and S. Wong, Phys. Rev. Lett. **48**, 738 (1982).

[110] B. Segard and B. Macke, Phys. Lett. **109 A**, 213 (1985).

[111] R.Y. Chiao, in *Amazing Light, a Volume Dedicated to C. H. Townes on His Eightieth Birthday*, Ed. R.Y. Chiao, (Springer, New York, 1996), pg. 91.

[112] R.Y. Chiao, Phys. Rev. A **48**, R34 (1993).

[113] E.L. Bolda, R.Y. Chiao, and J.C. Garrison, Phys. Rev. A **48**, 3890 (1993).

[114] R.Y. Chiao, J. Boyce, and J.C. Garrison, in *Fundamental Problems in Quantum Theory, in Honor of Professor John A. Wheeler*, D. M. Greenberg and A. Zeilinger, eds., Ann. N. Y. Acad. of Sci. **755**, 400 (1993).

[115] A.M. Steinberg and R.Y. Chiao, Phys. Rev. A **49**, 2071 (1994).

[116] M.W. Mitchell and R.Y. Chiao, Am. J. Phys. **66**, 14 (1998).

[117] E.L. Bolda, J.C. Garrison, and R.Y. Chiao, Phys. Rev. A **49**, 2938 (1994).

[118] R.Y. Chiao and A.M. Steinberg, in *Progress in Optics*, Ed. E. Wolf (Elsevier, Amsterdam, 1997), pg. 345.

[119] A.M. Steinberg, P.G. Kwiat, and R.Y. Chiao, Phys. Rev. Lett. **71**, 708 (1993).

[120] L.J. Wang, A. Kuzmich, and A. Dogariu, Nature(London) **406**, 277 (2000).

[121] A. Dogariu, A. Kuzmich, and L.J. Wang, Phys. Rev. A **63**, 053806 (2001).

[122] A. Dogariu, A. Kuzmich, H. Cao, and L.J. Wang, Opt. Exp. **8**, 344 (2001).

[123] A.M. Akulshin, S. Barreiro, and A. Lezama, Phys. Rev. Lett. **83**, 4277 (1999).

[124] A.M. Akulshin, A. Cimmino, A.I. Sidorov, P. Hannaford, and G.I. Opat Phys. Rev. A **67**, 011801 (2003).

[125] A.M. Akulshin, A. Cimmino, A.I. Sidorov, R. McLean, and P. Hannaford J. Opt. B **5**, S479 (2003).

[126] A.D. Wilson-Gordon and H. Friedmann, Opt. Commun. **94**, 238 (1992).

[127] C. Szymanowski and H. Keitel, J. Phys. B **27**, 5795 (1994); T. Quang and H. Freedhoff, Phys. Rev. A **48**, 3216 (1993).

[128] A. Wicht, M. Muller, R.-H. Rinkleff, A. Rocco, and K. Danzmann, Opt. Commun. **179**, 107 (2000).

[129] A. Rocco, A. Wicht, R.-H. Rinkleff, and K. Danzmann, Phys. Rev. A **66**, 053804 (2002).

[130] F. Schreier, M. Schmitz, and O. Bryngdahl, Opt. Commun. **163**, 1 (1999).

[131] C. Spielmann, R. Szipöcs, A. Stingl, and F. Krausz, Phys. Rev. Lett. **73**, 2308 (1994).

[132] A.M. Steinberg, P.G. Kwiat, and R.Y. Chiao, Phys. Rev. Lett. **71**, 708 (1993).

[133] D.L. Fisher, T. Tajima, M.C. Downer, and C.W. Siders, Phys. Rev. E **51**, 4860 (1993).

[134] R.G. Ghulghazaryan and Y. P. Malakyan, Phys. Rev. A **67**, 063806 (2003).

[135] Md. A.I. Talukder, Y. Amagishi, and M. Tomita Phys. Rev. Lett. **86**, 3546 (2001).

[136] D. Bortman-Arbiv, A. D. Wilson-Gordon, and H. Friedmann Phys. Rev. A **63**, 043818 (2001).

[137] K. Kim, H.S. Moon, C. Lee, S.K. Kim, and J.B. Kim Phys. Rev. A **68**, 013810 (2003).

[138] M.S. Bigelow, N.N. Lepeshkin, and R.W. Boyd, Science, **301**, 200 (2003).

[139] G. Diener, Phys. Lett. A **223**, 328 (1996).

[140] G. Diener, Phys. Lett. A **235**, 118 (1997).

[141] Y. Aharonov, B. Reznik, and Ady Stern, Phys. Rev. Lett. **81**, 2190 (1998).

[142] B. Segev, P.W. Milonni, J.F. Babb, and R.Y. Chiao Phys. Rev. A **62**, 022114 (2000).

[143] A. Kuzmich, A. Dogariu, L.J. Wang, P.W. Milonni, and R.Y. Chiao Phys. Rev. Lett. **86**, 3925 (2001).

[144] M.D. Stenner, D.J. Gautheir, and M.A. Neifeld, Nature(London), **425**, 695 (2003).

[145] P.W. Milonni, J. Phys. B: At. Mol. Opt. Phys. **35**, R31 (2002).

[146] D. Solli, R.Y. Chiao, and J.M. Hickmann, Phys. Rev. E **66**, 056601 (2002).

[147] R. Grobe, F. T. Hioe, and J. H. Eberly, Phys. Rev. Lett. **73**, 3183 (1994).

[148] J. H. Eberly and V. V. Kozlov, Phys. Rev. Lett. **88**, 243604 (2002).

[149] A. Rahman and J. H. Eberly, Phys. Rev. A **58**, R805 (1998).

[150] H. Taub and D.L. Schilling *Principles of Communication Systems*, Tata McGraw-Hill Publishing Company Limited, New Delhi (1986).

[151] L. W. Hillman, R. W. Boyd, J. Krasinski, and C. R. Stroud, Jr. , Opt. Commun. **45**, 416 (1983).

[152] T.H. Maiman, Phys. Rev. Lett. **4**, 564(1960).

[153] P. F. Liao and D. M. Bloom, Opt. Lett. **3**, 4 (1978).

[154] M. S. Malcuit, R. W. Boyd, L. W. Hillman, and C. R. Stroud, Jr., JOSA B **1**, 73 (1984); K. V. Yumashev, N. V. Kuleshov, P. V. Prokoshin, A. M. Malyarevich, and V. P. Mikhailov, Appl. Phys. Lett. **70**, 2523 (1997); Z. Burshtein, P. Blau, Y. Kalisky, Y. Shimony, and M. R. Kokta, IEEE J. Quantum Electron, **34**, 292 (1998).

[155] M.L. Shand, J.C. Walling, and R.C. Morris, J. Appl. Phys. **52**, 953 (1981).

[156] M.J.V. Bell, D.F. de Sousa and L.A.O. Nunes, J. Appl. Phys. **87**, 8264 (2000).

[157] B.R. Mollow, Phys. Rev. A **5**, 2217 (1972).

[158] F.Y. Wu, S. Ezekiel, M. Ducloy and B.R. Mollow, Phys. Rev. Lett. **38**, 1077 (1977); M.T. Gruneisen, K.R. MacDonald, and R.W. Boyd, J. Opt. Soc. Am. B **5**, 123 (1998); W.V. Davis, A.L. Gaeta, R.W. Boyd, and G.S. Agarwal, Phys. Rev. A **5**, 3625 (1996).

[159] G.S. Agarwal, Phys. Rev. A **19**, 923 (1979).

[160] D. Grandclement, G. Grynberg, and M. Pinard, Phys. Rev. Lett. **59**, 44 (1987); G. Grynberg and P. R. Berman, Phys. Rev. A **39**, 4016 (1989).

[161] C. Cohen-Tannoudji and S. Reynaud, J. Phys. B **10**, 345 (1977); For a detail discussion see, C. Cohen-Tanoudji, J. Dupont-Roc, and G. Grynberg, *Atom-photon Interactions: Basics Process and Applications* (Wiley, New York, 1992), Chap. VI.

[162] A. Javan, W.R. Bennett, Jr., and D.R. Herriott, Phys. Rev. Lett. **6**, 106 (1961).

[163] W. Demtroder, *Laser Spectroscopy Basic Concepts and Instrumentation*, (3^{rd}Edition, Springer-Verlag Berlin Heidelberg NewYork), pg. 450.

[164] S. Svanberg, G.-Y Yan, T.P. Duffey, and A.L. Schawlow Opt. Lett. **11**, 138 (1986).

[165] V.M. Agranovich and V.L. Ginzburg, *Spatial dispersion in crystal optics and the theory of excitons*, (Interscience Publishers, London, 1964).

[166] Y. Rostovtsev, O. Kocharovskaya, and M.O. Scully, J. Mod. Opt. **49**, 2637 (2002).

[167] G. Vemuri, G.S. Agarwal, and K.V. Vasavada, Phys. Rev. Lett. **79**, 3889 (1997).

List of Publications

I. Papers in Journals and Books:

1. *Knob for Changing Light Propagation from Subluminal to Superluminal*, G. S. Agarwal, T.N. Dey, and Sunish Menon, Phys. Rev. A **64**, 053809 (2001).

2. *Stoppage of Light Made Flexible by an Additional Control Field* , G. S. Agarwal, and T.N. Dey, J. Mod. Opt. **50**, 1469 (2003).

3. *Storage and Retrieval of light at Moderate Powers* , T.N. Dey, and G.S. Agarwal, Phys. Rev. A **67**, 033813 (2003); (selected in Virtual Journal of Ultrafast Science, April 2003).

4. *Slow light in Doppler-broadened two level systems* , G.S. Agarwal and T.N. Dey, Phys. Rev. A **68**, 063816 (2003).

5. *Sub and Super-Luminal Propagation of Intense Pulses in Media with Saturated and Reverse Absorption*, G.S. Agarwal and T.N. Dey, Phys. Rev. Lett. **92**, 203901 (2004).

II. In Proceedings/Abstracts of International and National Conferences:

1. *From Delocalization to Localization in Optical Waveguide Arrays* , Tarak Nath Dey, "International Conference on Perspectives in Theoretical Physics" Pg. 45, held at Physical Research Laboratory, Ahmedabad, India, 8-12, Jan., 2001.

2. *Ultra Slow light* , Tarak Nath Dey,"National Laser Smposium", Pg 34, held at Indian Institute of Technology, Kharagpur, India 22-24, Dec., 2003 (Invited talk).